IN SILICO IDENTIFICATION OF CANDIDATE *MECP2* TARGETS AND QUANTITATIVE ANALYSIS IN RETT SYNDROME

A THESIS SUBMITTED TO
THE DEPARTMENT OF MOLECULAR BIOLOGY AND GENETICS
AND
THE INSTITUTE OF ENGINEERING AND SCIENCE OF
BILKENT UNIVERSITY
IN PARTIAL FULFILLMENT OF THE REQUIREMENTS FOR
THE DEGREE OF MASTER OF SCIENCE

BY
ONUR EMRE ONAT
JULY, 2006

I certify that I have read this thesis and that in my opinion it is fully adequate, in scope and in quality, as a thesis for the degree of Master of Science.

Prof. Dr. Tayfun Özçelik

I certify that I have read this thesis and that in my opinion it is fully adequate, in scope and in quality, as a thesis for the degree of Master of Science.

Prof. Dr. Meral Topçu

I certify that I have read this thesis and that in my opinion it is fully adequate, in scope and in quality, as a thesis for the degree of Master of Science.

Assist. Prof. Rengül Çetin-Atalay

Approved for the Institute of Engineering and Science

Director of Institute of Engineering and Science
Prof. Mehmet Baray

ABSTRACT

IN SILICO IDENTIFICATION OF CANDIDATE *MECP2* TARGETS AND QUANTTITATIVE ANALYSIS IN RETT SYNDROME

Onur Emre Onat
M.S. in Molecular Biology and Genetics
Supervisor: Prof. Dr. Tayfun Özçelik
July 2006, 96 Pages

Rett syndrome (RTT) is an X-linked neuro-developmental disorder seen exclusively girls in the childhood. It is one of the most common causes of mental retardation with an incidence rate of 1/10,000-1/15,000. Mutations in *MECP2* gene was described as a common cause of RTT. *MECP2* is a transcriptional repressor that regulates gene expression. It is not fully understood which *MECP2* targets are affected in RTT and therefore contribute to disease pathogenesis. Researchers approached the problem in two directions: a) Global expression profile analysis and b) Candidate gene analysis. Global expression profile analysis revealed which a limited number of genes including those on the X-chromosome are de-regulated. Candidate gene analysis studies showed that loss of imprinting as exemplified by *DLX5* could also contribute to disease pathogenesis. We hypothesize that X-chromosome inactivation (XCI) is an important physiological epigenetic mechanism that could be involved in Rett pathogenesis. We predicted a *MECP2* binding motif by a distinctive bioinformatic approach. Using this algorithm we searched for the candidate *MECP2* target genes on the X-chromosome and whole genome. The genes *FHL1* and *MPP1,* whose interaction with *MECP2* were heuristically displayed were predicted by our algorithm. We identified more than 100 genes which are on the X-chromosome. 10 genes from the list were selected according to their *MECP2* binding homology score and X-inactivation status. In order to test this hypothesis we analyzed these genes with quantitative RT-PCR .We expect to identify the key genes that potentially contribute to RTT pathogenesis via disturbances in X-chromosome inactivation.

ÖZET

MECP2 HEDEF GENLERİNİN IN SILICO TANIMLANMASI VE RETT SENDROMU'NDA NİCELİKSEL ANALİZİ

Onur Emre Onat
Moleküler Biyoloji ve Genetik Yüksek Lisans
Tez Yöneticisi: Prof. Dr. Tayfun Özçelik
Temmuz 2006, 96 Sayfa

Rett sendromu (RTT) çocukluk çağında kız çocuklarında görülen nörogelişimsel bir hastalıktır. Mental retardasyonun başlıca sebeplerinden olup, 1/10000-1/15000 sıklıkla görülür. *MECP2* geninin mutasyonuna bağlı olarak gelişir. *MECP2* bir gen anlatımı baskılayıcısıdır. RTT'de anlatımı bozulan genlerin belirlenmesi hastalığın patogenezinin anlaşılması açısından çok önemlidir. Bu konuda araştırmacılar iki farklı yoldan ilerlemektedir: a) Global gen anlatım profili incelemeleri b) Aday gen incelemeleri. Mikroarray teknolojisi ile incelenen birinci yolda, kısıtlı sayıda genin anlatımının farklılaştığı gözlenmiştir. Aday gen çalışmaları ise önemli bir epigenetik düzenleme olan genomik imlemeye uğrayan *DLX5* geninin RTT hastalarında imlemeden kaçarak hastalık mekanizmasına katkıda bulunduğunu göstermiştir. Önemli bir fizyolojik epigenetik düzenleme X-etkinsizleştirilmesidir. RTT patogenezi ile ilişkisi henüz araştırılmamıştır. X-etkinsizleştirilmesinin RTT patogenezinde önemli bir rol oynadığını düşünüyoruz. Özgün bir biyoinformatik yazılım algoritmi geliştirerek *MECP2* bağlayan dizi motiflerinin varlığını özellikle X-kromozomu olmak üzere insan genomunda aradık. Bu inceleme sonunda saptanan genler arasında *MECP2* ile etkileşime girdiği deneysel olarak gösterilmiş *MPP1* ve *FHL1* genleride yer alıyordu. Listemizde bulunan genler arasında X-kromozomuna haritalanan yüzün üzerinde gen bulunmaktadır. Bu genlerin X-etkinsizleştirilmesi profillerine ve *MECP2* bağlayan dizi homolojisi değerlerine bağlı olarak on farklı aday gen seçtik. Ters yazılımlı polimeraz zincir reaksiyonu (RT-PCR) ile bu genlerin anlatımını incelemeye aldık. Bu çalışmaların RTT patogenezinde X-etkinsizleştirilmesinin rolü konusunda değerli bilgiler vermesi beklenmektedir.

TO MY PARENTS

GÜLSEREN, İSMAİL ONAT

AND

TO MY SISTER

EMEL ONAT (GÖLLÜ)

FOR THEIR LOVE AND SUPPORT

ACKNOWLEDGEMENTS

First of all, I would like to express my deepest gratitude to my advisor Prof. Tayfun Özçelik for his guidance, encouragement, patience, and continuous support throughout my thesis work. I not only benefit from his scientific advices but also improve my point of view on academic and social life during our conversations. It would be an honor for me to further my academic studies with him.

It is my pleasure to express my thanks to Prof. Meral Topçu for her help in clinical diagnosis and obtaining patient samples and their clinical data.

Moreover, I would particularly thank to Assist. Prof. Rengül Çetin Atalay and her student Murat İskar for their effort, guidance, and help in bioinformatic studies.

Very special thanks to my family for their support and understanding through my whole life. I know that what I am now is your creature. Having a family like you who just couldn't be loved more means so much.

I wish to express my thanks to Bilkent MBG family. What makes Bilkent MBG as attractive is its cordial and sincere environment. Thank all of you, my friends and instructors, for your warm friendships and suggestions.

I would like to thank my home-friends Emre Albay and Hüseyin Çevik (ex) for their understanding and sensibility during my thesis study. I believe one day we will create this country from the begining with our conversations which prolongs each time to the mornings with the help of tea and cigarettes.

Finally, my very special thanks go to Ezgi Özcan for her love and care. What really make you my special is simply being mine.

TABLE OF CONTENTS

LIST OF TABLES

LIST OF FIGURES

ABBREVIATIONS

bp	base pair
BSA	bovine serum albumin
Bisacrylamide	N, N, methylene bis-acrylamide
C-terminus	carboxy Terminus
CHIP	chromatin immuno-precipitation
CpG	cytosine guanine pair
CTCF	CCCTC-binding factor
ddH_2O	deionized water
del	deletion
DMR	differentially methylated region
DMSO	dimethyl sulphoxide
DNA	deoxyribonucleic acid
DNase	deoxyribonuclease
dNTP	deoxynucleotide triphosphate
EDTA	ethylenediaminetetraacetic acid
EtBr	ethidium bromide
EtOH	ethanol
FBS	fetal bovine serum
FCS	fetal calf serum
HCl	hydrochloric acid
HDAC	histone deacetylase
IRSA	International Rett Syndrome Association
kb	kilobase
KCl	potassium chloride
LCL	lymphoblastoid cell line
LOI	loss of imprinting
MBD	methyl binding domain

MBS	MECP2 binding site
$MgCl_2$	magnesium chloride
mM	milimolar
µl	microliter
mRNA	messenger RNA
NaOAc	sodium acetate
NaCl	sodium chloride
NaOH	sodium hydroxide
NLS	nuclear localization signal
PAGE	polyacrylamide gel electrophoresis
PBS	phosphate buffered saline
PCR	polymerase chain reaction
PSV	preserved speech variant
RCP	the red opsin
RE	restriction enzyme
RTT	Rett syndrome
RNA	ribonucleic acid
RT-PCR	reverse transcriptase PCR
SDS	sodium dodecyl sulphate
TAE	tric-acetic acid-EDTA
TBE	tric-boric acid-EDTA
TEMED	N, N, N, N-tetramethyl-1-2, diaminoethane
TRD	trancriptional repression domain
UV	Ultraviolet
XCI	X-chromosome inactivation
Xic	X-inactivation center

CHAPTER I. INTRODUCTION

1.1 Rett syndrome

Rett syndrome (RTT; OMIM #312750) is an X-linked neuro-developmental disorder first defined by Dr. Andreas Rett in 1966 (Rett, 1966; Rett, 1977). It is the second most common causes of mental retardation in females after Down syndrome (Ellaway *et al*., 2001). Population genetics studies estimated the frequency of Rett syndrome to be about 1 in 10,000 to 1 in 20,000 (Kerr *et al*, 1985; Hagberg *et al.*, 1985; Leonard *et al*., 1997; Miyamoto *et al*., 1997). It is seen almost exclusively in females and lethal in males. Unlike females which have two X chromosomes, males have one X and one Y chromosomes. So, there is no backup copy of X chromosomes in males that can compensate in the presence of defective copy. Rett patients appear to develop normally until 6–18 months of age, then gradually lose speech and purposeful hand use, and develop microcephaly, seizures, autism-like features, ataxia, intermittent hyperventilation and stereotypic hand movements (Armstrong, 1997).

1.1.1 Clinical features

When Andreas Rett defined Rett syndrome in two girls showing same unusual behaviors who were seated next to each other in the waiting room in 1966, it was largely ignored (Rett, 1966).

In 1983, Hagberg described 35 girls with a progressive encephalopathy. He

described RTT phenotype as rapid deterioration of high brain functions following developmental stagnation after normal development up to the age of 7 to 18 months. Within 1.5 years period autism, severe dementia, loss of purposeful hand use, ataxia, and microcephaly occurs (Hagberg *et al*., 1983)

The diagnosis criteria for Rett syndrome is summarized in Table 1.1. At the first 3 months after birth, growth and development are normal. At the age 3 to 6 months developmental delay and slowed head growth is noted, which is followed by autistic behavior, regression, and stereotyped hand movements. Between the age 6 to 18 months hypotonia (diminished muscle tone), deceleration in eye contact occurs. After the age 3 years up until the end of adolescence acquired microcephaly (decreased head circumference) and decline in body weight is seen, and it results in a short stature (Fitzgerald et al., 1990)

Table 1.1 Diagnostic criteria for Rett syndrome (Ellaway *et al*., 2001)

Necessary Criteria
• Apparently normal prenatal and perinatal period • Apparently normal psychomotor development within the first 6 months • Normal head circumference at birth • Deceleration of head growth between ages 5 months and 4 years • Loss of acquired purposeful hand skills between ages 6 and 30 months, temporally associated with communication dysfunction and social withdrawal • Development of severely impaired expressive and receptive language, and presence of apparent severe psychomotor retardation • Stereotypic hand movements such as hand writing/squeezing, clapping/tapping, mouthing and washing/rubbing automatisms appearing after purposeful hand skills are lost • Appearance of gait apraxia and truncal apraxia/ataxia between ages 1 and 4 years • Diagnosis tentative until 2 to 5 years of age
Supportive Criteria

• Breathing dysfunction
  o Periodic apnea during wakefulness
  o Intermittent hyperventilation
  o Breath-holding spells
  o Forced expulsion of air or saliva
• Electroencephalografic abnormalities
  o Slow waking background and intermittent rhythmical slowing (3-5 Hz)
  o Epileptiform discharges, with or without clinical seizures
• Seizures
• Spasticity, often with associated development of muscle wasting and dystonia
• Peripheral vasomotor disturbance
• Scoliosis
• Growth retardation
• Hypotrophic small feet

Exclusion Criteria
• Evidence of intrauterine growth retardation • Organomegaly of other signs of storage disease • Retinopathy or optic atrophy • Microcephaly at birth • Evidence of perinatally acquired brain damage • Existence of identifiable metabolic or other progressive neurological disorder • Acquired neurological disorders resulting from severe infections or head trauma

1.1.2 Stages of Rett syndrome

There are four stages of the RTT which are early onset (6-18 months), regressive stage (1-3 years), relative stabilization stage (3-10 years), and late motor impairment stage (10+ years) summarized in Table 1.2.

Table 1.2 Classic Rett syndrome: clinical characteristics and differential diagnosis by stage (Ellaway *et al*., 2001)

Stage	**Clinical characteristics**	**Differential diagnosis**
I. Early onset stagnation stage Onset: 6-18 months	Development stagnation/arrest Deceleration of head/brain growth Disinterest in play activity Hypotonia Nonspecific personality changes Diminished play interest Hand waving – nonspecific, episodic	Benign congenital hypotonia Prader-Willi syndrome Cerebral palsy
II. Rapid destructive stage Onset: 1-3 years	Rapid developmental regression with irritability Poor hand use Seizures Hand stereotypies: wringing Autistic manifestations Loss of expressive language Insomnia and irritability Self-abusive behaviour (e.g., chewing fingers) Mental deterioration Clumsy mobility/apraxia/ataxia Better preservation of gross motor functions Irregular breathing – hyperventilation	Autism Psychosis Hearing or visual disturbance Encephalitis Infantile spasms (West syndrome) Tuberous sclerosis Ornithine carbamoyl transferase deficiency Phenylketonuria Infantile neuronal ceroid lipofuscinosis

III. Pseudo-stationary stage Onset: 3-10 years	Severe mental retardation/apparent dementia Amelioration of autistic features Seizures and epileptic signs Typical hand stereotypies Prominent gait ataxia and apraxia Jerky truncal ataxia Spasticity; gross motor dysfunction Hyperventilation, breath-holding, aerophagia Apnea during wakefulness Weight loss with excellent appetite Early scoliosis, Bruxism	Spastic ataxic cerebral palsy Spinnocerebellar degeneration Leukodystrophies or other storage disorders Neuroaxonal dystrophy Lennox-Gastaut syndrome Angelmann syndrome
IV. Late motor deterioration stage Onset: 10+ years	Combined upper and lower motor neuron signs Progressive scoliosis, muscle wasting, and rigidity Severe multihandling syndrome Paraparesis or tetraparesis Decreasing mobility; wheelchair-bound Growth retardation, but normal puberty Staring, unfathomable gaze Emotional and eye contact "improving" Reduced seizure frequency Virtual absence of expressive and receptive language Trophic disturbance of feet Cachexia Respiratory abnormalities	Neurodegenerative disorders of unknown genes

In **stage I, early onset of stagnation**, there is stagnation in development and growth. Head growth slows and hypotonia is seen. The infant begins to show less eye contact and obtaining new skills slows down. Quite frequently these symptoms are not sufficient to be noticed. After several months, **stage II, the rapid regression stage** comes. At this stage most of the previously acquired skills such as spoken language and purposeful hand use (apraxia), and social interaction are lost. The characteristic hand

movements begin to emerge and slowing of head growth draw attention. At **Stage III, plateau or pseudo-stationary stage,** motor problems, and seizures develop. Autistic-like features clearly emerge. Many girls remain in this stage for most of their lives. The last stage, **stage IV – late motor deterioration stage –** is defined as reduced mobility. Spasticity, dystonia (increased muscle tone), muscle weakness, rigidity (stiffness), scoliosis are features of this stage. The majority of the girls with Rett syndrome survive into adulthood.

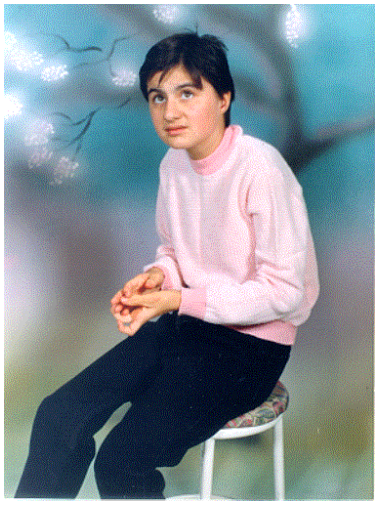

Figure 1.1 Girl with typical characteristics of RTT phenotype (Courtesy of Rett Syndrome Association – Turkey; Prof. Dr. Meral Topçu).

1.1.3 Rett variants

The clinical characteristics of Rett syndrome varies among patients. In general there are two phenotypes of Rett syndrome: Typical (classic) and atypical phenotypes. Besides, there are variants of the atypical form of Rett syndrome (Hagberg *et al.*, 1994)

Early onset seizure subgroup demonstrates the 5-10% of the cases, which occur in both classical and atypical forms (Hagberg *et al.,* 1994).

Form fruste subgroup is characterized by dyspraxic hand functioning and milder mental retardation but no classic Rett stereotypies. This group constitutes 25-30% of the cases (Hagberg *et al.,* 1994).

Congenital onset subgroup, which consists of severely affected girls, constitutes a very small percentage. These girls have abnormal development from birth (Hagberg *et al.,* 1995).

Girls with **Late childhood regression** subgroup develop more gradually with respect to classic RTT types (Gillberg, 1989).

Preserved speech variant (PSV) subgroup resembles classic RTT phenotype but differs in that patients recover some degree of speech and hand use (De Bona *et al.,* 2000).

The **male form** subgroup represents the same phenotypic characteristics with classic Rett syndrome (Christen et al., 1995; Topcu et al., 1991)

1.2 Molecular mechanisms of the disease

1.2.1 Identification of the Rett syndrome gene: *MECP2*

Since almost 99% percent of the RTT cases are sporadic, it was not easy to understand the genetic basis of the disease (Schanen et al., 1997). Several hypotheses

were put forward including the following:

First of all, Hagberg proposed that X-linked dominant inheritance is the best explanation of the involvement of the disease in females (Hagberg et al., 1983). This hypothesis was confounded because most RTT cases are sporadic. However, twin studies with Rett syndrome (Tariverdian et al., 1987; Tariverdian, 1990; Partington, 1988, Zoghbi et al. 1990) supported the hypothesis that Rett syndrome is a genetic disorder. Chromosomal rearrangements (Benedetti et al., 1992) and both uniparental heterodisomy and isodisomy (Webb et al., 1993) were excluded.

At the very beginning of 90s, it was suggested that the gene for Rett syndrome should be located on the short arm of the X chromosome because of a translocation t(X; 22) (p11.22; p11) (Journel et al., 1990) and t(X;3)(p22.1;q13.31) (Zoghbi et al., 1990). In the late 90s, following elegant exclusion mapping studies, RTT locus was mapped to Xq28 (Schanen et al., 1997).

Soon after identification of three de novo missense mutations in 5 of 21 sporadic Rett probands and an additional missense mutation in a family with two affected half sisters in the *MECP2* gene, revealed the long sought "RTT gene" (Amir et al., 1999).

In a more recent study, it was found that truncating frameshift and missense mutations in the *CDKL5* gene causes RTT-like phenotypes (Weaving et al., 2004; Tao et al., 2004). Missense mutations in *CDKL5* is also associated with infantile spasms and clinical phenotypes of neurodegenerative disorders, such as Rett syndrome and Angelman syndrome (Tao et *al., 2004*)

1.2.2 *MECP2* organization and expression

MECP2 gene is located on Xq28, and spans a region of 76 kb. It lies between the genes interleukin I receptor-associated kinase (IRAK) and the red opsin (RCP) (Quaderi *et al*., 1994; D'Esposito *et al.,* 1996) (Figure 1A) The *MECP2* gene has four exons and a CpG island which contains several potential binding sites for Sp1 (Marin *et al*., 1997, Reichwald *et al*., 2000).

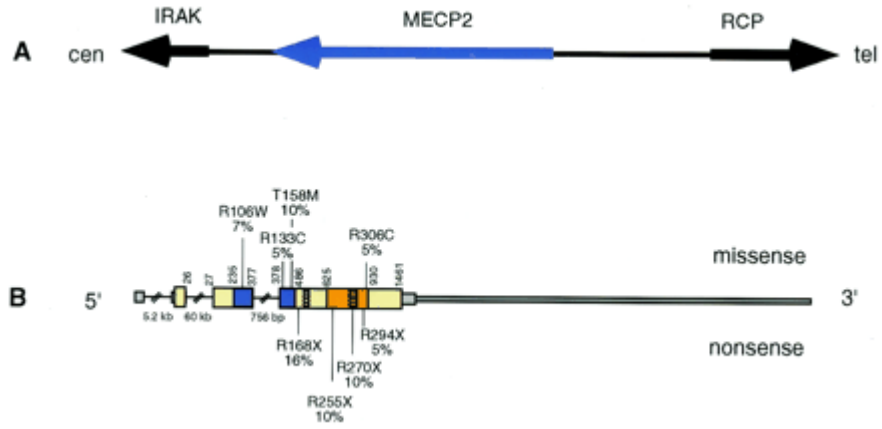

Figure 1.2 Location and organization of *MECP2*. A) The MECP2 gene in Xq28 is flanked by the IRAK and RCP loci in humans. B) The genomic organization of the MECP2 gene. It is comprised of four exons. The coding sequence for the methyl-binding domain is indicated in blue (Dragich et al., 2000).

Expression of *MECP2* gene is low during embryogenesis in mammals, but it is widely expressed in adult tissues. The highest expression is seen in adult brain and

spinal cord. There are three transcripts of *MECP2* gene: 1.8 kb, 7.6 kb and 10 kb. The shortest and longest transcripts are present in most tissues and have short half-lives (Dragich *et al*., 2000)

1.2.3 Structure and function of *MECP2*

As mentioned above, mutations in the gene encoding methyl CpG binding protein 2 (MeCP2) is the major cause of Rett syndrome. MeCP2 functions as a transcriptional repressor like MeCP1. Both MeCP family genes bind methylated CpG dinucleotides (Meehan *et al*., 1992). Most of the cytosine residues of the CpG dinucleotides are methylated in terms of regulation of gene expression (Ng et al., 1999; Jones et al., 1999).

Transcriptional repression via MeCP2 is probably important in epigenetic regulation such as imprinting (Pedone *et al.,* 1999), X-inactivation (Jeppesen *et al.,* 1993), tissue specific expression (Schubeler et al., 2000), and the silencing of endogenous retroviruses (Li *et al.,* 1992).

MeCP2 contains two domains: MBD (Methyl Binding Domain) (Nan *et al.,* 1993) and TRD (Transcriptional Repression Domain) (Nan *et al.,* 1998). Besides, MeCP2 has two NLSs (Nuclear Localisation Signals) (Nan *et al.,* 1996). MeCP2 binds methylated CpG base pairs on its target genes via MBD domain (Nan *et al.,* 1993), and represses its target genes by interacting with a co-repressor complex containing Sin3A and HDACs (histone deacetylases 1 and 2) via its TRD domain (Nan *et al.,* 1998; Jones *et al.*, 1998).

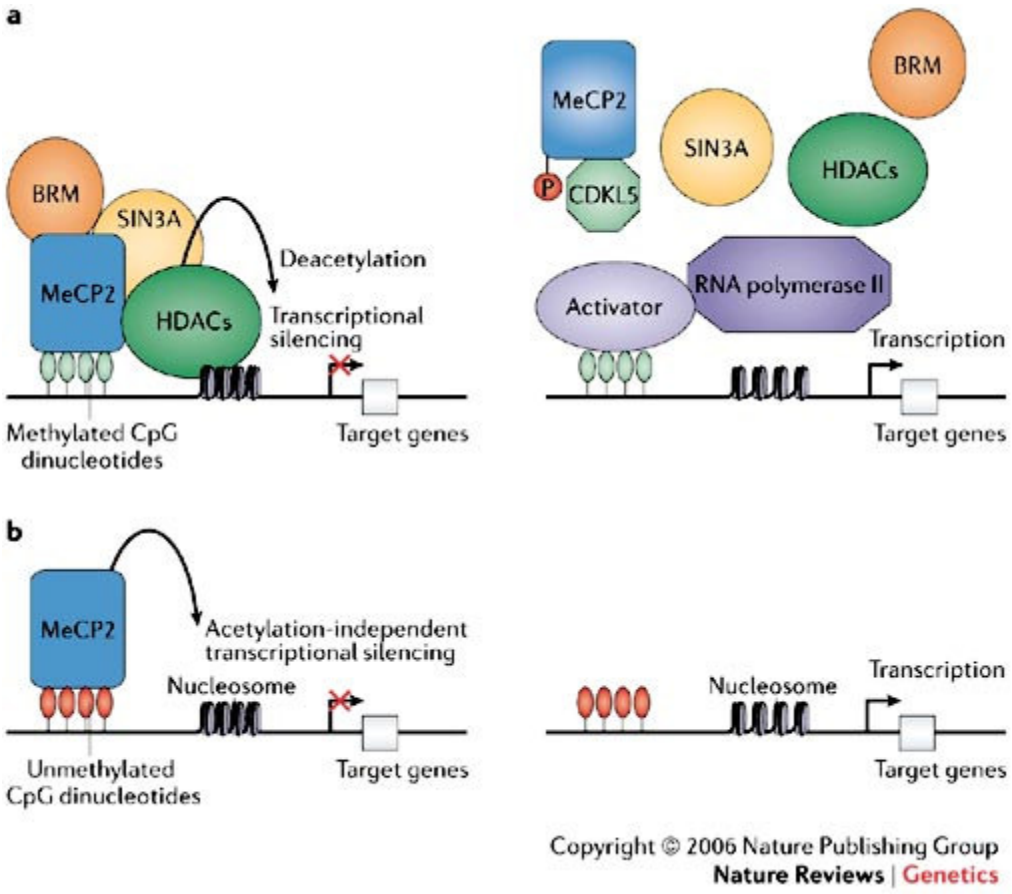

Figure 1.3 The schematic representation of *MECP2* repression activity. A) MeCP2 binds on methylated DNA and represses transcription by recruiting chromatin-remodeling complex including SIN3A (transcriptional co-repressor), BRM (SWI/SNF-related chromatin remodeling protein), and HDACs (histone deacetylases). Lack of MeCP2 binding on DNA can be due to inactivation of MeCP2 via phosphorylation by CDKL5 (Cyclin-dependent kinase-like 5) B) MeCP2 can also represses its target genes independent of DNA methylation (Bienvenu et al., 2006)

1.2.4 Mutations and polymorphisms of *MECP2* and their effects

MECP2 mutations are detected in up to 80% of classic RTT patients (Wan et al., 1999; Bienvenu *et al*., 2000). More than 2000 *MECP2* mutations have been reported in females (Amir et al., 2000; Miltenberger et al., 2003; Weaving et al., 2005; Philippe et al., 2006) but 8 C→T transitions given in Table-1.3 account for 65% of all mutations in RTT patients (Miltenberger *et al.*, 2003).

Table 1.3 *MECP2* mutation spectrum in Rett syndrome (Weaving *et al.*, 2003)

Base Change	AA Change	Incidence	Type of Mutation
473 C→T	T158M	9.64	Missense
502 C→T	R168X	9.25	Nonsense
763 C→T	R255X	7.93	Nonsense
808 C→T	R270X	7.70	Nonsense
880 C→T	R294X	6.30	Nonsense
916 C→T	R306C	5.13	Missense
397 C→T	R133C	4.04	Missense
316 C→T	R106W	3.73	Missense

Furthermore, there are several polymorphisms defined for *MECP2* in the coding or non-coding regions (Laccone *et al.*, 2002). The medical significance of these polymorphisms in hemizygous males need a clear definition.

Most mutations found in *MECP2* gene lie in the MBD and TRD functional domains. The majority of the RTT mutations are nonsense or frameshift mutations that lie in the last exon of *MECP2*. In general, there are five types of *MECP2* mutations: 1) Missense mutations, 2) Nonsense mutations, 3) Frameshift mutations, 4) Large deletions, 5) Splicing mutations, deletions, and insertions (Bienvenu *et al*., 2002).

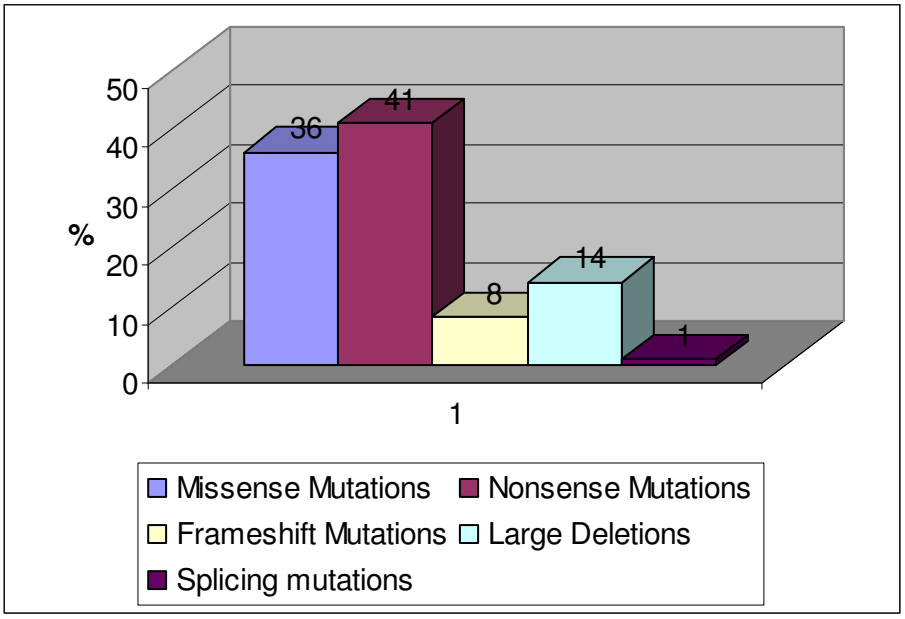

Figure 1.4 Type of *MECP2* mutations. Mutations are classified as nonsense mutations (%44), missense mutations (%36), large deletions (%14), frameshift mutations (%8), splicing mutations (%1) (Bienvenu *et al.*, 2002)

1.3 Phenotype - Genotype correlations in Rett syndrome

The phenotypic range of the RTT patients led to the classification of the cases from milder to the more severe. Form fruste and preserved speech variants are classified as mildest cases. These patients lack all supportive criteria mentioned before and they can also retain some communication and hand skills (Zappella, 1992).

The phenotype-genotype correlation studies indicated that the nonsense mutations cause more severe phenotype than missense mutations (Cheadle *et al.*, 2000). Another study indicates that early truncating mutations are more severe than late

truncating mutations (Weaving *et al.*, 2003). Besides that, the severity of the disorder is likely to depend on location and type of mutation present. Rett patients with PSV do not contain early truncating mutations; all the mutations found in these patients are either missense or late truncating mutations (*Zapella et al*., 2001).

More specifically, recent studies with RTT patients demonstrated that R133C mutation was associated with autistic presentation, R306C mutation is associated with slower disease progression (Smeets et al., 2003), and R270X mutation is associated with reduced survival (Jian et al., 2005).

1.4 Epigenetic mechanisms

The epigenetic mechanism of transcriptional silencing by methylation of CpG dinucleotides has a considerable importance for development. As mentioned, *MECP2* represses its target genes by binding to the methylated CpG dinucleotides that is why it is thought that *MECP2* repression has roles in epigenetic mechanisms such as X-inactivation and genomic imprinting (Cross *et al.*, 1995).

1.4.1 X-chromosome inactivation

X-chromosome inactivation occurs in females in order to equalize dosage compensation between females and males. Since males have only one X-chromosome, one of the X allele is silenced via X-inactivation mechanism in females (Plath *et al.,* 2002).

The X-inactivation mechanism is controlled via Xic (X-inactivation control center). Xic contains two major genes: *XIST* and *TSIX,* which are coding non-translated genes. *TSIX* gene is anti-sense mRNA transcript of *XIST* (Shibata et al., 2003; Takagi,

2003). In general terms, *XIST* is expressed from the inactive X and *TSIX* is expressed from the active X chromosome (Lee *et al.*, 2001).

In fact, the mechanism of X-chromosome inactivation is more complex. Once the *XIST* is expressed from one allele, *TSIX* is expressed from other allele at the same time. *TSIX* is the repressor of *XIST* (Lee *et al.*, 1999). Mouse-knock out studies reveal that *TSIX* disrupted mice express *XIST* and escape from X-inactivation (Lee *et al*., 1999). Therefore repression of *TSIX* leads an increase in the expression of *XIST.* Then the *XIST* mRNA coats the X allele in cis form (Clemson et al., 1996) and inactivates the allele via some modifications such as histone modifications, partially methylation of CpG islands, and action of trans-acting factors (Solari et al., 1974).

1.4.2 Genomic imprinting

Genomic imprinting is another epigenetic mechanism resulting in parent specific expression such that only one allele of a gene is expressed. Paternal imprinting means that the allele coming from father is modified to prevent transcription and maternal imprinting means that the allele coming from mother is transcriptionally repressed. In both conditions mono-allelic expression occurs (Surani, 1998).

DNA methylation on CpG dinucleotides is a key mechanism in imprinting (Costello-Plass, 2001). Genomic imprinting is heritable during cell divisions and reversible in gametogenesis (Gribnau *et al.*, 2003).

Two well known imprinted genes are *H19* and *IGF2*. *H19* gene is paternally imprinted and *IGF2* is maternally imprinted. DMR (Differentially Methylated Region) regulates the imprinting of both genes. DMR is methylated on the paternal chromosome and not methylated on the maternal chromosome (Croteau *et al.,* 2001).

The mechanism of imprinting in the *H19/IGF2* is more complex. *IGF2* expression depends on the CTCF (CCCTC-binding factor), which is a methylation sensitive insulator (Filippova *et al*., 1996). CTCF has binding sites on *H19* DMR and represses the expression of *IGF2* from maternal allele via DNA methylation (Schoenherr *et al*., 2003).
(Figure 1.5)

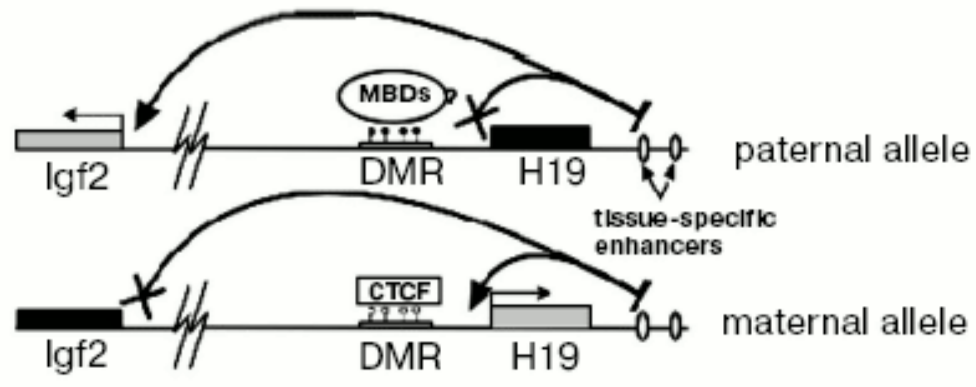

Figure 1.5 Schematic representation of *H19/IGF2* imprinting. White circles are non-methylated CpGs and black circles are methylated CpGs (Salozhin *et al*., 2005)

Errors in imprinting causes some defects such that errors in paternal imprinting can lead to an increase in cell growth and cell differentiation and errors in maternal imprinting can cause opposite effects (Leighton et al., 1995)

1.4.3 Association between epigenetic regulations and Rett syndrome

Epigenetic regulations via DNA methylation are associated with gene silencing. Transcriptional repression occurs in two ways: 1) DNA binding of transcription factors

on methyl-CpGs, 2) binding of proteins on methylated CpGs independent of their DNA sequences. These proteins include MeCP2, MBD1, MBD2, MBD4, and Kaiso (Bell *et al*., 2000; Hendrich *et al*., 1998; Prokhortchouk *et al*., 2001)

Defects in DNA methylation cause human diseases. Among the five genes, MeCP2 defects cause Rett syndrome exclusively in girls because *MECP2* is X-linked. Due to the random X-chromosome inactivation, RTT patients are mosaic for the mutant allele. Therefore, extremely skewed X-chromosome inactivation can lead to lethality or can prevent the disease (Villard *et al*., 2000).

Girls with Rett syndrome usually show random X-inactivation patterns. However, cases with skewed X-inactivation and milder phenotypes such as mild learning disabilities or incomplete diagnostic features have been reported (Amir *et al*., 2000; Wan *et al*., 1999).

Furthermore, Angelman syndrome, which is an imprinting disorder, shares some clinical similarities with Rett syndrome including developmental delay, language impairment, seizures, and stereotypic behaviors (Zoghbi, 2003). Angelman syndrome is defined by loss of imprinting in the maternal allele of chromosome 15q11-q13 due to the mutation of *UBE3A* (Lalande, 1996). Mice studies showed that *Mecp2* deficiency results in reduction of Ube3a and Gabrb3 in mice cerebrum without any change in allele specific expression (Moretti *et al*., 2005). The reduction in the expression levels of these genes in RTT patients confirmed the hypothesis (Samaco et al., 2005).

1.5 Targets of *MECP2* mediated repression

Biochemical evidences revealed that MeCP2 represses its target genes by binding to chromosomes, thus, defects in MeCP2 would result in deregulation of a large number of genes (Willard *et al*., 1999).

Investigators attempting to identify *MECP2* targets approached the subject in two ways: Global expression profile analysis and candidate gene analysis. To identify potential target genes regulated by MeCP2, Francke and colleagues looked for increased transcript levels in *MECP2* mutants. The differentially regulated genes identified as 49 with increased and 21 with decreased expression, leading to the conclusion that *MECP2* deficiency does not correlate with global deregulation of gene expression (Traynor *et al*., 2002). Subsequent experimental studies supported the proposal that *MECP2* deficiency does not lead to global alterations in transcription but instead leads to subtle changes of gene expression (Chen *et al*., 2003). Esteller and colleagues unveiled novel target genes of *MECP2*-mediated gene expression via cDNA microarray and ChIP analysis. They showed over-expressed X-linked genes in which the presence of methylation was highly likely because inactivation of one of the X chromosomes is mediated by methylation (Ballestar *et al*., 2004).

On the other hand, candidate gene analysis provided a different view on target gene search. Loss of imprinting in the maternally expressed *DLX5* gene in individuals with RTT provided a new mechanism underlying gene regulation by *MECP2* (Horike *et al*., 2005).

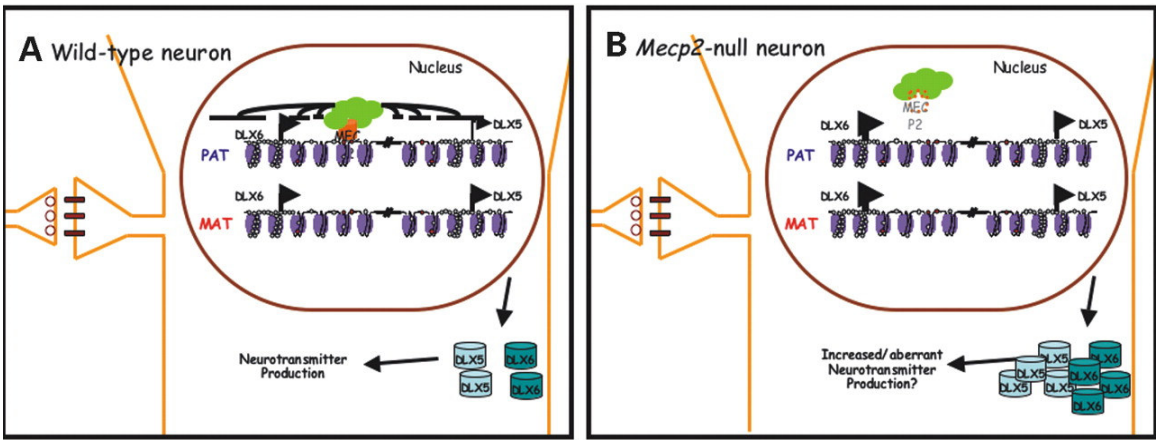

Figure 1.6 MeCP2 repression of *Dlx5* imprinted gene. A) In wild type neurons *Dlx5* is paternally imprinted via MeCP2 mediated repression by recruiting histone co-repressor complex. B) In Mecp2-null neurons *Dlx5* is biallelically expressed from both allele resulting in increased neurotransmitter production. (Cabellero *et al.*, 2005).

Another MeCP2 target gene identified by candidate gene approach is BDNF (Brain-derived Neurotrophic Factor) (Chen *et al*., 2003; Martinowich *et al*., 2003). MeCP2 deficiency in neuronal cells results in incomplete repression of *Bdnf* (Chen *et al*., 2003).

Table 1.4 Known MeCP2 target genes (Bienvenu *et al*., 2006)

Gene	Species	Function	Tissue in which gene is expressed	Change in expression level
BDNF	Mouse	Survival, neuronal plasticity	Cultured neurons	≈ +2-fold
hairy2	Xenopus	Neuronal differentiation	Whole embryo	≈ -2- fold
Fkbp5	Mouse	Hormonal signalling	Brain (74 days)	+2.26-fold
IGF2	Human	Cell proliferation	Lymphoblastoid cells	+2.21-fold
DLX5	Human	Transcription factor	Lymphoblastoid cells	≈ +2-fold
Dlx5	Mouse	Transcription factor	Brain	≈ +2-fold
Dlx6	Mouse	Transcription factor	Brain	≈ +2-fold
Ube3a	Mouse	Proteolysis	Brain	≈ -2-fold
UBE3A	Human	Proteolysis	Brain (2–20 years)	≈ -2-fold
Sgk1	Mouse	Cellular stress response	Brain (74 days)	+3.44-fold
MPP1	Human	Signal transduction	Lymphoblastoid cells	+3.32-fold

BDNF, brain-derived neurotrophic factor; DLX, distal-less homeobox; Fkbp5, FK506-binding protein 5; IGF2, insulin-like growth factor 2; MeCP2, methyl-CpG-binding protein 2; MPP1, palmitoylated membrane protein 1; Sgk1, serum/glucocorticoid kinase 1; Ube3a, ubiquitin protein ligase E3A.

1.6 Bioinformatics and algorithms

Bioinformatics can be defined as handling and processing the biological information via computers (Ouzounis *et al*., 2003). The birth of bioinformatic studies can be considered as the early 70s with the first sequence alignment algorithms (Gibbs *et al.,* 1970). One of the most important aspects of late 70s in terms of bioinformatics was collection of the biological information in computers for storage (Dayhoff, 1978). The collected data on computers were made available for the first time in the 80s and depending on that the first efficient algorithms and the theory of clustering were developed (Ouzounis *et al.*, 2003; Shepard *et al*., 1980).

In the early 90s, access to the Internet led to the formation of first databases such

as GenBank or MedLine and scientific tools such as BLAST (Ouzounis *et al.*, 2003).

Nowadays, with the advances in information technology such as large capacity storage, internet, and databases creates a revolution in bioinformatics (Soberon *et al.*, 2004).

The importance of analyzing sequences generated by molecular biology activities increased dramatically importance in recent years. In the algorithms of sequence analysis, the quantification of similarity is achieved by normalization and scoring which relies on aligning reference homologous sequences and then comparing them with the candidate alignments (Vinga *et al.*, 2003). Alignment and scoring is the more important aspects of the algorithms. In order to obtain optimal alignments dynamic programming or HMM (hidden markov model) which maximize the score, is used. Besides that BLAST and FASTA provides an experiment-based approach (Altschuletal *et al.*, 1997; Pearson *et al.*, 1988, Vinga *et al.*, 2003). On the other hand, scoring depends on the pair-wise alignments. There are several scoring systems such as PAM (amino acids substitution matrices) and BLOSUM matrices (Henikoff *et al.*, 1992; Dayhoff *et al.*, 1978; Vinga *et al.*, 2003).

MEME is a tool for discovering motifs among DNA or protein sequences which are related to each other. The sequence which occurs repeated among these DNA or protein sequences is called as motif. In the MEME tool motifs are extracted by a position dependent letter-probability matrix. The DNA or protein sequences, which are given as input in the MEME program, are called training sets. There are lots of expected outputs requested and MEME tool automatically aligns these motifs according to best width, description of each motif, and number of occurrence by statistical calculations. MEME firstly puts the most statistically significant motif in the first place. The most significant motif is the one which has the lowest *E*-value and the *E*-value is dependent on the motifs' log likelihood ratio, width and number of occurrences, the background

letter frequencies, and the size of the training set (http://meme.sdsc.edu/meme/meme-intro.html).

1.7 Aim and strategy

Mutations in *MECP2* (Xq28) was described in 1999 as a common cause of RTT. MeCP2 is a transcriptional repressor that regulates the expression pattern of many genes. It is not fully understood which MeCP2 targets are affected in RTT and therefore contribute to disease pathogenesis. Investigators approached the problem in two directions: a) Global expression profile analysis and b) Candidate gene analysis. Global expression profile analysis revealed that several genes including those on the X-chromosome are over-expressed in *MECP2* positive Rett patients (Traynor *et al*., 2002; Chen *et al*., 2003; Ballestar *et al*., 2004). Candidate gene analysis studies showed that loss of imprinting as exemplified by *DLX5* could also contribute to disease pathogenesis. Here modifications in silent-chromatin looping in *MECP2* mutants are strongly suspected (Horike *et al*., 2005). We hypothesize that X-chromosome inactivation (XCI) is an important physiological epigenetic mechanism that could be involved in Rett pathogenesis. Random XCI patterns in peripheral blood are characteristic for RTT that is caused by heterozygous *MECP2* mutations.

All in all, we expect to observe over-expression of X-linked genes which are transcribed exclusively from active X-chromosome and whose expression is controlled by MeCP2. These putative genes have the potential to contribute to RTT pathogenesis via disturbances in XCI.

We developed an algorithm which predicts potential MeCP2 targets on the X-chromosome and the entire genome. This algorithm is based on the identification of shared sequence motifs in known MeCP2 targets.

CHAPTER II. MATERIALS AND METHODS

2.1 MATERIALS

2.1.1 Patient samples

Rett syndrome patients were referred to Bilkent University, Faculty of Science, Department of Molecular Biology and Genetics (Ankara, Turkey) by collaborating physicians at Hacettepe University, Medical Faculty, Department of Pediatric Neurology (Ankara, Turkey). Blood samples were collected in EDTA containing tubes, with the consent forms signed by the parents of the patients.

2.1.2 Cell lines and cell culture reagents

Immortalized lymphoblastoid cell lines (LCLs) derived from three Rett patients with known *MECP2* mutations and one healthy individual were kindly supplied from Prof. Dr. Alessandra Renieri (University of Siena, Department of Molecular Biology, Medical Genetics Laboratory, Siena, Italy) (http://www.biobank.unisi.it/Elencorett.asp) (Table 2.1)

Table 2.1 Lymphoblastoid cell lines

LCL	Phenotype	Mutated Gene	Mutation Type	Nucleotide Change	AA Change
1195	Rett-Like	MECP2	missense	C316T	R106V
1198	Rett-Like	MECP2	missense	C397T	R133C
1211	Classic Rett	MECP2	late truncating	1162_1187del26	-
1213	Healthy	-	-	-	-

Table 2.2 Reagents used in the cell culture experiments

Reagents	Supplier
RPMI 1640 with L-Glutamine	Biological industries, Haemek, Israel
Fetal Bovine Serum	Sigma, St. Louis, MO, USA
Penicillin/streptomycin mixture	Biochrom AG, Berlin, Germany
L-Glutamine	Biochrom AG, Berlin, Germany
Tissue Culture Flasks	Costar Corp. (Cambridge, Englang)
Petri dishes	Costar Corp. (Cambridge, Englang)
15 ml polycarbonate centrifuge tubes with lids	Costar Corp. (Cambridge, Englang)
Cryotubes	Costar Corp. (Cambridge, Englang)
0.4% Trypan Blue Solution	Biochrom AG, Berlin, Germany

2.1.3 Oligonucletides

The oligonucleotides used in PCR and Real time RT-PCR were synthesized by IONTEK (Bursa, Turkey). The list of used primer sequences are given in tables below.

Table 2.3 Primers for mutation detection on MECP2 gene

Primer	Sequence (5'→3')	Primer Length	Gene Name	Expected Size (bp)
RTT3F	CCTGGTCTCAGTGTTCATTG	20	MECP2	597
RTT3R	CTGAGTGTATGATGGCCTGG	20		
RTT4.1F	TTTGTCAGAGCGTTGTCACC	20	MECP2	380
RTT4.1R	CTTCCCAGGACTTTTCTCCA	20		
RTT4.3F	GGCAGGAAGCGAAAAGCTGAG	21	MECP2	366
RTT4.3R	TGAGTGGTGGTGATGGTGGTGG	22		

Table 2.4 Primers for Real Time RT-PCR

Primer	Sequence (5'→3')	Primer Length	Gene Name	Expected Size (bp)
AFF2F	TCGGTAAATGAGGGAGACAC	20	AFF2	181
AFF2R	TAGAGGTGATGGTGGAAATGG	21		
PTCHD1F	AATTCCACCTTCCTGGGAGT	20	PTCHD1	165
PTCHD1R	GGCAGTGGTGAGAAAAGG	20		
HMGB3F	GTATGAGAAGGATGTTGCTG	20	HMGB3	102
HMGB3R	TCTTCATCTTCCTCTTCCAC	20		
FAM50AF	ATCATCCCTCACCATCACAG	20	FAM50A	135
FAM50AR	GGACTCATCCTTCTCCACAG	20		
RPS6KA3F	AAACTCCCAAAGATTCACCTG	21	RPS6KA3	154
RPS6KA3R	CTGTTCCTGTGTAACTGCTG	20		
SLC6A8F	TGGGAGAACAAAGTCTTGAG	20	SLC6A8	151
SLC6A8R	TGAAGTACACGATCTTTCCC	20		
RP11F	GTTCCCTGCTCTTCTATGAC	20	RP11-13E5.1	157
RP11R	CCAAAGTAGTTCACCCAGAC	20		
OTUD5F	AGGTACAAGCAGTCAGTTCTC	21	OTUD5	128
OTUD5R	AGTCATTCAGACCAAAGGCA	20		
TSPYL2F	GTCAAAGCATTCCTCAACCA	20	TSPYL2	105
TSPYL2R	ATGTCTGAGATCCTGTACCTG	21		
FHL1F	CATCACTGGGTTTGGTAAAGG	21	FHL1	165
FHL1R	GGACAATACACTTGCTCCTG	20		
MPP1F	ACCCTGTCCCATATACAACAC	21	MPP1	124
MPP1R	CTGCCAAACTCCAAGAACTC	20		
PGK1F	GTTCTTGAAGGACTGTGTAGG	21	PGK1	145
PGK1R	GGCTTTAACCTTGTTCCCAG	20		

Table 2.5 Primers for X-chromosome inactivation status determination

Primer	Sequence (5'→3')	Primer Length	Gene Name	Expected Size (bp)
RS-6	GTCCAAGACCTACCGAGGAG	20	AR	280
RS-7	CCAGGACCAGGTAGGCTGTG	20		

2.1.4 Chemicals and reagents

Table 2.6 Chemicals, reagents, and kits used in the experiments

Reagent	Supplier	Used for
Acrylamide	Sigma, St. Louis, MO, USA	Polyacrylamide Gel Electrophoresis
Agarose	Basica LE, EU	Agarose Gel electrophoresis
Bisacrylamide	Sigma, St. Louis, MO, USA	Polyacrylamide Gel Electrophoresis
Bromophenol Blue	Sigma, St. Louis, MO, USA	Gel Electrophoresis
Ethanol	Merck, Frankfurt, Germany	
Ethidium Bromide	Sigma, St. Louis, MO, USA	Gel Electrophoresis
Proteinase K	Appligene-Oncor, USA	Nucleic Acid Extraction
TEMED	Carlo Erba, Milano, Italy	Polyacrylamide Gel Electrophoresis
RNAse ZAP	Ambion, Inc., USA	RNA Extraction
pUC Mix Marker, 8	MBI Fermentas, Amh, NY, USA	Gel Electrophoresis
RevertAid™ cDNA Synthesis Kit	MBI Fermentas, Amh, NY, USA	cDNA Synthesis
DNeasy Tissue Kit	Qiagen, Chatsworth, CA, USA	DNA isolation
BSA	Promega, Madison, USA	Enzymatic Digestion
Sodium Chloride (NaCl)	Sigma, St. Louis, MO, USA	PBS
Sodium Acetate	Sigma, St. Louis, MO, USA	PBS
Tris-HCl	Sigma, St. Louis, MO, USA	Agarose Gel
Ficoll Type 400	Sigma, St. Louis, MO, USA	Agarose Gel Loading Buffer
Boric Acid	Sigma, St. Louis, MO, USA	TBE
Xylene Cyanol	Sigma, St. Louis, MO, USA	Agarose Gel Loading Buffer
APS	Carlo Erba, Milano, Italy	Polyacrylamide Gel Electrophoresis
EDTA pH 8.0	Carlo Erba, Milano, Italy	TAE, TBE
Tris	BioRad, CA, USA	TBE
Nucleospin® Blood kit	Macherey-Nagel Inc., PA, USA	DNA isolation

2.1.5 Restriction enzymes

Table 2.7 Restriction enzymes used in the mutation detection experiments

Enzyme Name	Supplier	Recognition Site	Buffer (1X)
Hsp92 II (NlaIII)	Promega, Madison, USA	5'-CATG↓-3' 3'-↑GTAC-5'	NE Buffer 4 50 mM Potassium acetate 20 mM Tris acetate 10 mM Magnesium acetate 1 mM DTT
BspLI (NlaIV)	Fermentas, Amh, NY, USA	5'-GGN↓NCC-3' 3'-CCN↑NGG-5'	Buffer Y^+/Tango™ 66 mM Potassium acetate 33 mM Tris acetate 10 mM Magnesium acetate 0.1 mg/ml BSA
HphI	Fermentas, Amh, NY, USA	5'-GGTGA$(N)_8$↓-3' 3'-CCACT$(N)_7$↑-5'	Buffer B^+ 10 mM Tris-HCl 10 mM $MgCl_2$ 0.1 mg/ml BSA
HinfI	Fermentas, Amh, NY, USA	5'-G↓ANTC-3' 3'-CTNA↑A-5'	Buffer Y^+/Tango™ 66 mM Potassium acetate 33 mM Tris acetate 10 mM Magnesium acetate 0.1 mg/ml BSA
Hin61 (HhaI)	Fermentas, Amh, NY, USA	5'-G↓CGC-3' 3'-CGC↑G-5'	Buffer Y^+/Tango™ 66 mM Potassium acetate 33 mM Tris acetate 10 mM Magnesium acetate 0.1 mg/ml BSA

Table 2.8 Restriction enzymes used in the X-inactivation determination

Enzyme Name	Supplier	Recognition Site	Buffer (1X)
HpaII	Fermentas, Amh, NY, USA	5'-C↓CGG-3' 3'-GGC↑C-5'	Buffer Y^+/Tango™ 66 mM Potassium acetate 33 mM Tris acetate 10 mM Magnesium acetate 0.1 mg/ml BSA
RsaI	Fermentas, Amh, NY, USA	5'-GT↓AC-3' 3'-CA↑TG-5'	Buffer Y^+/Tango™ 66 mM Potassium acetate 33 mM Tris acetate 10 mM Magnesium acetate 0.1 mg/ml BSA

2.1.6 Polymerase chain reaction materials

Three kinds of thermal cycler were used for PCR reactions: The GeneAmp System 9600 (Perkin-Elmer, USA), DNA Engine Tetrat, PTC-225 (MJ Research Inc., MA, USA), and Mastercycler Eppendorf Scientific, Inc. (NY, USA). PCR reaction kits were supplied from MBI Fermentas Inc. (Amherst, NY, USA). The kit contains the following reagents

Table 2.9 PCR kit reagents

Reagent	Concentrations
Thermus Aquaticus DNA Polymerase	5U/µl
10X PCR Buffer	100 mM Tris-HCl (ph 8.8 at 25°C) 500 mM KCl 0.8% Nonidet P40
$MgCl_2$ Solution	25 mM
dNTP mix	10 µM dCTP, dGTP, dATP, dTTP

2.1.7 Electrophoresis marker

PUC mix, 8 was used as DNA marker in both agarose and polyacrylamide gel electrophoresis. It is supplied with 2 ml 6X Loading Dye solution. The sizes of the fragments and their appearance on 1.7% agarose gel and 5% polyacrylamide gel are given in figure 2.1.

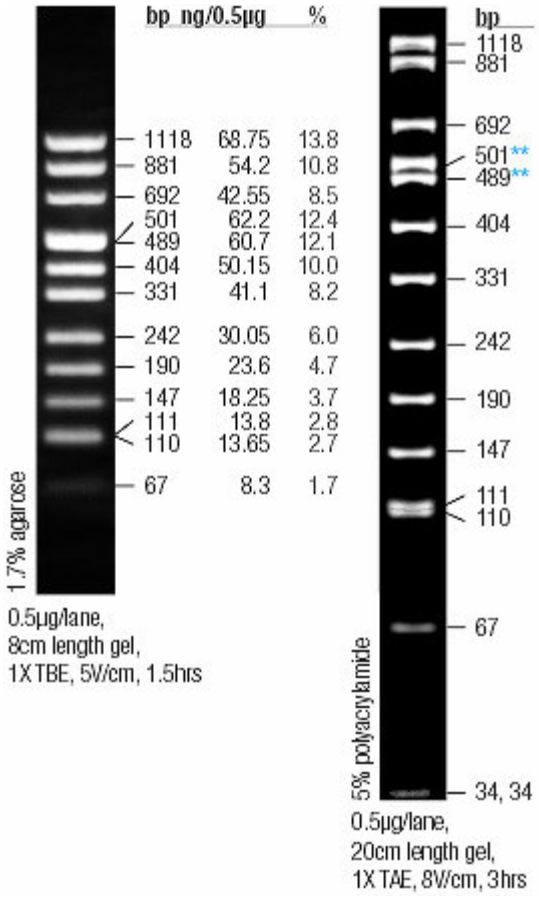

Figure 2.1 Sizes of the fragments of PUC mix marker, 8 and appearance on both agarose and polyacylamide gel electrophoresis (MBI Fermentas web site)

2.1.8 Real Time RT-PCR materials

The iCycler used for Real time RT-PCR was from BioRad (CA, USA). Real time RT-PCR kit was obtained from Qiagen (Chatsworth, CA, USA). The kit contains LightCycler-DNA Master SYBR Green I (Roche, Molecular Biochemicals, Germany) reagent.

2.1.9 Solutions and buffers

Table 2.10 Standard solutions and buffers used in the experiments

Reagents	Concentrations
1X TBE (Tris-Boric Acid-EDTA)	89 mM Tris-base 89 mM boric acid 2 mM EDTA pH 8.3
Ethidium Bromide	10 mg/ml in water (stock solution) 30 ng/ml (working solution)
Agarose Gel Loading Buffer (6X)	15% ficoll 0.05% bromophenol 0.05% xylene cyanol
Acrylamide:Biacrylamide Stock Solution (%30)	29.5 gr acrylamide 0.44 gr bisacrylamide 100 ml with ddH_2O
1X TAE (Tris-Acetic Acid-EDTA)	40 nm Tris-Acetate 2 mM EDTA pH 8.0

2.2 METHODS

2.2.1 Mutation detection of Rett patients

2.2.1.1 DNA isolation from blood samples

Blood samples have been reached us in tubes containing EDTA, and they were divided into 1 ml aliquots in 1.5 ml eppendorf tubes. The DNA isolation was carried out from 200 µl bloods via Nucleospin® Blood kit (Macherey-Nagel Inc., PA, USA) according to manufacturer's instructions. The remaining bloods were stored at -80°C for later use.

The concentration of the DNA was checked by spectrophotometric reading and horizontal 1% agarose gel electrophoresis in 1X TBE or TAE buffer. The DNA samples were loaded on gel after mixed with 6X loading buffer. 1 µg/ml ethidium bromide was added in agarose gel and the gel was run in electrophoresis buffer (1X TBE or 1X TAE) at different voltages and time depending on the size of the gels. After the run, the DNA samples were visualized with UV transilluminator.

2.2.1.2 Polymerase chain reaction (PCR)

PCR reaction carried out to amplify the 3 different fragments on 2 different exons of *MECP2*: Exon1 (Primer: RTT3F and RTT3R), exon4.1 (Primers: RTT4.1F and RTT4.1R), and exon4.3 (Primers: RTT4.3F and RTT4.3R). The cocktail and the conditions are given in Table 2.11 and Figure 2.2, 2.3, 2.4.

Table 2.11 PCR cocktail for mutation detection

Reaction Ingredients	Volume
DNA (100-150 ng)	3 µl
Mg Buffer (10X)	2.5 µl
$MgCl_2$ solution (1.5 mM)	1.5 µl
Forward Primer (20 pmol)	0.5 µl
Reverse Primer (20 pmol)	0.5 µl
dNTP (10 mM)	0.5 µl
Taq Polymerase (1.25 U)	0.25 µl
ddH_2O	16.25 µl
Total	**25 µl**

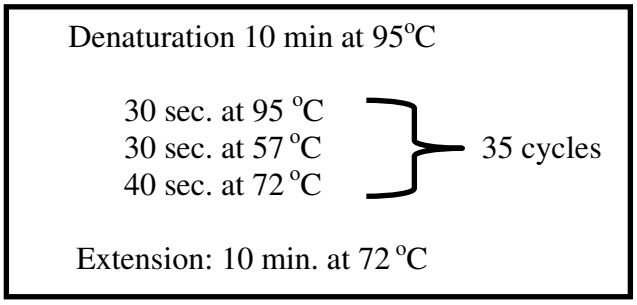

Figure 2.2 PCR conditions for RTT 3F/3R primers

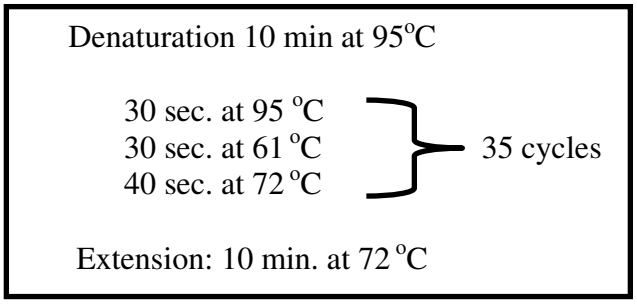

Figure 2.3 PCR conditions for RTT 4.1F/4.1R primers

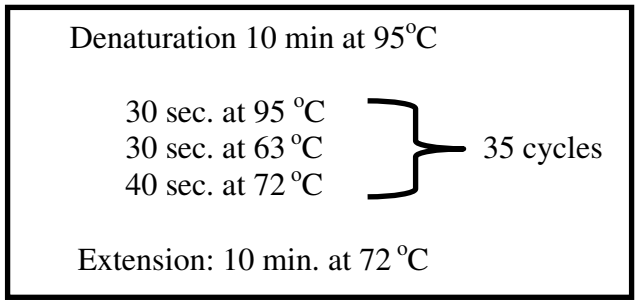

Figure 2.4 PCR conditions for RTT 4.3F/4.1R Primers

2.2.1.3 Restriction enzyme digestions

Restriction enzyme digestion of PCR products were performed in 20 µl reaction volumes in 500 µl tubes. The amount of PCR products needed for digestion determined by 2% agarose gel electrophoresis before the reaction. Reactions were carried out using the conditions and materials (reaction buffer and BSA) given in the manufacturer's instructions. One unit of enzyme was used for each reaction.

The digestion reactions were incubated at 37°C in the water bath overnight. Restriction enzymes, mutations, and expected product sizes after digestion are given below.

Reaction 1: MECP2 exon 3

RE 1: *Nla*III. For R106W
Uncut amplicon: 597 bp
Mutant profile: 152 bp, 141 bp, 121 bp, 67 bp, 50 bp, 35 bp, 31 bp
Normal profile: 156 bp, 152 bp, 141 bp, 67 bp, 50 bp, 31 bp

Reaction 2: MECP2 exon 4.1

RE 2: *Nla*IV. For P152R
Uncut amplicon: 380 bp
Mutant profile: 213 bp, 95 bp, 49 bp, 23 bp
Normal profile: 175 bp, 95 bp, 49 bp, 38 bp, 23 bp

RE 3: *Hinf*I. For T197M
Uncut amplicon: 380 bp
Mutant profile: 197 bp, 183 bp
Normal profile: 380 bp

RE 4: *Nla*III. For T158M
Uncut amplicon: 380 bp
Mutant profile: 197 bp, 183 bp
Normal profile: 380 bp

RE 5: *Hph*I. For R168X
Uncut amplicon: 380 bp
Mutant profile: 235 bp, 123 bp, 22 bp
Normal profile: 358 bp, 22 bp

Reaction 3: MECP2 exon 4.3

RE 6: *Nla*IV. For R270X & V288X
Uncut amplicon: 366 bp
Mutant profile: 366 bp
Normal profile: 314 bp, 52 bp

RE 7: *Hha*I. For R306C
Uncut amplicon: 366 bp
Mutant profile: 308 bp, 47 bp, 11 bp
Normal profile: 164 bp, 144 bp, 47 bp, 11 bp

2.2.1.4 Agarose and polyacrylamide gel electrophoresis

Based on the recurrent mutation detection protocol on page 33, the digested samples RE2 (*Nla*IV), RE3 (*Hinf*I), RE4 (*Nla*III), RE5 (*Hph*I), RE6 (*Nla*IV), and RE7 (*Hha*I) were loaded in 3% agarose gel (3 g agarose, 1X TAE, and 3 µl Ethidium Bromide). The digests were mixed with 5 µl 6X loading buffer and then loaded on the gel. The gel was run in 1X TAE buffer at different voltages and time depending on the size of the gels. After the run, the DNA samples were visualized with UV transilluminator.

The digested sample RE1 (*Nla*III) was loaded in 6% polyacrylamide gel (12 ml acrylamide: bisacrylamide (29:1) solution, 6 ml 10X TBE buffer, 38 ml ddH_2O, 40 µl TEMED, and 500 µl 10X APS) in order to detect the fragments with small differences in length. The polyacrylamide solution was poured into the vertical apparatus and the digests was run at constant 20W for 3 hours in 1X TBE buffer. After the run the gel was put into ethidium bromide staining solution for 10 minutes, and then into ddH_2O washing for 10 minutes. The digests were visualized with UV transilluminator.

2.2.2 *MECP2* target gene search via bioinformatics analysis

Shigematsu and colleagues defined in vivo binding sequences of MECP2 by sequencing 100 Mecp2-binding sites (MBSs). Among these binding sequences, they mapped 33 genes located within 100 kb region on either side of each unique MBSs. 24 genes out of 33 were known to have a role in neurogenesis, muscle and skeletal development (Horike et al., 2005).

By using the human homolog promoters (-2000, +400) of these genes (Appendix B) we defined a motif via MEME program (http://meme.sdsc.edu/meme/intro.html) (Figure 2.5 and Figure 2.6)

MEME gives all the possible motifs; therefore, in order to select the right motif, several criteria were being taken into account:

1. The sequence of the motif should be C-G rich.
2. The length of the motif should be between 40-70 bases.
3. Motif should not be searched by one per sequence to lower blurriness. Instead, zero or one per sequence should be selected.
4. Higher number of reference sequences is desired for a good motif.
5. E-value should be smaller.
6. Distribution of these motifs over sequences is also important such that more compact regions would mean functional roles in transcription (Timothy et al. 1994)

Motif extracted over -2000 +400 promoters:
CCGCCCGCGCGGCCGCGGCCGCCGCCGCCGCCGCCGCCGCCCCCGCCG
CCCC (55 bp, 100% C-G rich sequence)

At first, our motif was aligned over -600 +400 promoters of human X-chromosome (1107 genes) according to the Jaligner algorithms (http://jaligner.sourceforge.net/). Jaligner uses an open source Java implementation of the Smith-Waterman algorithm with Gotoh's improvement for biological local pair-wise sequence alignment using the affine gap penalty model. According to Jaligner algorithms gap open penalty was selected as 25, and gap extension penalty was selected as 2. Then, our motif was aligned over -600 +400 promoters of human genome (32649 reference sequences and 24017 genes) by the same procedure.

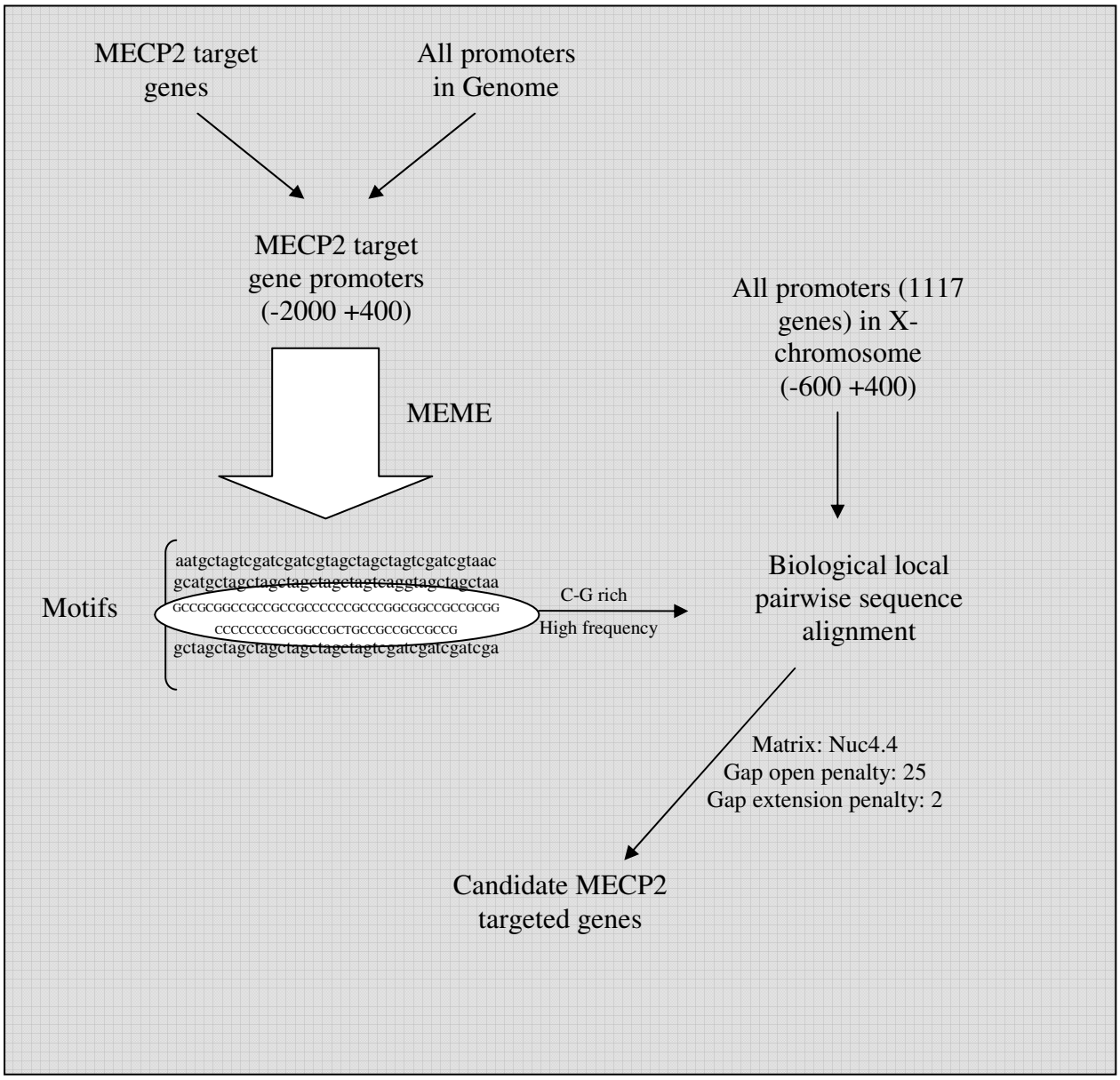

Figure 2.5 Schematic Representation of *MECP2* target gene search on X chromosomes via bioinformatic analysis.

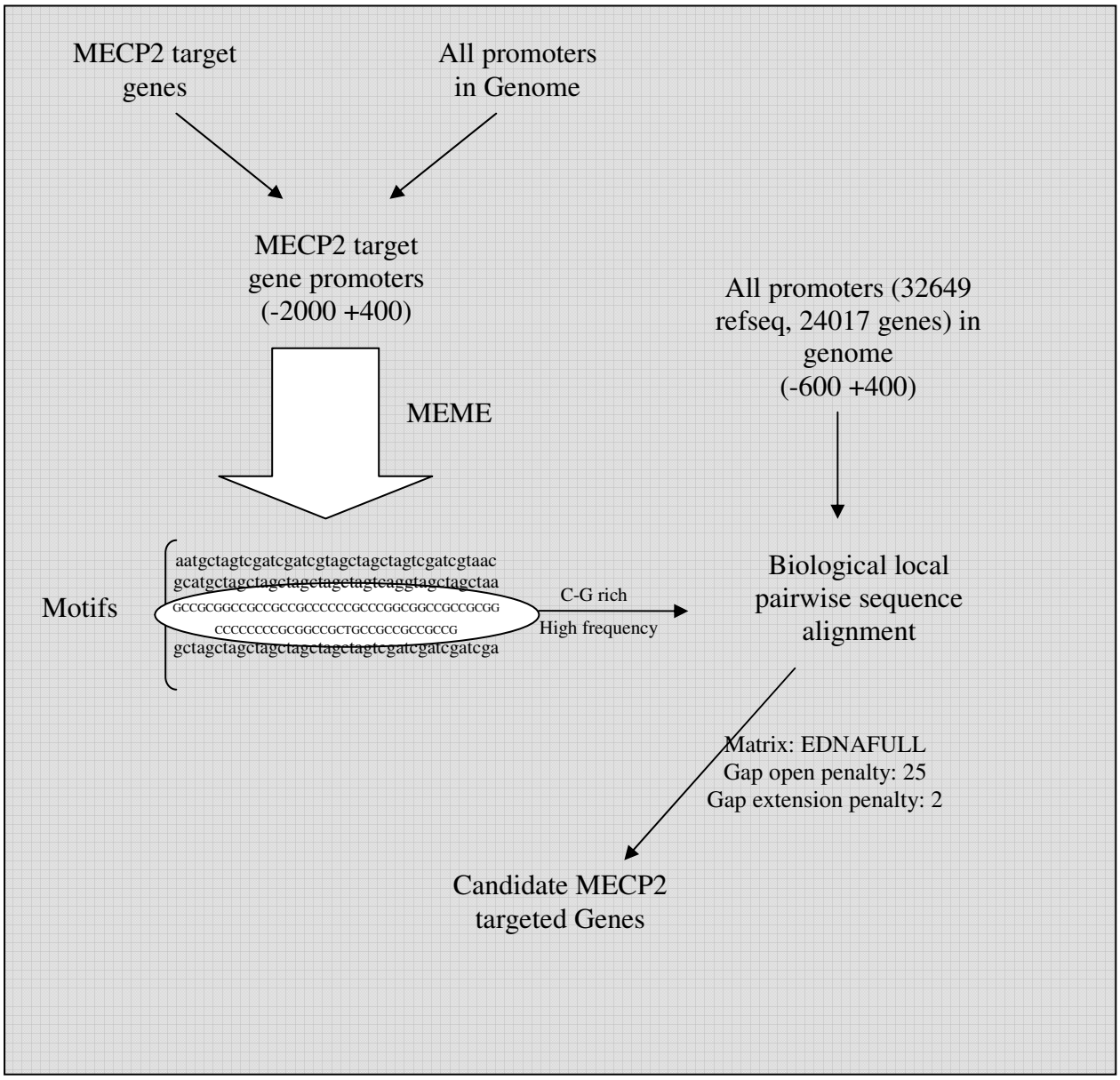

Figure 2.6 Schematic representation of *MECP2* target gene search on human genome via bioinformatic analysis

2.2.3 Cell culture techniques

2.2.3.1 Establishment of lymphoblastoid cell lines

Lymphoblastoid cell lines (LCLs) obtained from Siena University laboratories were established by Epstein-Bar Virus transformation of peripheral blood cells from patients with known *MECP2* mutations and from healthy individuals.

2.2.3.2 Culturing and subculturing of lymphoblastoid cell lines

Human lymphoblastoid cell lines are usually cultured in RPMI-1640 medium containing 10% fetal calf serum and they grow in suspension. EBV transformed cell lines grow in clumps (Sigma catalog, commonly used tissue culture techniques, 1988).

Suspension LCLs were cultured into RPMI-1640 medium with L-glutamine. Medium was supplied with 10% fetal calf serum. Before culturing the cell lines 5 ml (1%) L-Glutamine, 5 ml (1%) penicillin/streptomycin were added into the medium. The cells were cultured into T25 tissue culture flask with 15 ml medium. The flasks were incubated at 37^{o}C under 5% carbon dioxide in upright position. Lymphoblastoid cell lines were either subcultured or refed with fresh medium in every 5 to 7 days. The subculturing the cells the clumps should bring into single cell suspension by pipetting or mixing.

2.2.3.3 Cell counting

The cells were counted before storage because too high or too low cell count lowers the recovery viability. Cell counting can be used for different kinds of operations on cell cultures such as transfections, cell fusions, cryopreservation, and subculturing. Optimum number of cells is necessary for optimum growth and it will help to

standardize other techniques. (Cryomed Technical Manual for Model 700 Preprogrammed Freezing Controller, 1985)

In order to count the cells, the cell suspension centrifuged and resuspend with a fresh medium in a small volume. The clumps were broken up by pipetting or mixing. 200 µl of cell suspension was mixed with the same amount of Trypan Blue. A cover-slip was attached on the haemocytometer by moistening with the breath. Both sides of the chamber were filled with the mixture. The bright cells (non-viable cells were stained blue) were counted under microscope. The concentrations of the cells were counted by the formula:

Number of viable cells = Mean number of viable cells counted x Dilution factor x correction factor x Total volume of the suspension

2.2.3.4 Cryopreservation of cell lines

Cryopreservations of the cell cultures are the most reliable and reproducible way to freeze cells. Freezing media contained 70% RPMI-1640, 20% Fetal Calf Serum, 10% DMSO. DMSO (dimethyl sulphoxide) is used as a cryoprotectant.

One day before freezing the cells the medim of the cell suspension were changed. The cells were centrifuged at 5000 rpm for 5 minutes and the cell pellet was resuspend at a concentration of $4x10^6$ to $9x10^6$ cells per ml in freezing medium. 1 ml of aliquots were added to each cyroprotective ampules. The ampules were put in $+4^oC$ freezer for one hour, -20^oC freezer for 4 hours, and then put into -80^oC freezer overnight, respectively. Lastly they were put into liquid nitrogen storage vessel for long term preservation.

2.2.4 Determination of X-chromosome inactivation statuses of cell lines

2.2.4.1 DNA isolation from cell lines

Cells were counted as previously described before DNA isolation. The DNA isolation was carried out from up to $5x10^6$ cells via DNeasy® Tissue Kit (Qiagen, Chatsworth, CA, USA) according to manufacturer's instructions. The isolated DNAs were stored at $+4^oC$ for later applications.

The concentration of the DNA was checked by horizontal 2% agarose gel electrophoresis in TAE buffer. The DNA samples were loaded on gel after mixed with 6X loading buffer. 1 µg/ml ethidium bromide was added in agarose gel and the gel was run in 1X TAE buffer. After the run, the DNA samples were visualized with UV transilluminator.

2.2.4.2 Restriction enzyme digestions

Restriction enzyme digestion was carried out from 1 µl genomic DNA isolated from the cells in 20 µl reaction volumes in 500 µl tubes. Methylation specific *Hpa*II and *Rsa*I enzymes were used for determination of X-inactivation statuses. The uncut control samples were only digested with *Rsa*I enzyme using the conditions and materials (reaction buffer and BSA) given in the manufacturer's instructions. One unit from each enzyme was used for the reaction. The digestion reactions were incubated at 37^oC in the water bath overnight.

2.2.4.3 Polymerase chain reaction (PCR)

PCR reaction carried out to amplify 280 bp region in the exon1 of Androgen

Receptor (AR) gene (Primers: RS6 and RS7). The cocktail and the conditions are given in Table 2.12 and Figure 2.7.

Table 2.12 PCR cocktail for X-chromosome inactivation detection

Reaction Ingredients	Volume
DNA (100-150 ng)	3 µl
Mg Buffer (10X)	2.5 µl
$MgCl_2$ solution (1.5 mM)	1 µl
Forward Primer (20 pmol)	0.5 µl
Reverse Primer (20 pmol)	0.5 µl
dNTP (10 mM)	0.5 µl
Taq Polymerase (1.25 U)	0.25 µl
ddH_2O	16.75 µl
Total	**25 µl**

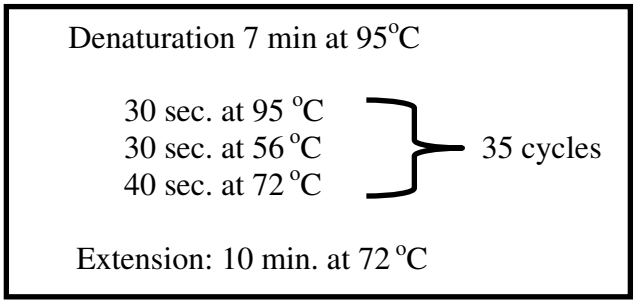

Figure 2.7 PCR conditions for *AR* RS6/7 primers

2.2.4.4 Polyacrylamide gel electrophoresis

The PCR products were loaded in 10% polyacrylamide gel (20 ml acrylamide: bisacrylamide (29: 1) solution, 6 ml 10X TBE buffer, 34 ml ddH_2O, 40 µl TEMED, and 500 µl 10X APS). The polyacrylamide solution was poured into the vertical apparatus and the digests was run at constant 20W for 5 hours in 1X TBE buffer. After the run the

gel was put into ethidium bromide staining solution for 10 minutes, and then into ddH_2O washing for 10 minutes. The digests were visualized by UV transilluminator.

2.2.5 Construction of cDNA library from the cell lines

2.2.5.1 RNA isolation from cell lines

Cells were counted as previously described before RNA isolation. The DNA isolation was carried out from up to $5x10^6$ cells via NucleoSpin® RNA II Kit (Macherey Nagel, Inc., PA, USA) according to manufacturer's instructions. The isolated RNAs were stored at -80°C for later applications.

The concentrations and purities of the total RNAs were checked by spectrophotometer (Beckman Instruments Du640, Inc. CA, USA).

2.2.5.2 cDNA synthesis from RNAs

cDNA synthesis was carried out via RevertAid™ First Strand cDNA Synthesis Kit (MBI Fermentas, Amh, NY, USA) from 2 µg RNA according to manufacturer's instructions.

2.2.5.3 Polymerase chain reaction (PCR)

PCR reaction carried out from cDNAs of LCL1195 to amplify AFF2 (181 bp), PTCHD1 (165 bp), HMGB3 (102 bp), FAM50A (135 bp), RPS6KA3 (154 bp), SLC6A8F (151 bp), RP11-13E5.1 (157 bp), OTUD5 (128 bp), TSPYL2 (105 bp), FHL1 (165 bp), MPP1 (124 bp), PGK1 (145 bp). After PCR the products were loaded in 2% agarose gel (2 g agarose, 1X TAE, and 3 µl Ethidium Bromide) to check optimization of the primers. The cocktail and the conditions are given in table 13 and figure 6.

Table 2.13 PCR cocktail for candidate MeCP2 target gene primers

Reaction Ingredients	Volume
cDNA (100 ng)	1 µl
Mg Buffer (10X)	2.5 µl
$MgCl_2$ solution (1.5 mM)	1,5 µl
Forward Primer (20 pmol)	0.5 µl
Reverse Primer (20 pmol)	0.5 µl
dNTP (10 mM)	0.5 µl
Taq Polymerase (1.25 U)	0.25 µl
ddH_2O	18.25 µl
Total	**25 µl**

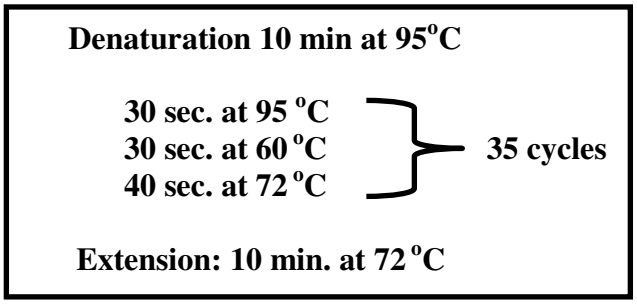

Figure 2.8 PCR conditions for MeCP2 target gene primers

2.2.6 Real Time RT-PCR

The real time RT-PCR assays were carried out with iCycler instrument (BioRad, CA, USA) using LightCycler-DNA Master SYBR Green I (Roche, Molecular Biochemicals, Germany) from cDNAs of the LCLs. The cocktail and the conditions were given in table 14 and figure 7.

Table 2.14 Real Time RT-PCR cocktail for candidate MeCP2 target gene primers

Reaction Ingredients	Volume
cDNA (100 ng)	1 µl
SYBR Green I Master Mix	12,5
Forward Primer (20 pmol)	0.25 µl
Reverse Primer (20 pmol)	0.25 µl
Nuclease free ddH_2O	11 µl
Mineral Oil	25 µl
Total	**50 µl**

Cycle 1:(1X)
Step 1: 95.0ºC for 10:00
Cycle 2:(50X)
Step 1: 95.0ºC for 00:30
Step 2: 60.0ºC for 00:30
Step 3: 72.0ºC for 00:30
Data collection enabled.
Cycle 3:(1X)
Step 1: 72.0ºC for 10:00
Step 2: 95.0ºC for 00:30
Cycle 4:(1X)
Step 1: 55.0ºC for 00:30
Cycle 5:(80X)
Step 1: 55.0ºC for 00:15
Increase setpoint temperature after cycle 2 by 0.5ºC
Melt curve data collection and analysis enabled.
Cycle 6:(1X)
Step 1: 4.0ºC HOLD

Figure 2.9 Real Time RT-PCR conditions for candidate MeCP2 target gene primers

The amounts of the cDNAs of the LCLs were equalized against *GAPDH*. Each of the primers was normalized by diluting cDNAs form 1 µl to 10^{-4} µl. Relative expression levels were calculated according to the formula:

$$\text{Expression change} = n^{-(\Delta CT\ \text{patient} - \Delta CT\ \text{control})}$$

Where; n is the normalization number (depends on the efficiency of the primers), C_T is the threshold cycle for each cell line, and ΔC_T represents the difference between the candidate *MECP2* target genes and *GAPDH* threshold cycles.

CHAPTER III. RESULTS

3.1 Mutation spectrum of *MECP2* in Rett patients

In order to provide a mutation spectrum of Rett patients, eight recurrent mutations shown in Table 3.1 and Figure 3.1 were screened in 235 patients. The mutations were selected according to their incidence rates and frequencies given in Appendix A.

Table 3.1 Selected *MECP2* mutations

Exon	Amino Acid Change	Nucleotide Change	Mutation Type	Domain	Restriction Enzyme
3	R106W	316 C→T	Missense	MBD	NlaIII
4.1	P152R	455 C→G	Missense	MBD	NlaIV
4.1	T158M	473 C→T	Missense	MBD	NlaIII
4.1	R168X	502 C→T	Nonsense	IDR	HphI
4.1	F155S	590 C→T	Missense	IDR	HinfI
4.3	V288X	806 delG	Nonsense	TRD	NlaIV
4.3	R270X	808 C→T	Nonsense	TRD	NlaIV
4.3	R306C	916 C→T	Missense	TRD	HhaI

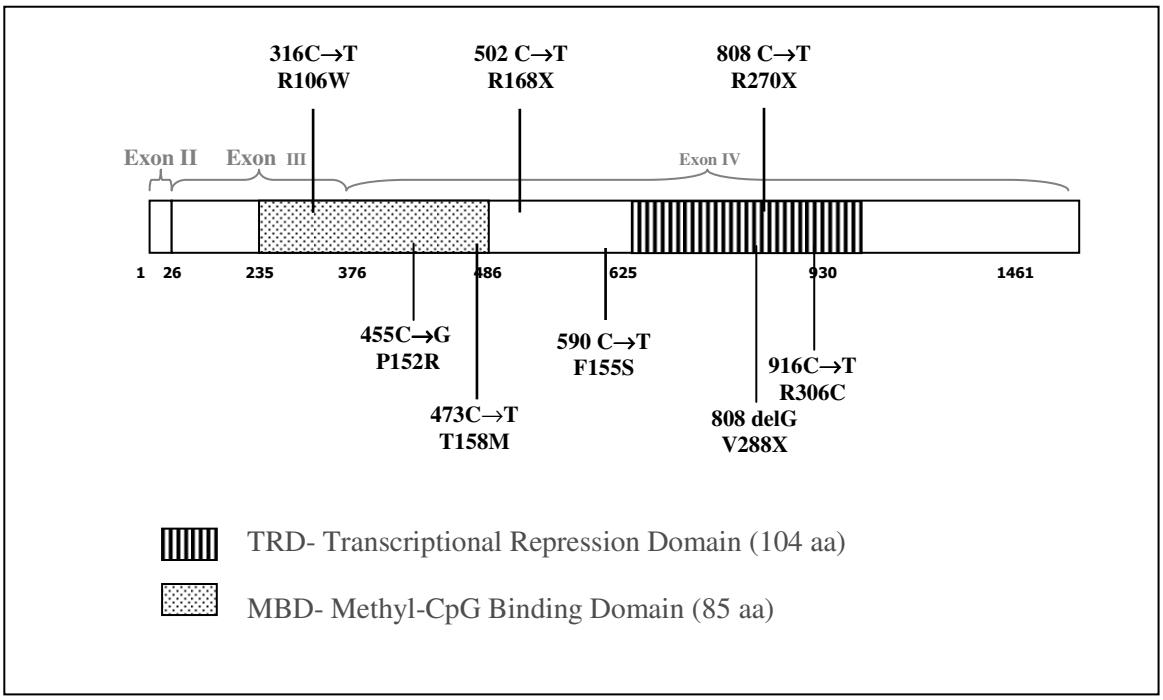

Figure 3.1 Selected *MECP2* mutations

The genomic DNAs isolated from the peripheral bloods of the patients were evaluated quantitatively by agarose gel. The PCR reactions with exon 3, exon 4.1, and exon 4.3 primers from the genomic DNAs were analyzed by agarose gel electrophoresis. The expected size of the PCR products were: 597 bp (exon 3 primer), 380 bp (exon 4.1 primer), and 366 bp (exon 4.3 primer).

The restriction enzyme digestion was carried out as explained in the methods part. The digestion enzymes and expected product sizes after digestion is given in the materials part. The pictures of the enzymatic digestions visualized by transilluminator are given in Figure 3.2.

A

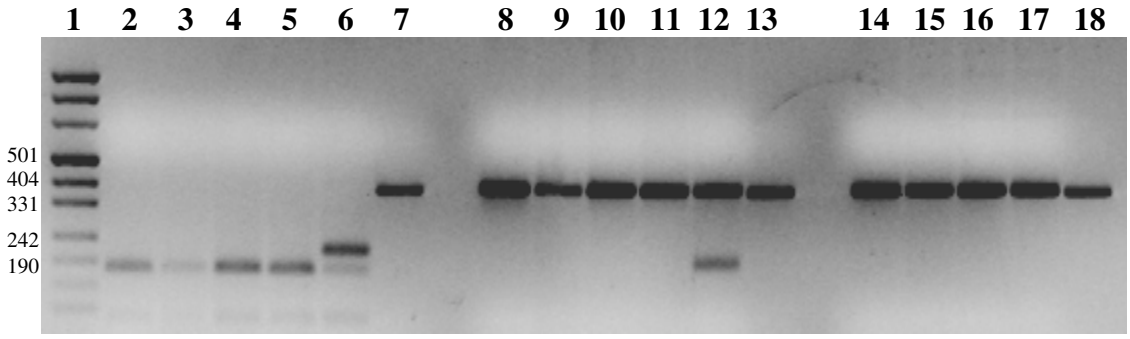
1 2 3 4 5 6 7 8 9 10 11 12 13 14 15 16 17 18
501
404
331
242
190

B

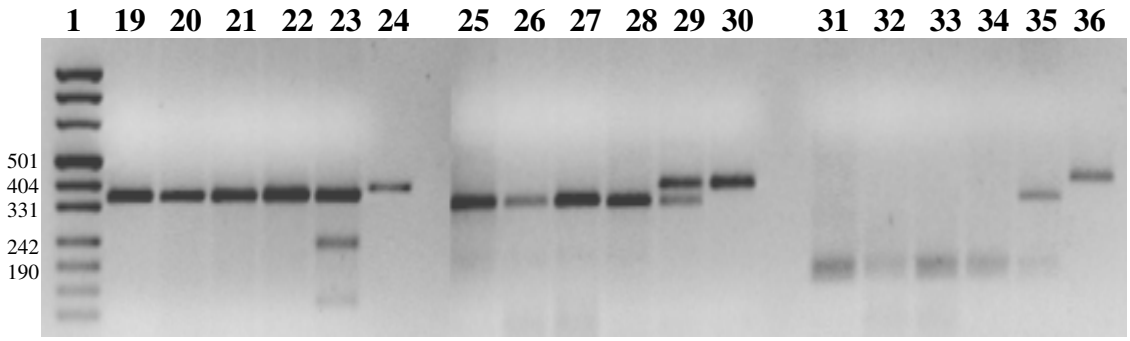
1 19 20 21 22 23 24 25 26 27 28 29 30 31 32 33 34 35 36
501
404
331
242
190

C

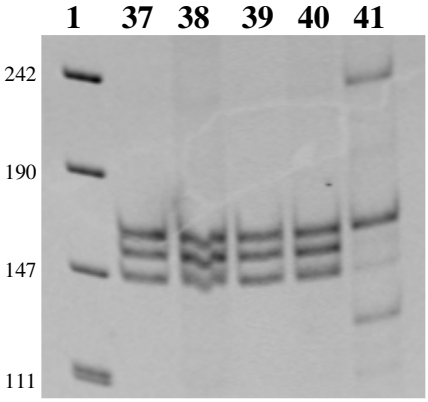
1 37 38 39 40 41
242
190
147
111

Figure 3.2 Mutation detection via enzymatic digestion. *MECP2* mutation detections of the RTT patients at 3% agarose gel electrophoresis (A,B) and 8% polyaccrylamide agarose gel (C). Lane 1s: pUC mix marker, 8. 20 µl digest + 5 µl 6x loading buffer were loaded on gels. A) Lanes 2-7: NlaIV restriction, lane 6: Patient 00-133 with P152R mutation, lane 7: Uncut sample. Lanes 8-13: NlaIII restriction, lane 12: Patient 00-188 with T158M mutation, lane 13: Uncut digest. Lanes 14-18: HinfI restriction, no patients with F155S mutation detected, lane 18: Uncut digest. B) Lanes 19-24: HphI restriction, lane 23: Patient 00-381 with R168X mutation, lane 24: Uncut sample. Lanes 25-30: NlaIV restriction, lane 29: Patient 00-104 with R270X mutation, lane 30: Uncut digest. Lanes 31-36: Hin61 restriction, lane 35: Patient 02-28 with R306C mutation, lane 36: Uncut digest. C) Lanes 37-41: NlaIII restriction, lane 41: Patient 99-91 with R106W mutation.

Analysis of the eight recurrent MECP2 mutations in 235 patients revealed a mutation n 48 patients. The frequencies of the mutations are given in Table 3.2.

Table 3.2 *MECP2* mutation spectrum in Rett patients

Exon	Amino Acid Change	Nucleotide Change	Number observed
3	R106W	316 C→T	5/235
4.1	P152R	455 C→G	5/235
4.1	T158M	473 C→T	13/235
4.1	R168X	502 C→T	6/235
4.1	F155S	590 C→T	0/235
4.3	V288X	806 delG	4/235
4.3	R270X	808 C→T	8/235
4.3	R306C	916 C→T	7/235

3.2 X-chromosome inactivation profile in cell lines

In order to determine the X-chromosome inactivation patterns in the cell lines, the androgen receptor assay was performed as explained in the methods section. Androgen receptor assay depends on the methylation of the inactive X-chromosome. Methylated inactive X-chromosome is resistant to methylation specific HpaII enzyme but unmethylated X-chromosome can be digested. A highly polymorphic triplet repeat adjacent to the methylation site in the androgen receptor provides difference in lengths of the alleles. The concentration difference of more than 80% between the two alleles is considered as skewed X-chromosome inactivation (Allen *et al*., 1992; Naumova *et al.*, 1996). X-inactivation statuses of the cells are given in Figure 3.3 and Table 3.3. According to these results, whereas LCL 1198 and LCL1213 are not informative, LCL 1195 and LCL1211 display skewed X-chromosome inactivation.

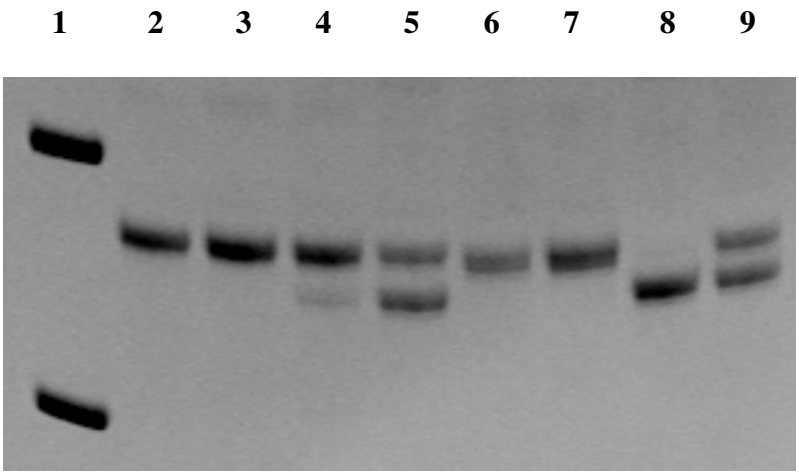

Figure 3.3 X-chromosome inactivation statuses via AR assay. Lane 1: pUC mix marker, 8, lane 2: HpaII digested PCR product of LCL1213, lane 3: Undigested PCR product of LCL1213, lane 4: HpaII digested PCR product of LCL1211, lane 5: Undigested PCR product of LCL1211, lane 6: HpaII digested PCR product of LCL1198, lane 7: Undigested PCR product of LCL1198, lane 8: HpaII digested PCR product of LCL1195, lane 9: Undigested PCR product of LCL1195

Table 3.3 X-inactivation statuses of the cell lines

LCL	Phenotype	Nucleotide Change	AA Change	X-inactivation status	X-inactivation pattern
1195	Rett-Like	C316T	R106V	%90.1	Skewed
1198	Rett-Like	C397T	R133C	-	Not informative
1211	Classic Rett	1162_1187del26	-	%84.8	Skewed
1213	Healthy	-	-	-	Not informative

3.3 Candidate *MECP2* target genes determination via bioinformatic analysis

The candidate gene analysis was carried out by bioinformatic analysis as explained in the methods part. At first, candidate *MECP2* target genes on the X-chromosome were searched (Table 3.4 and Appendix C). On the second round, candidate *MECP2* target genes on the whole chromosomes were searched (Table 3.5 and Appendix D).

Table 3.4 Candidate *MECP2* target genes identified by bioinformatic analysis

No	Gene	Score	Localization	X-Inactivation Status
1	AFF2	242	Xq28	-
2	PTCHD1	223	Xp22.11	-
3	HMGB3	201	Xq28	0/9
4	FAM50A	185	Xq28	-
5	RPS6KA3	179	Xp22.12-p22.1	0/9
6	SLC6A8	173	Xq28	-
7	RP11-13E5.1	161	Xq25	-
8	OTUD5	152	Xp11.23	-
9	TSPYL2	150	Xp11.2	0/5
10	FHL1	150	Xq26	1/9
11	MPP1	-	Xq28	0/9
12	PGK1	-	Xq26	0/9

Table 3.5 Candidate *MECP2* target genes on whole chromosomes

Symbol	Chr	Score	Gene Name	Location	Go Term	Kegg Title	Phenotype
AFF2	X	242	AF4/FMR2 family, member 2	Xq28	brain development/learning and/or memory	---	Mental retardation, X-linked, FRAXE type
BTBD2	19	228	BTB (POZ) domain containing 2	19p13.3	protein binding	---	---
PTCHD1	X	223	patched domain containing 1	Xp22.11	---	---	---
WIZ	19	214	---	---	---	---	---
FLJ37478	4	211	---	---	---	---	---
PRKCA	17	209	protein kinase C, alpha	17q22-q23.2	ATP binding/calcium ion binding/cell surface receptor linked signal transduction	Wnt signaling pathway/MAPK signaling pathway/Focal adhesion	Pituitary tumor, invasive
LOC116349	5	206	---	---	---	---	---
NOVA2	19	201	neuro-oncological ventral antigen 2	19q13.3	RNA binding/nucleus	---	---
HMGB3	X	201	high-mobility group box 3	Xq28	DNA bending activity	---	---
QKI	6	195	quaking homolog, KH domain RNA binding (mouse)	6q26-q27	nucleic acid binding	---	---
WNT4	1	192	wingless-type MMTV integration site family, member 4	1p36.23-p35.1	cell-cell signaling/development	Wnt signaling pathway/Hedgehog signaling pathway	Rokitansky-Kuster-Hauser syndrome
RHOT1	17	192	ras homolog gene family, member T1	17q11.2	GTP binding	---	---
ZNF480	19	192	zinc finger protein 480	19q13.41	metal ion binding	---	---
SLC35F1	6	189	solute carrier family 35, member F1	6q22.1-q22.31	---	---	---
NDRG3	20	189	NDRG family member 3	20q11.21-q11.23	catalytic activity/cell differentiation	---	---
RBPMS2	15	188	RNA binding protein with multiple splicing 2	15q22.31	---	---	---
HOXC8	12	187	homeobox C8	12q13.3	development	---	---
CAMK2N2	3	186	calcium/calmodulin-dependent protein kinase II inhibitor 2	3q27.1	---	---	---
CHD3	17	186	chromodomain helicase DNA binding protein 3	17p13.1	ATP binding/ATP-dependent DNA helicase activity	---	---
CNOT6L	4	185	CCR4-NOT transcription complex	4q13.3	---	---	---
FAM50A	X	185	family with sequence similarity 50, member A	Xq28	nucleus	---	---

3.4 Real Time RT-PCR

Relative expression levels of the 12 candidate *MECP2* target genes on the X-chromosome given in Table 3.4 were determined by Real time RT-PCR as explained in the methods part. The genes *MPP1* and *PGK1* were selected from the literature as a positive control (Ballester *et al.*, 2005).

3.4.1 Relative expressions of *AFF2* and *FHL1*

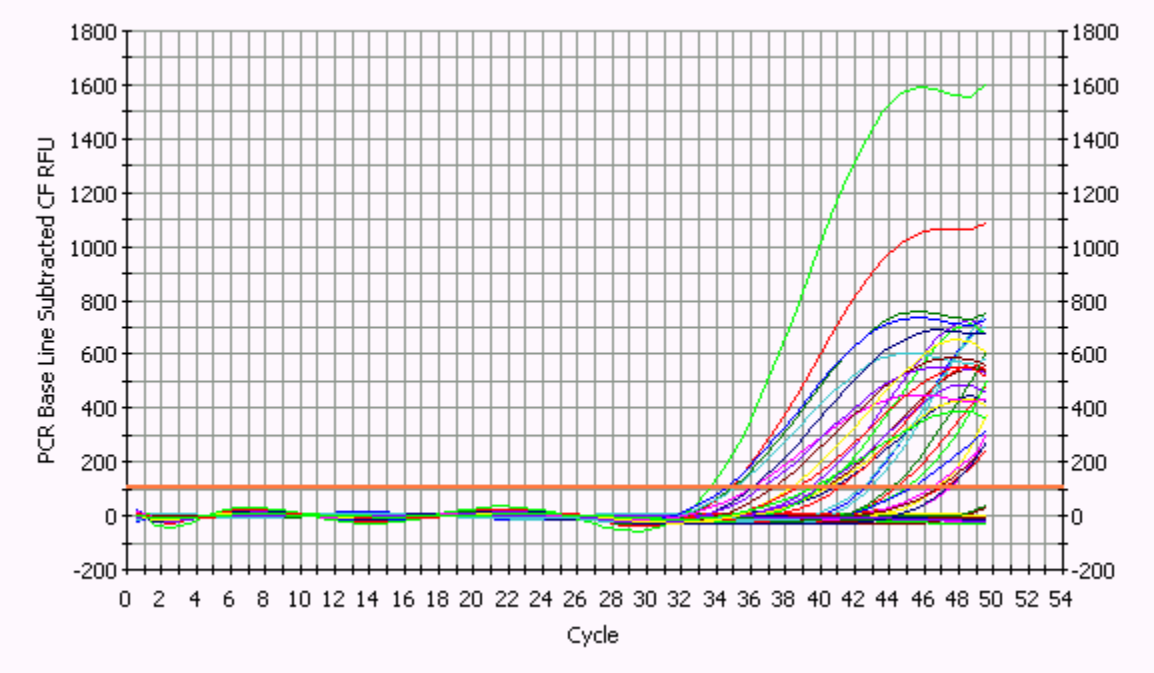

Figure 3.4 PCR Amp/Cycle Graph for *AFF2* and *FHL1*. Calculated threshold using the maximum curvature approach is 106.4.

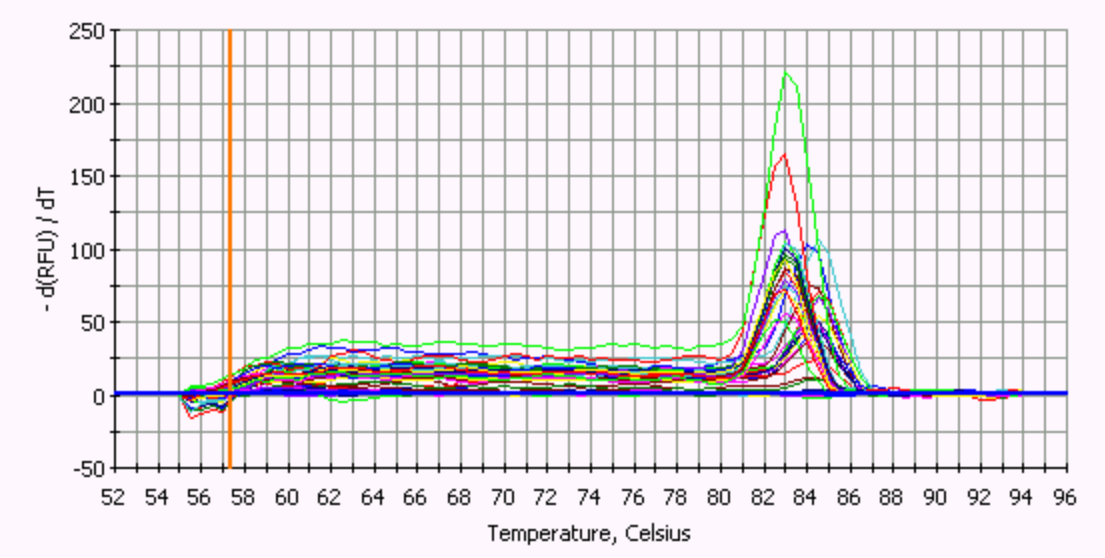

Figure 3.5 Melt curve graph for *AFF2* and *FHL1*. Threshold for automatic peak detection is set at 1.00.

3.4.2 Relative expression of *MPP1*

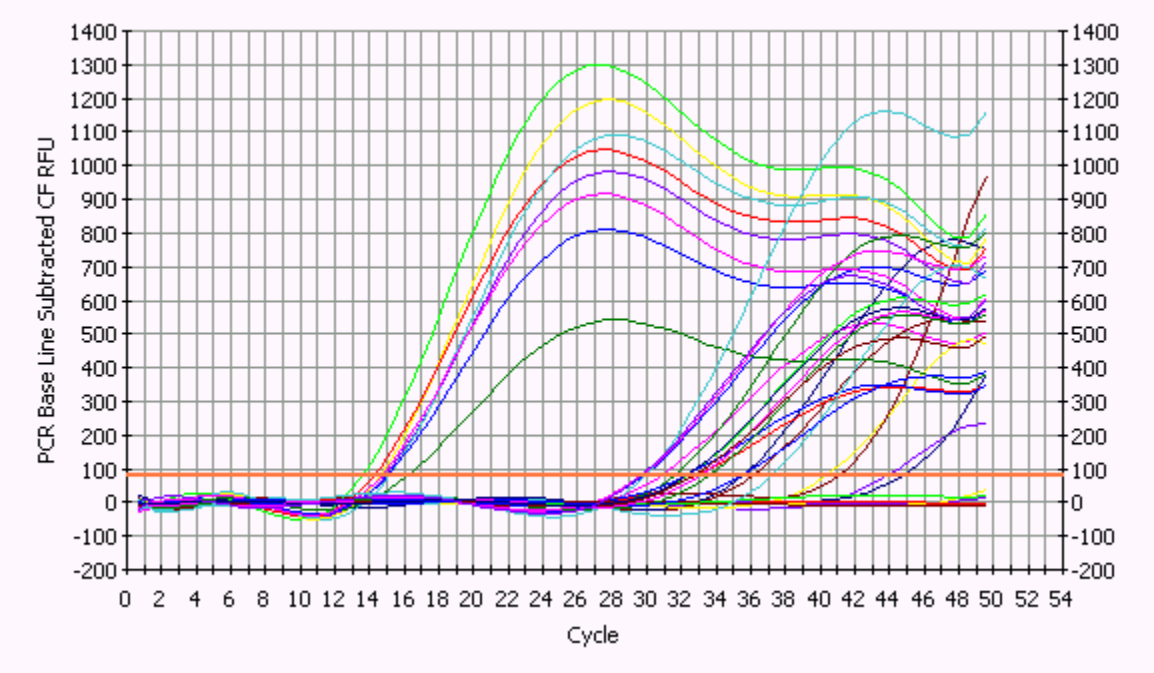

Figure 3.6 PCR Amp/Cycle Graph for *MPP1*. Calculated threshold using the maximum curvature approach is 77.0.

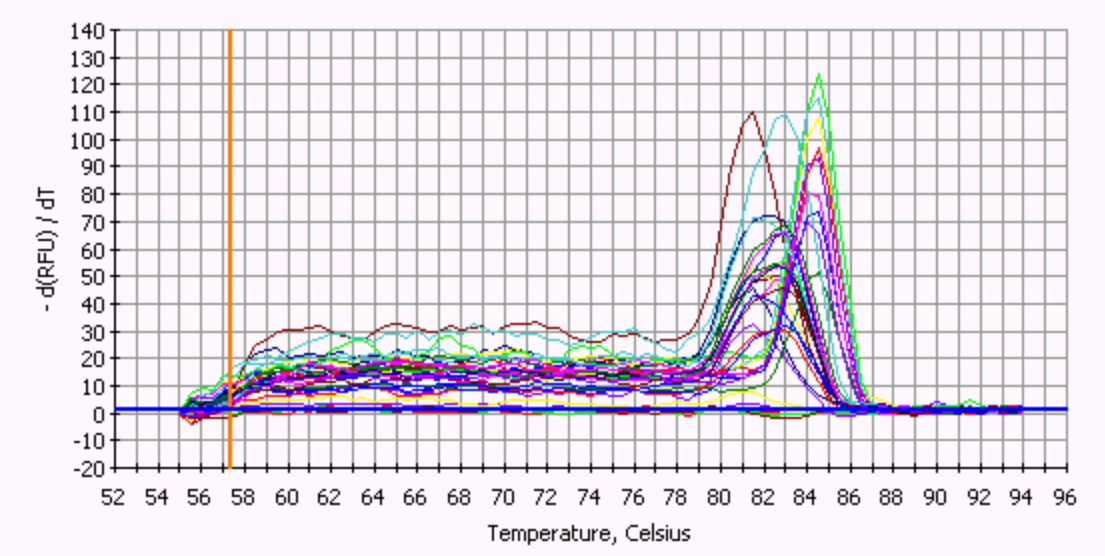

Figure 3.7 Melt curve graph for *MPP1*. Threshold for automatic peak detection is set at 1.00.

3.4.3 Relative expression of *RPS6KA3*

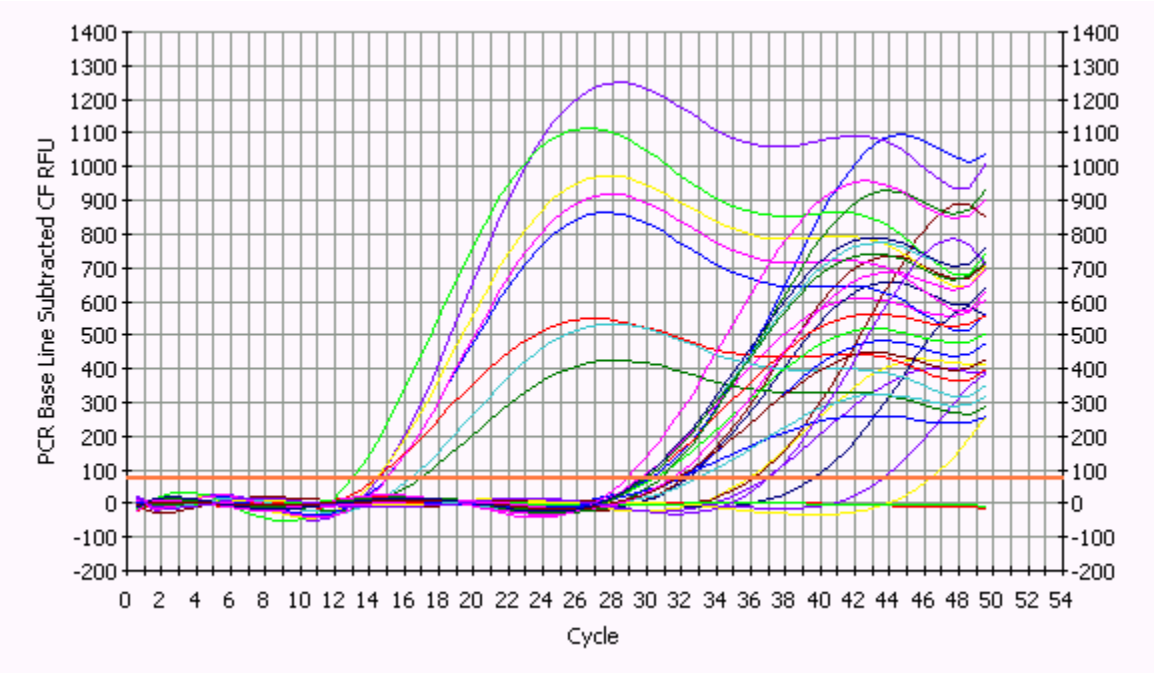

Figure 3.8 PCR Amp/Cycle Graph for *RPS6KA3*. Calculated threshold using the maximum curvature approach is 73.4.

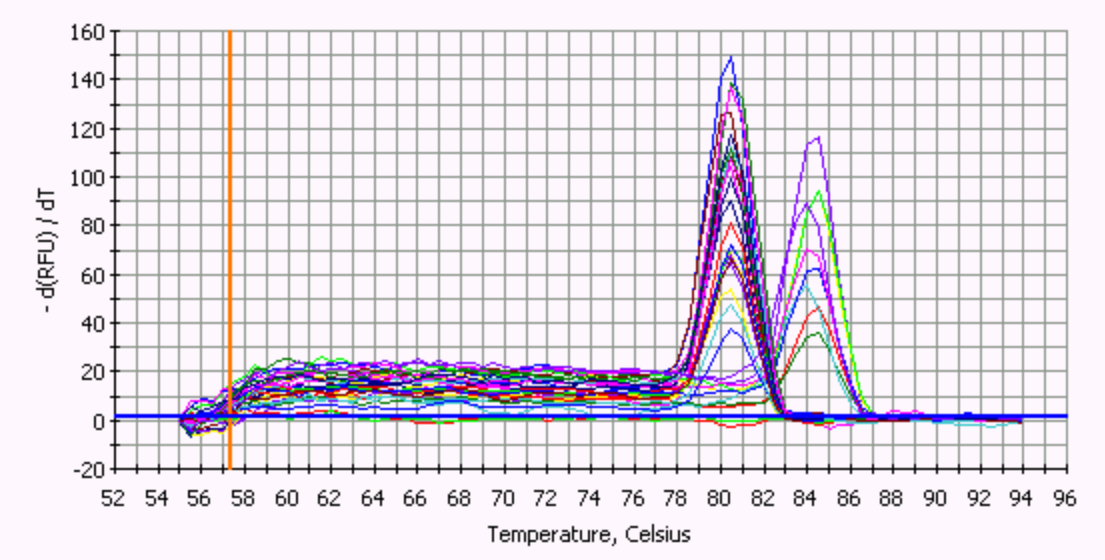

Figure 3.9 Melt curve graph for *RPS6KA3*. Threshold for automatic peak detection is set at 1.00.

3.4.4 Relative expression of *RP11.13E5.1*

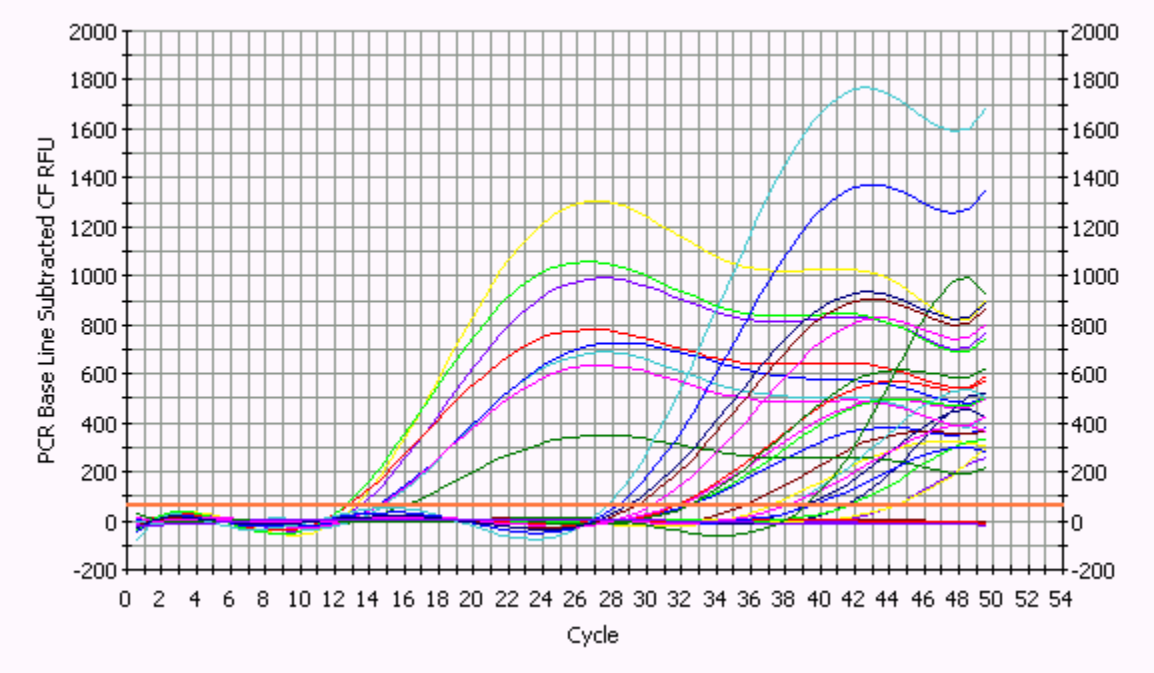

Figure 3.10 PCR Amp/Cycle Graph for *RP11.13E5.1*. Calculated threshold using the maximum curvature approach is 59.2.

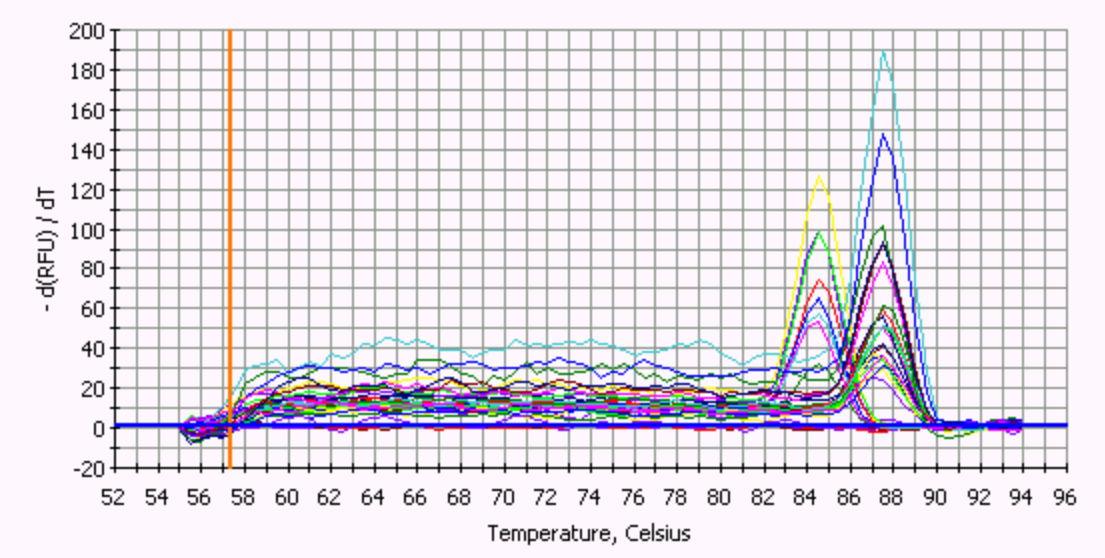

Figure 3.11 Melt curve graph for *RP11.13E5.1*. Threshold for automatic peak detection is set at 1.00.

3.4.5 Relative expression of *OTUD5*

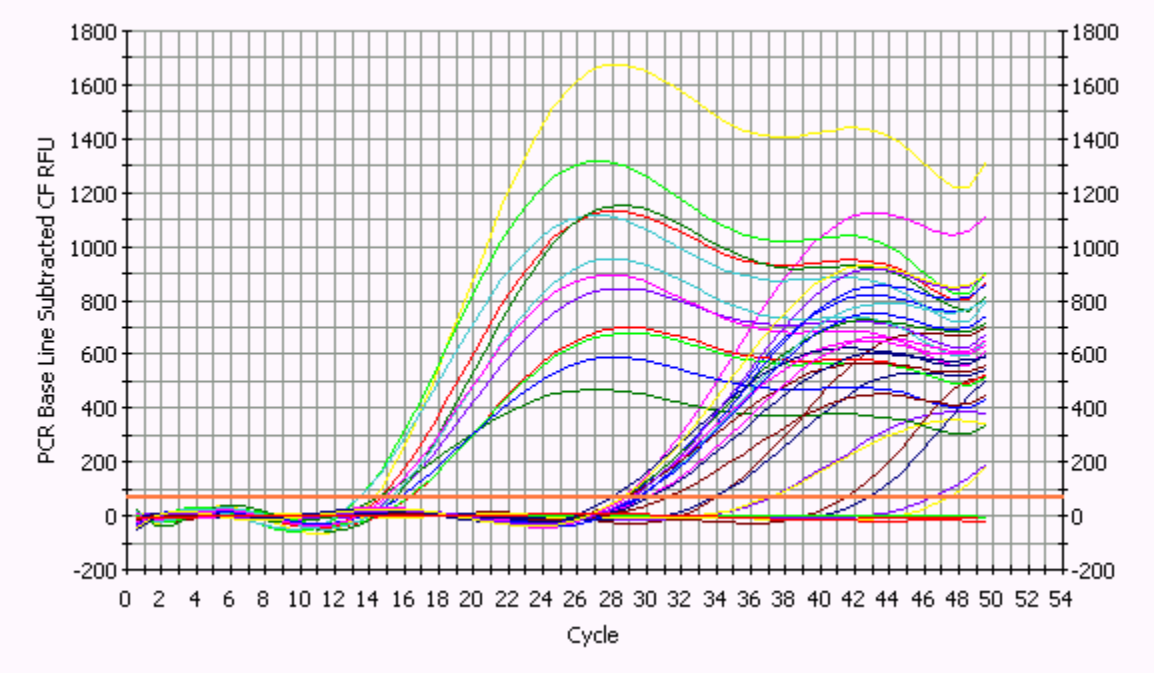

Figure 3.12 PCR Amp/Cycle Graph for *OTUD5*. Calculated threshold using the maximum curvature approach is 71.3.

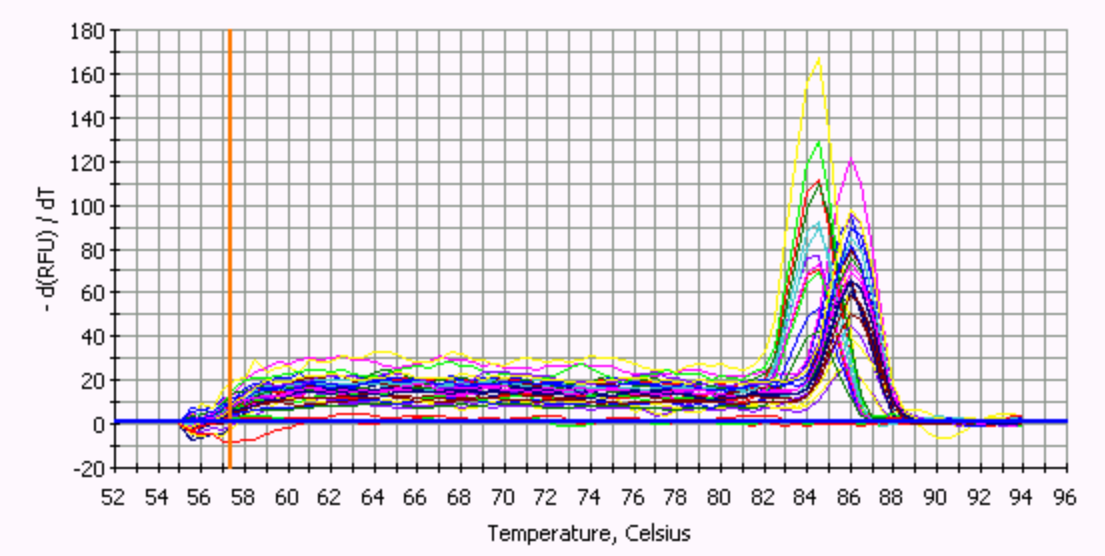

Figure 3.13 Melt curve graph for *OTUD5*. Threshold for automatic peak detection is set at 1.00.

3.4.6 Relative expression of *FAM50A*

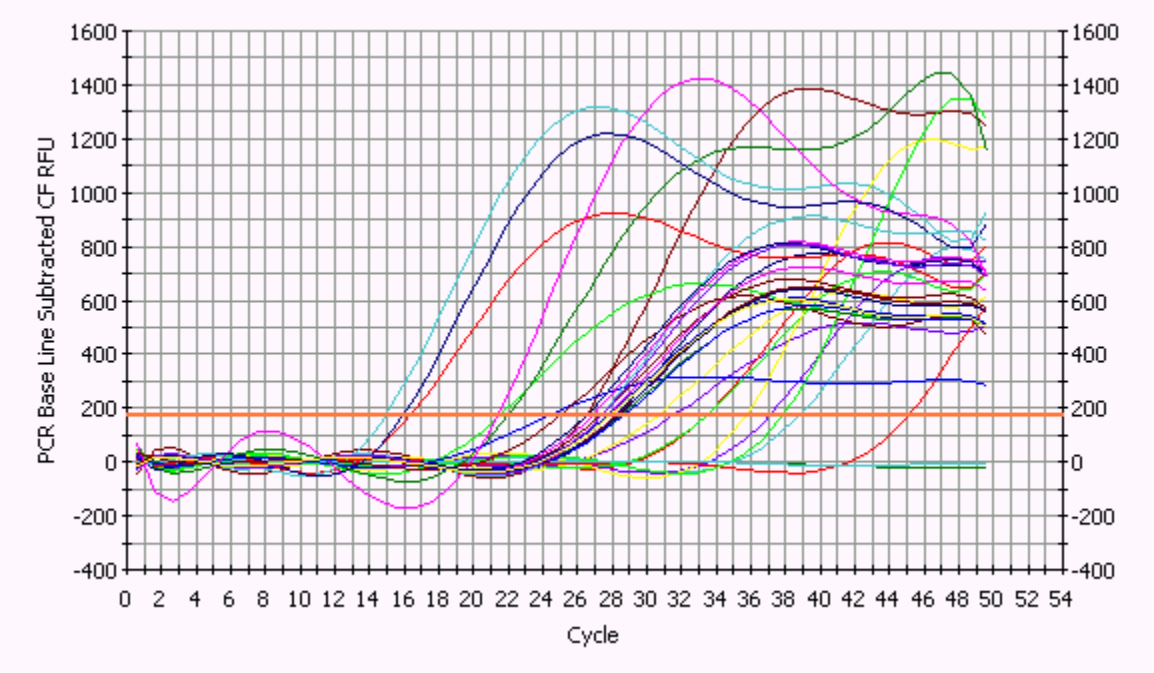

Figure 3.14 PCR Amp/Cycle Graph for *FAM50A*. Calculated threshold using the maximum curvature approach is 113.3.

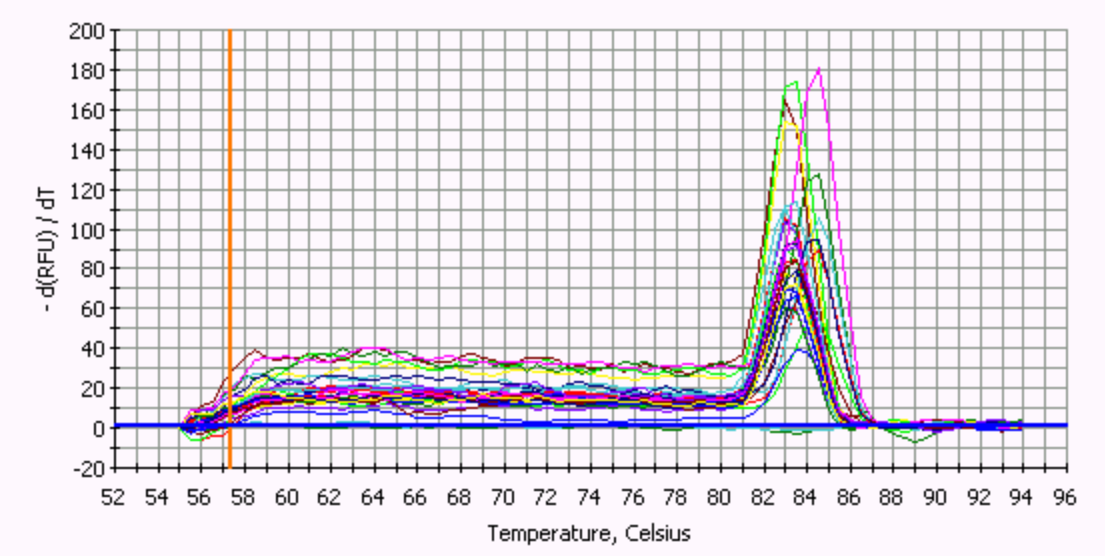

Figure 3.15 Melt curve graph for *FAM50A*. Threshold for automatic peak detection is set at 1.00.

3.4.7 Relative Expression of *PGK1*

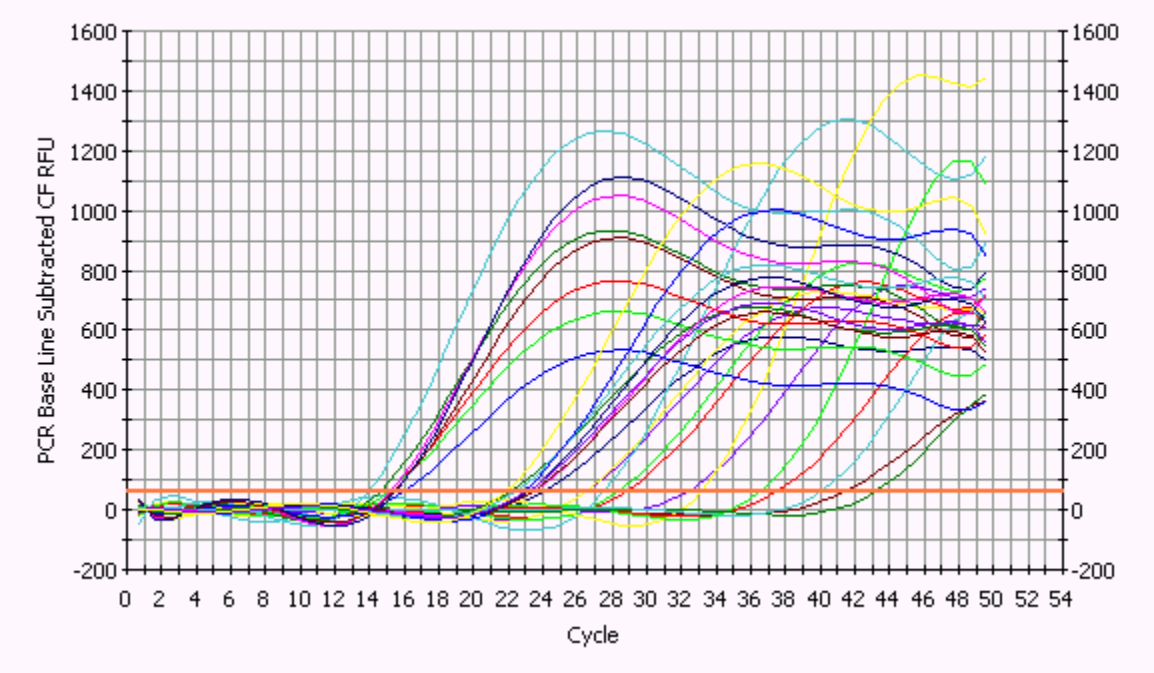

Figure 3.16 PCR Amp/Cycle Graph for *PGK1*. Calculated threshold using the maximum curvature approach is 60.0.

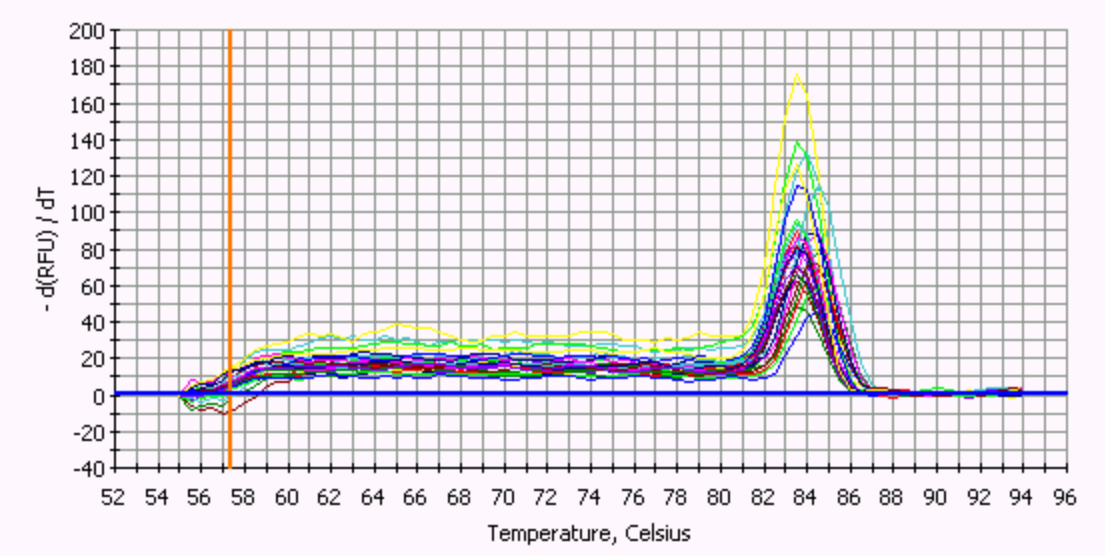

Figure 3.17 Melt curve graph for *PGK1*. Threshold for automatic peak detection is set at 1.00.

3.4.8 Relative expression of *PTCHD1* and *SLC6A8*

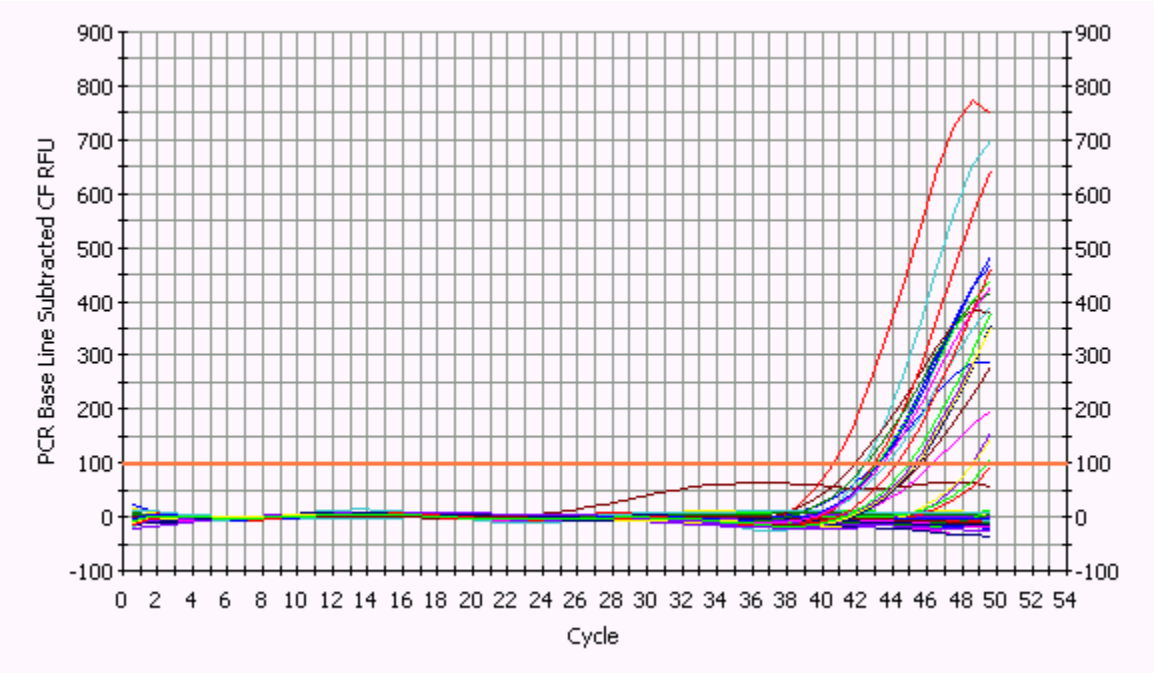

Figure 3.18 PCR Amp/Cycle Graph for *PTCHD1* and *SLC6A8*. Calculated threshold using the maximum curvature approach is 97.8.

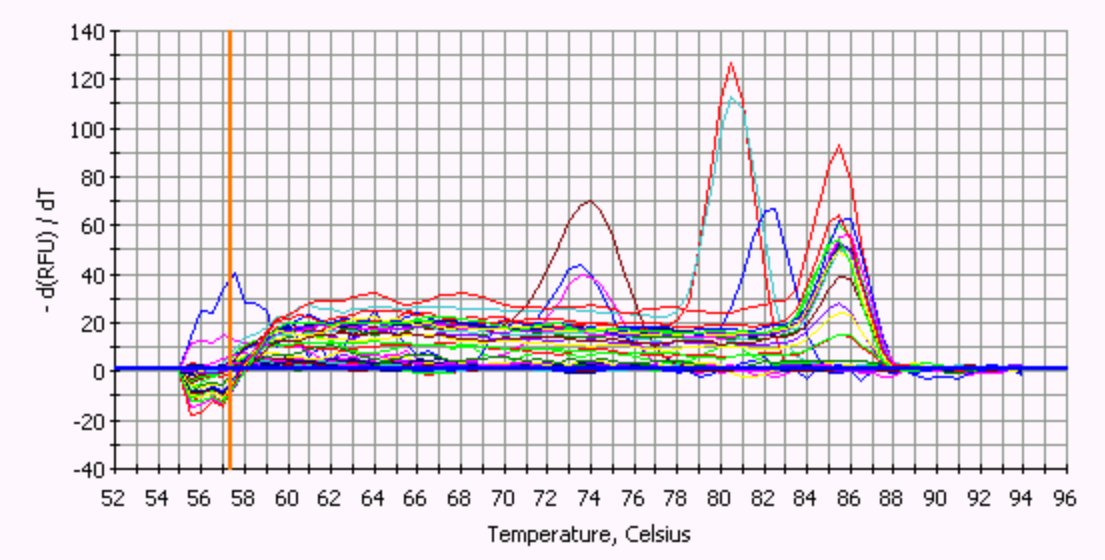

Figure 3.19 Melt curve graph for *PTCHD1* and *SLC6A8*. Threshold for automatic peak detection is set at 1.00.

3.4.9 Relative expressions of *TSPYL2* and *HMGB3*

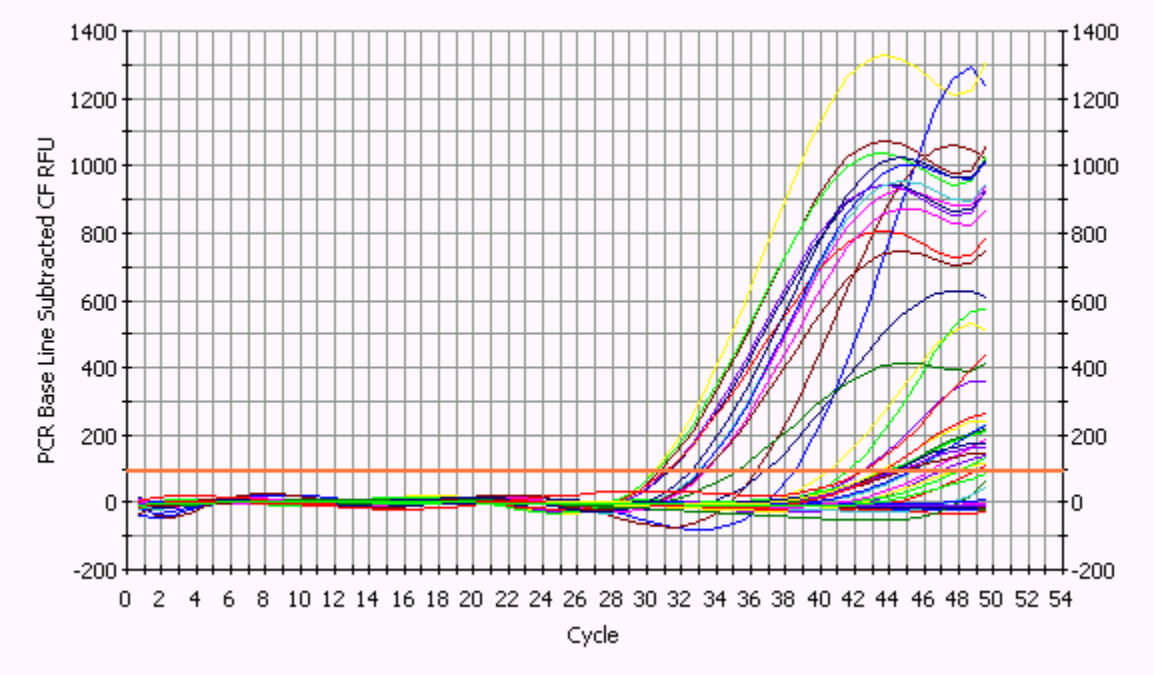

Figure 3.20 PCR Amp/Cycle Graph for *TSPYL21* and *HMGB3*. Calculated threshold using the maximum curvature approach is 91.8.

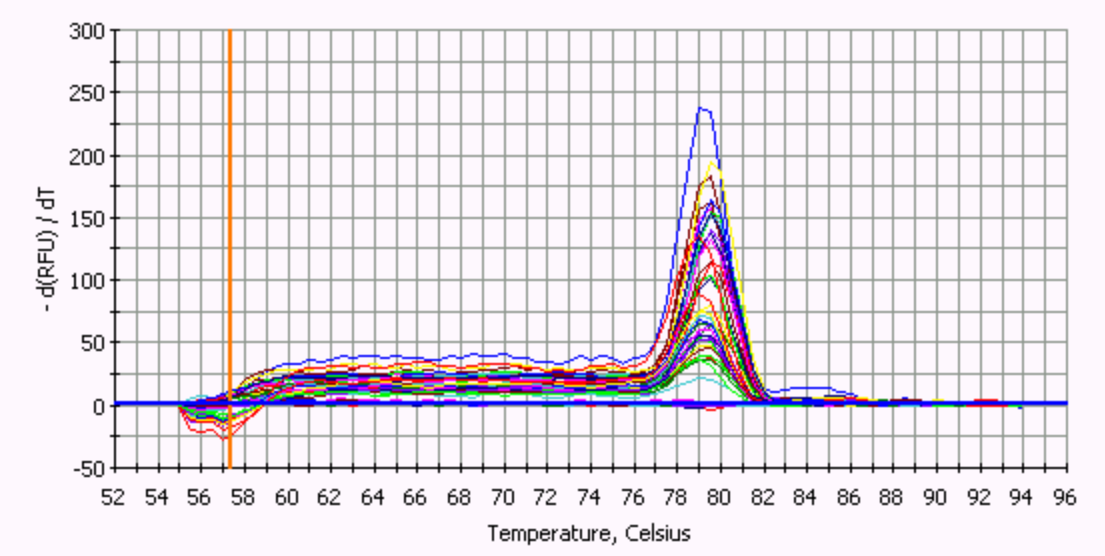

Figure 3.21 Melt curve graph for *TSPYL2* and *HMGB3*. Threshold for automatic peak detection is set at 1.00.

Table 3.6 Relative expressions of the candidate *MECP2* target genes in cell lines

Gene Name	Normalization	Relative Expression of LCL1195	Relative Expression of LCL1198	Relative Expression of LCL1211	Mean Relative Expression
AFF2	2.00	+84.45	+1.52	+13.00	+32.99
PTCHD1	2.00	-	+1.32	+1.00	+1.16
HMGB3	2.00	+1.07	-7.46	+1.00	-1.79
FAM50A	2.00	-3.25	-2.00	+5.66	+0.14
RPS6KA3	1.94	-1.30	-2.37	-2.21	-1.96
SLC6A8	2.00	+3.73	+1.32	+1.23	+2.09
RP11-13E5.1	2.24	-21.43	-1.91	-2.81	-8.72
OTUD5	1.68	-1.30	-1.44	-1.11	-1.28
TSPYL2	1.80	+3.24	+2.28	+1.12	+2.21
FHL1	2.00	+21.11	+6.50	+8.57	+12.06
MPP1	1.69	+1.23	+1.88	-2.57	+0.18
PGK1	1.92	-2.48	-2.55	-1.69	-2.24

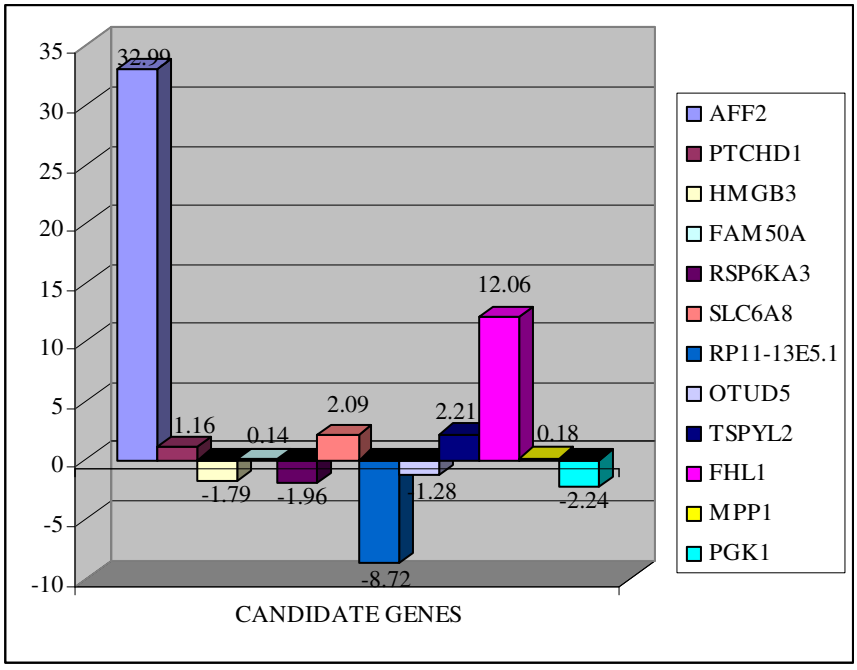

Figure 3.22 Relative expressions of the candidate *MECP2* target genes in cell lines

CHAPTER IV. DISCUSSION

Rett Syndrome is the second most common causes of mental retardation after Down syndrome (Ellaway *et al*., 2001). It is seen exclusively in girls with an incidence rate of 1 in 10,000 to 1 in 20,000 (Kerr *et al*, 1985; Hagberg *et al.*, 1985; Leonard *et al*., 1997; Miyamoto *et al*., 1997). The discovery of mutations in *MECP2* as the cause of the disease imply that Rett syndrome is the first human disease caused by a gene that is involved in transcriptional regulation (Amir *et al.*, 1999; Wan *et al.*, 1999).

4.1 Mutation spectrum of Rett syndrome

As mentioned before, there are up to 2000 *MECP2* mutations defined in classic female RTT patients (Amir et al., 2000; Miltenberger et al., 2003; Weaving et al., 2005; Philippe et al., 2006). We screened our patients for 7 frequent mutations: R106W, P152R, T158M, R168X, V288X, R270X, R306C and 1 rare mutation: F155S.

In the present mutation detection study which is an extension of a previous thesis conducted in our laboratory (Ayça Sayı, 2001), a total of 235 patients were analyzed for *MECP2* mutations (Table 3.2) and 48 mutations were detected with a 20% mutation detection rate.

Table 4.1 Frequencies comparison of *MECP2* mutations in our study.

Amino Acid Change	Nucleotide Change	Number observed
T158M	473 C→T	13/235
R270X	808 C→T	8/235
R306C	916 C→T	7/235
R168X	502 C→T	6/235
R106W	316 C→T	5/235
P152R	455 C→G	5/235
V288X	806 delG	4/235
F155S	590 C→T	0/235

Table 4.1 gives the frequencies of the selected *MECP2* mutations in the literature and in our study group.

4.2 Algorithms and Bioinformatics

MeCP2 functions as a transcriptional repressor by binding directly to the promoters of its target genes, thus, it is believed that MeCP2 has a great number of downstream targets (Willard *et al*., 1999). Recent potential target gene studies provided a different view on Rett pathogenesis and a limited number of candidate genes were defined as listed in Table 1.4 (Traynor *et al*., 2002; Ballestar *et al*., 2004; Horike *et al*., 2005; Bienvenu *et al*., 2006).

According to general overview, bioinformatics is the application of computer technology to the management of the biological information. With the recent developments in biotechnology in terms of high capability of computers to store, interpret, and analyze large amounts of data, internet, and databases bioinformatics become more popular in biological research (Soberon *et al*., 2004).

In order to find potential target genes of MeCP2 we derived a candidate *MECP2* binding motif using an algorithm. The motif is extracted from the genes taken from the article described in methods part via MEME program. The next step was biological local pair-wise sequence alignment of the motif with the 1107 X-linked genes' promoters using the affine gap penalty model.

In general terms, sequence alignment can be explained as the definition of a distance of number of sequences. By extracting the mismatch scores and gap open penalties from the total match scores alignment score is obtained (Barton *et al.*, 1993; Gotoh *et al.*, 1982). In our algorithm of target gene search higher scores of a gene means biological similarity between the motif of the *MECP2* and the gene on X chromosome. We further our experiments with the first ten genes with the higher scores.

4.3 De-regulated genes in *MECP2* mutant cell lines

MeCP2 has a function of regulating gene expression via transcriptional repression by directly binding to promoters of its target genes (Meehan *et al.*, 1992). Therefore, MeCP2 mutations would be result in deformations in MeCP2 transcriptional repression activity. Direct targets of MeCP2 would show increased expression in *MECP2* mutant cell lines.

We selected nine candidate genes according to the results of our bioinformatic study with the score more than 150, and 2 genes from micro-array data that are shown to be over-expressed in RTT cell lines (Ballester *et al.*, 2005). Besides that, *FHL1* gene was resided both in the microarray data with an increased expression and in our bioinformatic results with a higher score (150), suggesting that our algorithm gave a experimental approach.

Our RT-PCR results demonstrated that *FHL1* and *AFF2* showed a 12-fold and 33-fold increase, respectively, in their expression in *MECP2* mutant cell lines in comparison with a control cell line. Besides that, *SLC6A* (2-fold) and *TSPYL2* (2-fold) were also over-expressed in RTT cell lines. *HMGB3* (2-fold)*, RP11-13E5.1* (9-fold), and *PGK1* (2-fold) genes were down-regulated in RTT cell lines. Moreover, *PTCHD1, FAM50A, OTUD5,* and *MPP1* genes showed no significant alteration in their expression patterns (Figures 3.4 - 3.21 and Table 3.7).

4.4 Future Perspectives

RTT phenotype is described as rapid deterioration of high brain functions following developmental stagnation, autism, severe dementia, loss of purposeful hand use, ataxia, and microcephaly (Hagberg *et al*., 1983).

According to Gene Ontology database (http://www.geneontology.org/), *AFF2* gene functions in brain development, learning, and memory and *FHL1* gene functions in muscle growth and organ morphogenesis. Besides that, *SLC6A8* gene takes role in mental retardation. Therefore, these genes have a high potential to link with RTT phenotype. Our results showed increased expression of these genes in *MECP2* mutant cell lines, that is what we expect to find, however, in order to confirm the interactions between these genes and *MECP2,* further experimentation is needed.

In order to obtain a more significant data we are planning to collect RNA samples from peripheral bloods of our Rett patients with known MECP2 mutation and broaden our sample size. Confirming our hypothesis will provide a new perspective on candidate gene research via identifying new X-linked target genes and therefore contribute to disease pathogenesis via disturbances in X-chromosome inactivation. Moreover, confirming our data will show the importance of collaboration between

Bioinformatics and Molecular Genetics and will provide a different view on target gene research experiments.

As explained before, *MECP2* regulation of gene expression takes role in epigenetic mechanisms such as imprinting and X-chromosome inactivation. *DLX5* gene escapes from imprinting and biallelically expressed from both paternal and maternal alleles in *MECP2* mutant RTT patients (Horike *et al*., 2005). However, the role of X-inactivation in RTT pathogenesis is still an unknown issue. We expect to show that the increase in over-expression in the X-linked *MECP2* target genes depends on the biallelic expression from both active and inactive X-chromosome by escaping from X-chromosome inactivation via quantitative RT-PCR and clonal analysis of cells (single heterezygote clones) for intragenic polymorphisms. So we expect to conclude that the biallelic expression would be one of the causes of Rett syndrome by creating dosage problem.

Furthermore, we are planning to broaden our target gene research on whole human chromosomes. We derived the *MECP2* potential target genes data via our bioinformatic algorithm (APPENDIX D) as the next step of our hypothesis. We are aiming to identify the key genes contributing RTT pathogenesis on Human genome as a future direction.

CHAPTER V. REFERENCES

Allen RC, Zoghbi HY, Moseley AB, Rosenblatt HM, Belmont JW (1992). "Methylation of HpaII and HhaI sites near the polymorphic CAG repeat in the human androgen-receptor gene correlates with X chromosome inactivation." *Am J Hum Genet*. 51: 1229-39.

Altschul SF, Madden TL, Schaffer AA, Zhang J, Zhang Z, Miller W and Lipman DJ (1997). "Gapped BLAST and PSI-BLAST: a new generation of protein data base search programs." *Nucleic Acids Res*. 25: 3389–3402.

Amir RE, Van den Veyver IB, Wan M, Tran CQ, Francke U, Zoghbi HY (1999). "Rett syndrome is caused by mutations in X-linked MECP2, encoding methyl-CpG-binding protein 2." *Nature Genet.* 23: 185-188.

Amir RE, Van den Veyver IB, Schultz R, Malicki DM, Tran CQ, Dahle EJ, Philippi A, Timar L, Percy AK, Motil KJ, Lichtarge O, Smith EO, Glaze DG, Zoghbi HY.(2000). "Influence of mutation type and X chromosome inactivation on Rett syndrome phenotypes." *Ann Neurol.* 47: 670-9.

Amir RE, Zoghbi HY (2000). "Rett syndrome: methyl-CpG-binding protein 2 mutations and phenotype-genotype correlations." *Am J Med Genet*. 97: 147-52.

Armstrong DD (1997). Review of Rett syndrome. *J Neuropathol Exp Neurol*. 56: 843-9

Ayça Sayı (August, 2001). "Analysis of *MECP2* gene mutations in Rett Syndrome patients." *Thesis* submitted to Bilkent University.

Ballestar E, Ropero S, Alaminos M, Armstrong J, Setien F, Agrelo R, Fraga MF, Herranz M, Avila S, Pineda M, Monros E, Esteller M (2005). "The impact of MECP2 mutations in the expression patterns of Rett syndrome patients." *Hum Genet*. 116: 91-104.

Barton GJ (1993). "An efficient algorithm to locate all locally optimal alignments between two sequences allowing for gaps." *Comput Appl Biosci.* 9: 729-34.

Bell AC and Felsenfeld G (2000). "Methylation of a CTCF-dependent boundary controls imprinted expression of the Igf2 gene." *Nature* 405: 482–485.

Benedetti L, Munnich A, Melki J, Tardieu M, Turleau C (1992). "Parental origin of the X chromosomes in Rett syndrome." *Am. J. Med. Genet.* 44: 121-122.

Bienvenu T, Carrie A, de Roux N, Vinet MC, Jonveaux P, Couvert P, Villard L, Arzimanoglou A, Beldjord C, Fontes M (2000). "*MECP2* mutations account for most cases of typical forms of Rett syndrome." *Hum. Mol. Genet.* 9: 1377–1384.

Bienvenu T, Villard L, De Roux N, Bourdon V, Fontes M, Beldjord C, Tardieu M, Jonveaux P, Chelly J (2002). "French Consortium for MECP2 Gene Analysis. Spectrum of MECP2 mutations in Rett syndrome." *Genet Test*. 6: 1-6.

Bienvenu T, Chelly J (2006). "Molecular genetics of Rett syndrome: when DNA methylation goes unrecognized." *Nat Rev Genet*. 7: 415-26.

Caballero IM, Hendrich B (2005). "MeCP2 in neurons: closing in on the causes of Rett syndrome." *Hum Mol Genet*. 14: 2089.

Cheadle JP, Gill H, Fleming N, Maynard J, Kerr A, Leonard H, Krawczak M, Cooper DN, Lynch S, Thomas (2000). "Long-read sequence analysis of the *MECP2* gene in Rett syndrome patients: correlation of disease severity with mutation type and location." *Hum. Mol. Genet.* 9: 1119–1129

Chen WG, Chang Q, Lin Y, Meissner A, West AE, Griffith EC, Jaenisch R, Greenberg ME (2003). "Derepression of BDNF transcription involves calcium-dependent phosphorylation of *MeCP2*." *Science* 302: 885-9.

Clemson CM, McNeil JA, Willard HF and Lawrence JB (1996). "XIST RNA paints the inactive X chromosome at interphase: evidence for a novel RNA involved in nuclear/chromosome structure." *J. Cell Biol.* 132: 259–275.

Costello JF & Plass C (2001). "Methylation matters." *Journal of Medical Genetics* 38: 285–303.

Cross SH, Bird AP (1995). "CpG islands and genes." *Curr Opin Genet Dev*. 5: 309-14.

Croteau, S., Polychronakos, C., and Naumova, A. K. (2001) *Genesis*, 31, 11-16.

Dayhoff MO (1978). "Atlas of Protein Sequence and Structure." *National Biomedical Research Foundation* Vol. 4, Supp l.3.

De Bona C, Zappella M, Hayek G, Meloni I, Vitelli F, Bruttini M, Cusano R, Loffredo P, Longo I, Renieri A (2000). "Preserved speech variant is allelic of classic Rett syndrome." *Europ. J. Hum. Genet.* 8: 325-330.

D'Esposito M, Quaderi NA, Ciccodicola A, Bruni P, Esposito T, D'Urso M and Brown SD (1996). "Isolation, physical mapping and northern analysis of the X-linked human gene encoding methyl CpG-binding protein, MECP2." *Mamm. Genome* 7: 533–535.

Dragich J, Houwink-Manville I, Schanen C (2000). "Rett syndrome: a surprising result of mutation in MECP2." *Hum Mol Genet*. 9: 2365-75.

Ellaway C, Christodoulou J (2001). "Rett syndrome: clinical characteristics and recent genetic advances." *Disabil Rehabil*. 23: 98-106.

Filippova GN, Fagerlie S, Klenova EM, Myers C, Dehner Y, Goodwin G, Neiman PE, Collins SJ, and Lobanenkov VV (1996). "An exceptionally conserved transcriptional repressor, CTCF, employs different combinations of zinc fingers to bind diverged promoter sequences of avian and mammalian c-myc oncogenes." *Mol. Cell Biol.* 16: 2802-2813.

FitzGerald PM, Jankovic J, Percy AK (1990). "Rett syndrome and associated movement disorders." *Mov Disord*. 5: 195-202.

Gibbs AJ, McIntyre GA (1970). "The diagram, a method for comparing sequences. Its use with amino acid and nucleotide sequences." *Eur J Biochem.* 16: 1-11.

Gillberg C (1989). "The borderland of autism and Rett syndrome: five case histories to highlight diagnostic difficulties." *J Autism Dev Disord*. 19: 545-59.

Gribnau J, Hochedlinger K, Hata K, Li E, and Jaenisch R (2003). *Genes Dev.* 17: 759-773.

Gotoh O (1982). "An Improved Algorithm for Matching Biological Sequences." J. Mol. Biol. 162: 705-708.

Hagberg B, Aicardi J, Dias K, Ramos O (1983). "A progressive syndrome of autism, dementia, ataxia, and loss of purposeful hand use in girls: Rett's syndrome: report of 35 cases." *Ann. Neurol.* 14: 471-479.

Hagberg B (1985). "Rett syndrome: Swedish approach to analysis of prevalence and cause." *Brain Dev.* 7: 277-280.

Hagberg BA, Skjeldal OH (1994). “Rett variants: a suggested model for inclusion criteria.” *Pediatr Neurol* 11: 5-11.

Hagberg B (1995). “Rett syndrome: clinical peculiarities and biological mysteries.” *Acta Paediatr.* 84: 971-976.

Christen HJ, Hanefeld F (1998). “Male Rett variant.” *Neuropediatrics* 26: 81-82.

Hendrich B and Bird A (1998). “Identification and characterization of a family of mammalian methyl-CpG binding proteins.” *Mol. Cell. Biol.* 18: 6538–6547.

Henikoff S and Henikoff JG (1992). “Amino acid substitution matrices from protein blocks.” *Proc. Natl Acad. Sci*. 89: 10915–10919.

Horike S, Cai S, Miyano M, Cheng JF, Kohwi-Shigematsu T (2005). “Loss of silent-chromatin looping and impaired imprinting of DLX5 in Rett syndrome.” *Nat Genet*. 37: 31-40.

Jeppesen P and Turner BM (1993). “The inactive X chromosome in female mammals is distinguished by a lack of histone H4 acetylation, a cytogenetic marker for gene expression.” *Cell* 74: 281–289.

Jian L, Archer HL, Ravine D, Kerr A, de Klerk N, Christodoulou J, Bailey MES, Laurvick C, Leonard H (2005). “p.R270X MECP2 mutation and mortality in Rett syndrome.” *Europ. J. Hum. Genet.* 13: 1235-1238.

Jones PL, Veenstra GJ, Wade PA, Vermaak D, Kass SU, Landsberger N, Strouboulis J and Wolffe AP (1998). “Methylated DNA and MeCP2 recruit histone deacetylase to repress transcription.” *Nature Genet.* 19: 187–191.

Jones PL and Wolffe AP (1999). “Relationships between chromatin organization and DNA methylation in determining gene expression.” *Semin. Cancer Biol.* 9: 339–347.

Journel H, Melki J, Turleau C, Munnich A, de Grouchy J (1990). “Rett phenotype with X/autosome translocation: possible mapping to the short arm of chromosome X.” *Am. J. Med. Genet.* 35: 142-147.

Kerr AM, Stephenson JB (1985). “Rett's syndrome in the west of Scotland.” *Br Med J*. 291: 579-82.

Kriaucionis S, Bird A (2003). “DNA methylation and Rett syndrome.” *Hum Mol Genet*. 12: 221-7.

Laccone F, Zoll B, Huppke P, Hanefeld F, Pepinski W, Trappe R (2002). “MECP2 gene nucleotide changes and their pathogenicity in males: proceed with caution.” *J Med Genet*. 39: 586-8.

Lalande M (1996). “Parental imprinting and human disease.” *Annu. Rev. Genet.* 30: 173–195.

Lee JT, Davidow LS and Warshawsky D (1999). “*Tsix*, a gene antisense to Xist at the X-inactivation centre.” *Nat. Genet.* 21: 400–404.

Lee JT and Lu N (1999). “Targeted mutagenesis of Tsix leads to nonrandom X inactivation.” *Cell* 99: 47–57.

Lee JT (2000). “Disruption of imprinted X inactivation by parent-of-origin effects at Tsix.” *Cell* 103: 17–27.

Leighton PA, Ingram RS, Eggenschwiler J, Efstratiadis A and Tilghman SM (1995). *Nature* 375: 34-39.

Leonard H, Bower C, English D (1997). “The prevalence and incidence of Rett syndrome in Australia.” *Eur Child Adolesc Psychiatry*. 6: 8-10.

Li E, Bestor TH and Jaenisch R (1992). “Targeted mutation of the DNA methyl-transferase gene results in embryonic lethality.” *Cell* 69: 915–926.

Lyon MF (1961). “ Gene action in the X-chromosome of the mouse.” *Nature* 190: 372–373.

Lyon MF (1968). “Chromosomal and subchromosomal inactivation.” *Ann Rev Genet.* 2: 31–52.

Marin M, Karis A, Visser P, Grosveld F and Philipsen S (1997). “Transcription factor Sp1 is essential for early embryonic development but dispensable for cell growth and differentiation.” *Cell* 89: 619–628.

Martinowich K, Hattori D, Wu H, Fouse S, He F, Hu Y, Fan G and Sun YE (2003). “DNA methylation-related chromatin remodeling in activity-dependent BDNF gene regulation.” *Science* 302: 890–893.

Meehan RR, Lewis JD and Bird AP (1992). “Characterization of MeCP2, a vertebrate DNA binding protein with affinity for methylated DNA.” *Nucleic Acids Res.* 20: 5085–5092.

Miltenberger-Miltenyi G, Laccone F (2003). “Mutations and polymorphisms in the human methyl CpG-binding protein MECP2.” *Hum Mutat*. 22: 107-15.

Miyamoto A, Yamamoto M, Takahashi S, Oki J (1997). “Classical Rett syndrome in sisters: variability of clinical expression.” *Brain Dev.*19: 492-494.

Moretti P, Bouwknecht JA, Teague R, Paylor R and Zoghbi HY (2005). “Abnormalities of social interactions and home cage behavior in a mouse model of Rett syndrome.” *Hum. Mol. Genet.* 14: 205–220.

Nan X, Meehan RR and Bird A (1993). “Dissection of the methyl-CpG binding domain from the chromosomal protein MeCP2.” *Nucleic Acids Res.* 21: 4886–4892.

Nan X, Ng HH, Johnson CA, Laherty CD, Turner BM, Eisenman RN and Bird A (1998). “Transcriptional repression by the methyl-CpG-binding protein MeCP2 involves a histone deacetylase complex.” *Nature* 393: 386–389.

Nan X, Tate P, Li E and Bird A (1996). “DNA methylation specifies chromosomal localization of MeCP2.” *Mol. Cell. Biol.* 16: 414–421.

Nance WE (1964). “ Genetic tests with a sex-linked marker: glucose-6-phosphate dehydrogenase.” *Cold Spring Harbor Symp Quant Biol* 29: 415–424.

Naumova AK, Plenge RM, Bird LM, Leppert M, Morgan K, Willard HF, Sapienza C (1996). “Heritability of X chromosome--inactivation phenotype in a large family.” *Am J Hum Genet*. 58: 1111-9.

Ng HH and Bird A (1999). “DNA methylation and chromatin modification.” *Curr. Opin. Genet. Dev.* 9: 158–163.

Nyhan WL, Bakay B, Connor JD, Marks JF, Keele DK (1970). “Hemizygous expression of glucose-6-phosphate dehydrogenase in erythrocytes of heterozygotes for the Lesch-Nyhan syndrome.” *Proc Natl Acad Sci* 65: 214–218.

Ouzounis CA, Valencia A (2003). “Early bioinformatics: the birth of a discipline--a personal view.” *Bioinformatics* 19: 2176-90.

Partington MW (1988). “Rett syndrome in monozygotic twins.” *Am. J. Med. Genet.* 29: 633-637.

Pearson WR and Lipman DJ (1988). “Improved tools for biological sequence comparison.” *Proc. Natl Acad. Sci.* 85: 2444–2448.

Pedone PV, Pikaart MJ, Cerrato F, Vernucci M, Ungaro P, Bruni CB and Riccio A (1999). “Role of histone acetylation and DNA methylation in the maintenance of the imprinted expression of the H19 and Igf2 genes.” *FEBS Lett.* 458: 45–50.

Philippe C, Villard L, De Roux N, Raynaud M, Bonnefond JP, Pasquier L, Lesca G, Mancini J, Jonveaux P, Moncla A, Chelly J, Bienvenu T (2006). “Spectrum and distribution of MECP2 mutations in 424 Rett syndrome patients: a molecular update.” *Eur J Med Genet*. 49: 9-18.

Plath K, Mlynarczyk-Evans S, Nusinow DA and Panning B (2002). *Annu. Rev. Genet.* 36: 233-278.

Prokhortchouk A, Hendrich B, Jorgensen H, Ruzov A, Wilm M, Georgiev G, Bird A and Prokhortchouk E (2001). “The p120 catenin partner Kaiso is a DNA methylation-dependent transcriptional repressor.” *Genes Dev.* 15: 1613–1618.

Quaderi NA, Meehan RR, Tate PH, Cross SH, Bird AP, Chatterjee A, Herman GE and Brown SD (1994). “Genetic and physical mapping of a gene encoding a methyl CpG binding protein, Mecp2, to the mouse X chromosome.” *Genomics* 22:648–651.

Reichwald K, Thiesen J, Wiehe T, Weitzel J, Poustka WA, Rosenthal A, Platzer M, Strätling WH and Kioschis P (2000). “Comparative sequence analysis of the MECP2-locus in human and mouse reveals new transcribed regions.” *Mamm. Genome* 11: 182–190.

Rett A (1977). “Cerebral atrophy associated with hyperammonaemia.” In: Vinken PJ, Bruyn GW (1977). “Handbook of Clinical Neurology. Amsterdam: North Holland” 29: 305-329.

Rett A (1966). “Ueber ein eigenartiges hirnatrophisches Syndrom bei Hyperammoniamie in Kindesalter.” *Wien. Med. Wschr.* 116: 723-738.

Salozhin SV, Prokhorchuk EB, Georgiev GP (2005). “Methylation of DNA--one of the major epigenetic markers.” *Biochemistry* 70: 525-32.

Samaco RC, Hogart A, LaSalle JM (2005). “Epigenetic overlap in autism-spectrum neurodevelopmental disorders: MECP2 deficiency causes reduced expression of UBE3A and GABRB3.” *Hum Mol Genet.* 14: 483-92.

Schanen NC, Dahle EJR, Capozzoli F, Holm VA, Zoghbi HY, Francke U (1977). "A new Rett syndrome family consistent with X-linked inheritance expands the X chromosome exclusion map." *Am. J. Hum. Genet.* 61: 634-647.

Schanen NC, Kurczynski TW, Brunnelle D, Woodcock MM, Dure LS, Percy AK (1998). "Neonatal encephalopathy in two boys in families with recurrent Rett syndrome." *J. Child Neurol.* 13: 229-231.

Schoenherr CJ, Levorse JM, and Tilghman SM (2003). *Nat. Genet.* 33: 66-69.

Schubeler D, Francastel C, Cimbora DM, Reik A, Martin DIK and Groudine M (2000). "Nuclear localization and histone acetylation: a pathway for chromatin opening and transcriptional activation of the human beta-globin locus." *Genes Dev.* 14: 940–950.

Shepard RN (1980). "Multidimensional scaling, tree-fitting and clustering." *Science* 210: 390–398.

Shibata S and Lee JT (2003). "Characterization and quantitation of differential Tsix transcripts: implications for Tsix function." *Hum. Mol. Genet.*, 12, 125-136.

Sirianni N, Naidu S, Pereira J, Pillotto RF, Hoffman EP (1998). "Rett syndrome: confirmation of X-linked dominant inheritance, and localization of the gene to Xq28." *Am. J. Hum. Genet.* 63: 1552-1558.

Smeets E, Schollen E, Moog, U, Matthijs G, Herbergs J, Smeets H, Curfs L, Schrander-Stumpel C, Fryns JP (2003). "Rett syndrome in adolescent and adult females: clinical and molecular genetic findings." *Am. J. Med. Genet.* 122A: 227-233.

Soberon J, Peterson AT (2004). "Biodiversity informatics: managing and applying primary biodiversity data." *Philos Trans R Soc Lond B Biol Sci*. 359: 689-98.

Solari A (1974). "The behaviour of the XY pair in mammals." *Rev. Cytol.* 38: 273–317.

Surani MA (1998). "Imprinting and the initiation of gene silencing in the germ line." *Cell* 93: 309–312.

Takagi N (2003). "Imprinted X-chromosome inactivation: enlightenment from embryos in vivo" *Semin. Cell Dev. Biol.* 14: 319-329.

Tao J, Van Esch H, Hagedorn-Greiwe M, Hoffmann K, Moser B, Raynaud M, Sperner J, Fryns JP, Schwinger E, Gecz J, Ropers HH, Kalscheuer VM (2004). "Mutations in the X-linked cyclin-dependent kinase-like 5 (CDKL5/STK9) gene are associated with severe neurodevelopmental retardation." *Am. J. Hum. Genet.* 75: 1149-1154.

Tariverdian G, Kantner G, Vogel F (1087). "A monozygotic twin pair with Rett syndrome." *Hum. Genet.* 75: 88-90.

Tariverdian G (1990). "Follow-up of monozygotic twins concordant for the Rett syndrome." *Brain Dev.* 12: 125-127.

Timothy L, Bailey and Charles E (1994). "Fitting a mixture model by expectation maximization to discover motifs in biopolymers" *Proceedings of the Second International Conference on Intelligent Systems for Molecular Biology* pp. 28-36, AAAI Press, Menlo Park, California.

Traynor J, Agarwal P, Lazzeroni L, Francke U (2002). "Gene expression patterns vary in clonal cell cultures from Rett syndrome females with eight different *MECP2* mutations." *BMC Med Genet*. 3: 12.

Topçu M, Topaloglu H, Renda Y, Berker M, Turanli G (1991). "The Rett syndrome in males." *Brain Dev*. 13: 62.

Villard L, Kpebe A, Cardoso C, Chelly PJ, Tardieu PM and Fontes M (2000). "Two affected boys in a Rett syndrome family: clinical and molecular findings." *Neurology* 55: 1188–1193

Vinga S, Almeida J (2003). "Alignment-free sequence comparison-a review." *Bioinformatics* 19: 513-23.

Wan M, Lee SS, Zhang X, Houwink-Manville I, Song HR, Amir RE, Budden S, Naidu S, Pereira JL, Lo IF, Zoghbi HY, Schanen NC, Francke U (1999). "Rett syndrome and beyond: recurrent spontaneous and familial MECP2 mutations at CpG hotspots." *Am J Hum Genet*. 65: 1520-9.

Weaving LS, Williamson SL, Bennetts B, Davis M, Ellaway CJ, Leonard H, Thong MK, Delatycki M, Thompson EM, Laing N, Christodoulou J (2003). "Effects of MECP2 mutation type, location and X-inactivation in modulating Rett syndrome phenotype." *Am J Med Genet A*. 118: 103-14.

Weaving LS, Christodoulou J, Williamson SL, Friend KL, McKenzie OLD, Archer H, Evans J, Clarke A, Pelka GJ, Tam PPL, Watson C, Lahooti H, Ellaway CJ, Bennetts B, Leonard H, Gecz J (2004). "Mutations of CDKL5 cause a severe neurodevelopmental disorder with infantile spasms and mental retardation." *Am. J. Hum. Genet.* 75: 1079-93.

Weaving LS, Ellaway CJ, Gecz J, Christodoulou J (2005). "Rett syndrome: clinical review and genetic update." *J Med Genet.* 42: 1-7.

Webb T, Watkiss E, Woods CG (1993). "Neither uniparental disomy nor skewed X-inactivation explains Rett syndrome." *Clin. Genet.* 44: 236-240.

Willard HF and Hendrich BD (1999). "Breaking the silence in Rett syndrome." *Nat. Genet.* 23: 127–128.

Zappella M (1992). "The Rett girls with preserved speech." .*Brain Dev*. 14: 98-101.

Zappella M, Meloni I, Longo I, Hayek G, Renieri A (2001). "Preserved speech variants of the Rett syndrome: molecular and clinical analysis." *Am. J. Med. Genet.* 104: 14-22.

Zoghbi HY, Ledbetter DH, Schultz R, Percy AK, Glaze DG (1990). "A de novo X;3 translocation in Rett syndrome." *Am. J. Med. Genet.* 35: 148-151.

Zoghbi HY, Percy AK, Schultz RJ, Fill C (1990). "Patterns of X chromosome inactivation in the Rett syndrome." *Brain Dev.* 12: 131-135.

Zoghbi HY (2003). "Postnatal neurodevelopmental disorders: meeting at the synapse?" *Science* 302: 826–830.

CHAPTER VII. APPENDICIES

Appendix A The incidence rates and frequencies of some of the Rett mutations

(http://mecp2.chw.edu.au/cgi-bin/mecp2/views/basic.cgi?form=amino-freq)

Amino acid change	Frequency	Percentage
p.T158M	190	9.2
p.R168X	186	9.01
p.R255X	166	8.04
p.R270X	146	7.07
p.R294X	118	5.71
p.R306C	96	4.65
p.R133C	91	4.41
p.R106W	71	3.44
intronic variation	54	2.62
p.L386fs	47	2.28
p.P388fs	30	1.45
p.G269fs	30	1.45
p.P152R	29	1.4
p.S194S	23	1.11
p.M1?	23	1.11
p.E397K	22	1.07
p.T299T	19	0.92
3'UTR variation	19	0.92
p.A140V	18	0.87
p.S411S	15	0.73
p.R306H	14	0.68
p.P302R	12	0.58
p.S134C	12	0.58
p.G237fs	12	0.58
p.P376S	11	0.53
p.P225R	10	0.48
p.R9fs	10	0.48
p.R106Q	10	0.48
p.P387fs	9	0.44

p.Y141X	9	0.44
p.K345K	8	0.39
p.R270fs	7	0.34
p.G428S	7	0.34
p.T197M	7	0.34
p.T203M	7	0.34
p.A201V	7	0.34
p.S359P	6	0.29
p.P251fs	6	0.29
p.P384fs	6	0.29
p.P385fs	6	0.29
p.A439T	6	0.29
p.A259A	5	0.24
p.F142F	5	0.24
p.P387_M466del80	5	0.24
p.(N126+S486)	5	0.24
p.A444T	5	0.24
p.P402L	5	0.24
p.R250fs	5	0.24
p.G232fs	5	0.24
p.G252fs	4	0.19
p.P361A	4	0.19
p.H366fs	4	0.19
p.P390_P391delPP	4	0.19
p.Q406X	4	0.19
p.P272L	4	0.19
p.D156E	4	0.19
5'UTR variation	4	0.19
p.S204X	4	0.19
p.S70S	4	0.19
p.L386fsX403	4	0.19
p.R133H	4	0.19
p.T240T	4	0.19
p.S401N	4	0.19
p.P302L	4	0.19
ambiguous mutation data	4	0.19
p.K286fs	4	0.19
p.L100V	4	0.19
p.V412I	3	0.15
p.P405P	3	0.15
MECP2_e1:p.G16dupG	3	0.15

p.P322L	3	0.15
p.S332fs	3	0.15
p.G273G	3	0.15
p.S49X	3	0.15
p.R106G	3	0.15
p.P101S	3	0.15
p.P399L	3	0.15
p.T158T	3	0.15
p.R250R	3	0.15
p.P399P	3	0.15
p.A278A	3	0.15
p.I125I	3	0.15
[p.R168X] + [p.G232A]	3	0.15
p.Q170X	3	0.15
[p.L328L + p.388delP]	3	0.15
p.K305R	3	0.15
p.P56P	3	0.15
p.Q244X	3	0.15
p.A281A	3	0.15
p.L328L	3	0.15
p.R458C	2	0.1
p.P101R	2	0.1
p.T445T	2	0.1
p.K200X	2	0.1
p.H368fs	2	0.1
p.P322A	2	0.1
p.S357S	2	0.1
p.K22X	2	0.1
p.F155S	2	0.1
p.Q297X	2	0.1
p.P376fs	2	0.1
p.P225L	2	0.1
p.S229L	2	0.1
p.C413C	2	0.1
p.A280A	2	0.1
p.R250H	2	0.1
p.P302A	2	0.1
p.D34fs	2	0.1
p.Q16X	2	0.1
p.K36fs	2	0.1
p.T158A	2	0.1

Appendix B Gene list used in motif search

Gene Name	Accession Number	Chromosome
CTSS	NM_004079	1
S100A10	NM_002966	1
CLK2	NM_003993	1
IGFBP2	NM_000597	2
MYCN	NM_005378	2
LHCGR	NM_000233	2
AGTR1	NM_032049	3
PPID	NM_005038	4
ITGA2	NM_002203	5
PAM	NM_138822	5
SEPT7	NM_001788	7
NET1	NM_005863	10
MARCH8	NM_145021	10
PTPRCAP	NM_005608	11
BIRC2	NM_001166	11
IGF2	NM_000612	11
SLC2A3	NM_006931	12
CDH1	NM_004360	16
TOP2A	NM_001067	17
ITGA3	NM_005501	17
DNAJB1	NM_006145	19
CSE1L	NM_177436	20
GNAS	NM_080426	20
PGK1	NM_000291	X
RNF113A	NM_006978	X
RBBP7	NM_002893	X
SMARCA1	NM_139035	X
AFF2	NM_002025	X
FHL1	NM_001449	X
MPP1	NM_002436	X

Appendix C Whole list of candidate *MECP2* target genes on X chromosomes determined by bioinformatic analysis

No	Gene	Score	Localization	X-Inactivation Status
1	AFF2	242	Xq28	
2	PTCHD1	223	Xp22.11	
3	HMGB3	201	Xq28	0/9
4	FAM50A	185	Xq28	
5	RPS6KA3	179	Xp22.12-p22.1	0/9
6	SLC6A8	173	Xq28	
7	RP11-13E5.1	161	Xq25	
8	OTUD5	152	Xp11.23	
9	TSPYL2	150	Xp11.2	0/5
10	FHL1	150	Xq26	1/9
11	UTX (DUSP21)	149	Xp11.2	9/9
12	SH3KBP1	147	Xp22.1-p21.3	4/9
13	TSPAN7	147	Xp11.4	
14	KIAA1280	145	Xp22.32	1/9
15	TBL1X	141	Xp22.3	7/9
16	LOC158572	139	Xp11.23	0/9
17	PRKX	138	Xp22.3	7/9
18	CRSP2	137	Xp11.4-p11.2	6/6
19	USP27X	137	Xp11.23	
20	LOC286495	137	Xq13.3	
21	AP1S2	135	Xp22.2	9/9
22	LOC402395	135	Xp11.4	
23	UBQLN2	134	Xp11.23-p11.1	2/9
24	TMEM28	134	Xq13.1	
25	NHS	133	Xq22.13	3/9
26	APXL	132	Xq22.3	
27	ARD1A	132	Xq28	
28	PPP1R3F	129	Xq11.23	0/9
29	LOC401621	129	Xq28	
30	PLXNA3	129	Xq28	0/9
31	LOC139952	128	Xp22.2	
32	PRPS2	127	Xp22.3-p22.2	0/5
33	RGAG4 (KIAA2001)	127	Xq13.1	0/9

34	CXorf38	126	Xp11.4	
35	REPS2 (POB1)	124	Xp22.2	2/9
36	LOC139334	124	Xp11.3	
37	BRCC3	124	Xq28	
38	RBBP7 (RpAp46)	123	Xp22.2	9/9
39	PDZK4	123	Xq28	0/9
40	SLC9A7	122	X	1/9
41	SYN1	122	Xp11.23	0/9
42	NAP1L3	122	Xq21.3-q22	7/9
43	DOCK11	122	Xq24	3/9
44	IRAK1	122	Xq28	1/9
45	ATP6AP2	121	Xp11.4	1/9
46	MSL3L1	120	Xp22.3	3/9
47	TMEM47	120	Xp11.4	
48	CXorf17	120	Xp11.22	
49	GPC3	120	Xq26.1	
50	SRPX (ETX1)	119	Xp21.1	0/9
51	ZNF6	119	Xq21.1-q21.2	
52	FMR1	118	Xq27.3	1/9
53	F8	118	Xq28	0/9
54	MAGEA11	117	Xq28	
55	MTMR1	117	Xq28	0/9
56	ZMAT1	116	Xq21	
57	TMEM32	116	Xq26.3	
58	LOC441488	115	Xp21.1	
59	LOC340602	115	Xp11.22	0/9
60	AMMECR1	115	Xq22.3	2/9
61	FLJ25444	114	Xp22.11	
62	ELK1	114	Xp11.2	0/6
63	XK	113	Xp21.1	
64	SMC1L1	113	Xp11.22-p11.21	7/9
65	MSN	113	Xq11.2-q12	1/9
66	IL13RA1	113	Xq24	0/9
67	PNMA3	113	Xq28	
68	CXorf12	113	Xq28	5/9
69	CNKSR2	112	Xp22.12	
70	MBTPS2	112	Xp22.1-p22.2	0/9
71	PCDH19	112	Xq13.3	
72	LOC392510	112	Xq22.1	
73	LOC389895	111	Xq27.1	
74	ABCD1	111	Xq28	3/9

75	GPR143	110	Xp22.3	7/9
76	CASK	110	Xp11.4	0/6
77	USP51	110	Xp11.22	
78	CITED1	110	Xq13.1	1/9
79	LOC401602	110	Xq21.32	
80	SLC25A5	109	Xq24-q26	0/6
81	DKFZP564B147	109	Xq26.3	0/9
82	MGC39606	109	Xq26.3	
83	GAB3	109	Xq28	8/9
84	SMS	108	Xp22.1	0/6
85	ACOT9	108	Xp22.11	
86	SUV39H1	108	Xp11.23	0/9
87	ELF4	108	Xq26	0/9
88	LOC389842	107	Xp21.3	
89	LOC347454	107	Xq24	
90	WDR40B	107	Xq25	
91	SMARCA1	107	Xq25	0/9
92	APLN	107	Xq25-26.3	0/9
93	CXorf50	106	Xq13.1	
94	GPC4	106	Xq26.1	2/9
95	SLC9A6	106	Xq26.3	0/9
96	TREX2	106	Xq28	0/9
97	RAB9B	105	Xq22.1-q22.3	1/9
98	SUHW3	105	Xq25	
99	PNMA6A	105	Xq28	0/9
100	LOC392423	104	Xp22.33	
101	ARL13A	104	Xq22.1	
102	ZIC3	104	Xq26.2	
103	LDOC1	104	Xq27	1/9
104	PLCXD1	103	Xp22.33; Yp11.32	9/9
105	FAM51A1	103	Xp22.2	9/9
106	ZFX	103	Xp21.3	9/9
107	NROB1	103	Xp21.3-p21.2	
108	PJA1	103	Xq13.1	1/9
109	RP11-130N24.1	103	Xq13.3	
110	LOC286425	103	Xq21.1	
111	GABRE	103	Xq28	0/9
112	DUSP9	103	Xq28	0/9
113	SLC25A6	102	Xp22.32; Yp11.3	9/9
114	PHF16	102	Xp11.3	0/9
115	SYP	102	Xp11.23-p11.22	2/9

116	LOC389863	102	Xq12	
117	LOC158948	102	Xq22.1	
118	NUDT11	101	Xp11.22	0/9
119	AR	101	Xq11.2-q12	0/6
120	LOC402422	101	Xq25	
121	FLNA	101	Xq28	0/9
122	IQSEC2	100	Xp11.22	
123	DLG3	100	Xq13.1	0/9
124	UBE2A	100	Xq24-q25	0/9

APPENDIX D Whole list of candidate *MECP2* target genes on whole chromosomes determined by bioinformatic analysis

Symbol	Chr	Score	Gene Name	Location	Go Term	Kegg Title	Phenotype
AFF2	X	242	AF4/FMR2 family, member 2	Xq28	brain development/learning and/or memory	---	Mental retardation, X-linked, FRAXE type
BTBD2	19	228	BTB (POZ) domain containing 2	19p13.3	protein binding	---	---
PTCHD1	X	223	patched domain containing 1	Xp22.11	---	---	---
WIZ	19	214	---	---	---	---	---
FLJ37478	4	211	---	---	---	---	---
PRKCA	17	209	protein kinase C, alpha	17q22-q23.2	ATP binding/calcium ion binding/cell surface receptor linked signal transduction	Wnt signaling pathway/MAPK signaling pathway/Focal adhesion	Pituitary tumor, invasive
LOC116349	5	206	---	---	---	---	---
NOVA2	19	201	neuro-oncological ventral antigen 2	19q13.3	RNA binding/nucleus	---	---
HMGB3	X	201	high-mobility group box 3	Xq28	DNA bending activity	---	---
QKI	6	195	quaking homolog, KH domain RNA binding (mouse)	6q26-q27	nucleic acid binding	---	---
WNT4	1	192	wingless-type MMTV integration site family, member 4	1p36.23-p35.1	cell-cell signaling/development	Wnt signaling pathway/Hedgehog signaling pathway	Rokitansky-Kuster-Hauser syndrome
RHOT1	17	192	ras homolog gene family, member T1	17q11.2	GTP binding	---	---
ZNF480	19	192	zinc finger protein 480	19q13.41	metal ion binding	---	---
SLC35F1	6	189	solute carrier family 35, member F1	6q22.1-q22.31	---	---	---
NDRG3	20	189	NDRG family member 3	20q11.21	catalytic activity/cell differentiation	---	---
RBPMS2	15	188	RNA binding protein with multiple splicing 2	15q22.31	---	---	---
HOXC8	12	187	homeobox C8	12q13.3	development	---	---
CAMK2N2	3	186	calcium/calmodulin-dependent protein kinase II inhibitor 2	3q27.1	---	---	---
CHD3	17	186	chromodomain helicase DNA binding protein 3	17p13.1	ATP binding/ATP-dependent DNA helicase activity	---	---
CNOT6L	4	185	CCR4-NOT transcription complex	4q13.3	---	---	---
FAM50A	X	185	family with sequence similarity 50, member A	Xq28	nucleus	---	---

RNF170	8	184	ring finger protein 170	8p11.21	metal ion binding/protein binding/zinc ion binding	---	---
NPAS3	14	184	neuronal PAS domain protein 3	14q12-q13	DNA binding	---	---
RKHD2	18	184	ring finger and KH domain containing 2	18q21.1	---	---	---
FAM44A	4	183	family with sequence similarity 44, member A	4p16.1	---	---	---
CPEB2	4	183	cytoplasmic polyadenylation element binding protein 2	4p15.33	nucleic acid binding/nucleotide binding	---	---
HCN2	19	183	hyperpolarization activated cyclic nucleotide-gated potassium channel 2	19p13.3	cAMP binding/cation transport/cell-cell signaling	---	---
CACNG2	22	183	calcium channel, voltage-dependent, gamma subunit 2	22q13.1	calcium ion binding	MAPK signaling pathway	---
EIF4E3	3	181	eukaryotic translation initiation factor 4E member 3	3p14	---	---	---
TMEM99	17	180	transmembrane protein 99	17q21.2	---	---	---
NKRF	X	180	NF-kappaB repressing factor	Xq24	DNA binding	---	---
RPS6KA3	X	179	ribosomal protein S6 kinase, 90kDa, polypeptide 3	Xp22.2-p22.1	ATP binding/central nervous system development/ skeletal development	MAPK signaling pathway/Long-term potentiation	Coffin-Lowry syndrome/Mental retardation, X-linked
KLF11	2	178	Kruppel-like factor 11	2p25	negative regulation of cell proliferation/	---	---
DGKI	7	178	diacylglycerol kinase, iota	7q32.3-q33	cytoplasm/diacylglycerol kinase activity	Phosphatidylinositol signaling system/Glycerolipid metabolism/	---
ANKRD13D	11	178	ankyrin repeat domain 13 family, member D	11q13.2	---	---	---
FLJ46347	2	177	---	---	---	---	---
LOC642931	9	176	---	---	---	---	---
LOC644689	9	176	---	---	---	---	---
LOC644722	9	176	---	---	---	---	---
JPH3	16	175	junctophilin 3	16q24.3	biological process unknown	---	Huntington disease-like 2
KIAA1713	18	175	KIAA1713	18q11	---	---	---
CUL3	2	174	cullin 3	2q36.3	G1/S transition of mitotic cell cycle	Ubiquitin mediated proteolysis	---
ELF2	4	174	E74-like factor 2	4q28	regulation of transcription from RNA polymerase II promoter	---	---
LMX1B	9	174	LIM homeobox transcription factor 1, beta	9q34	development/dorsa ventral pattern formation/embryonic development/ embryonic limb morphogenesis/ neuron differentiation	---	Nail-patella syndrome/Nail-patella syndrome with open-angle glaucoma
RCOR1	14	174	REST corepressor 1	14q32.32	---	---	---

MAZ	16	174	MYC-associated zinc finger protein	16p11.2	transcription termination from RNA polymerase II promoter	---	---
PP2447	22	174	---	---	---	---	---
TP53BP2	1	173	tumor protein p53 binding protein, 2	1q42.1	NF-kappaB binding/SH3/SH2 adaptor activity/apoptosis	---	---
C9orf28	9	173	chromosome 9 open reading frame 28	9q33.3	---	---	---
DAPK2	15	173	death-associated protein kinase 2	15q22.31	ATP binding/apoptosis/	---	---
CDYL2	16	173	chromodomain protein, Y-like 2	16q23.2	chromatin assembly or disassembly	---	---
NCAM2	21	173	neural cell adhesion molecule 2	21q21.1	cell adhesion /neuron adhesion	Cell adhesion molecules (CAMs)	---
ANAPC11	17	172	APC11 anaphase promoting complex subunit 11 homolog	17q25.3	anaphase-promoting complex /protein ubiquitination	Ubiquitin mediated proteolysis/Cell cycle	---
PCBP1	2	171	poly(rC) binding protein 1	2p13-p12	Ribonucleoprotein complex	---	---
GNB2	7	171	guanine nucleotide binding protein (G protein), beta polypeptide 2	7q21.3-q22.1	signal transducer activity/signal transduction	---	---
FBXO11	2	170	F-box protein 11	2p16.3	protein ubiquitination	---	---
LOC644873	5	170	---	---	---	---	---
LOC653483	6	170	---	---	---	---	---
MLL5	7	170	myeloid/lymphoid or mixed-lineage leukemia 5	7q22.1	regulation of transcription, DNA-dependent	---	---
RNF165	18	170	ring finger protein 165	18q21.1	---	---	---
HDGF2	19	170	---	---	---	---	---
USF2	19	170	upstream transcription factor 2	19q13	RNA polymerase II transcription factor activity	---	---
RIMS4	20	170	Regulating synaptic membrane exocytosis 4	20q13.12	exocytosis/neurotransmitter transport/synapse	---	---
KIF13A	6	169	kinesin family member 13A	6p23	microtubule motor activity	---	---
RXRA	9	169	retinoid X receptor, alpha	9q34.3	retinoid-X receptor activity	Adipocytokine signaling pathway	---
ARID2	12	169	AT rich interactive domain 2 (ARID, RFX-like)	12q12	chromatin modification	---	---
NOTUM	17	169	Notum pectinacetylesterase homolog	17q25.3	---	---	---
ACAA2	18	169	acetyl-Coenzyme A acyltransferase 2	18q21.1	acetyl-CoA C-acyltransferase activity	Fatty acid metabolism	---
ADNP	20	169	activity-dependent neuroprotector	20q13.13	Sequence-specific DNA binding	---	---
DNAJC5	20	169	DnaJ (Hsp40) homolog, subfamily C, member 5	20q13.33	heat shock protein binding	---	---

PRKACB	1	168	protein kinase, cAMP-dependent, catalytic, beta	1p36.1	cAMP-dependent protein kinase activity/ protein amino acid phosphorylation	Calcium signaling pathway/Insulin signaling pathway/ MAPK signaling pathway /Wnt signaling pathway/ Hedgehog signaling	---
MAD2L1BP	6	168	MAD2L1 binding protein	6p21.1	regulation of exit from mitosis	---	---
LOC644640	9	168	---	---	---	---	---
CENTG3	7	167	centaurin, gamma 3	7q36.1	small GTPase mediated signal transduction	---	---
ZDHHC2	8	167	zinc finger, DHHC-type containing 2	8p21.3-p22	acyltransferase activity	---	---
EIF2C2	8	167	Eukaryotic translation initiation factor 2C, 2	8q24	protein biosynthesis/translation initiation factor activity	---	---
NKX6-2	10	167	NK6 transcription factor related, locus 2 (Drosophila)	10q26	---	---	---
GNPTAB	12	167	N-acetylglucosamine-1-phosphate transferase, alpha and beta subunits	12q23.3	---	---	Mucolipidosis IIIA
CRLF1	19	167	cytokine receptor-like factor 1	19p12	antimicrobial humoral response /cytokine binding/	---	Cold-induced sweating syndrome
CABP7	22	167	calcium binding protein 7	22q12.2	calcium ion binding	---	---
JAZF1	7	166	---	---	---	---	---
CLN8	8	166	ceroid-lipofuscinosis, neuronal 8	8p23	ER-Golgi intermediate compartment /nervous system development	---	Ceroid lipofuscinosis, neuronal 8
C9orf75	9	166	chromosome 9 open reading frame 75	9q34.3	---	---	---
DAZAP1	19	166	DAZ associated protein 1	19p13.3	cell differentiation /spermatogenesis	---	---
NOTCH3	19	166	Notch homolog 3 (Drosophila)	19p13.2-p13.1	Notch signaling pathway /regulation of development	Dorso-ventral axis formation/Notch signaling pathway	Cerebral arteriopathy
PBX3	9	165	pre-B-cell leukemia transcription factor 3	9q33-q34	anterior compartment specification/ embryonic development/ hindbrain development/ posterior compartment specification	---	---
PPM1A	14	165	protein phosphatase 1A magnesium-dependent, alpha	14q23.1	positive regulation of I-kappaB kinase/NF-kappaB cascade	MAPK signaling pathway	---
NCK2	2	164	NCK adaptor protein 2	2q12	T cell activation /cytoskeletal adaptor activity	T cell receptor signaling pathway/Axon guidance	---
CHCHD7	8	164	coiled-coil-helix- domain 7	8q12.1	---	---	---
LOC653569	8	164	---	---	---	---	---
MLLT10	10	164	myeloid/lymphoid leukemia translocated to 10	10p12	transcription factor activity	---	Leukemia, acute T-cell lymphoblastic
ENO2	12	164	enolase 2 (gamma, neuronal)	12p13	phosphopyruvate hydratase activity	Phenylalanine, tyrosine and tryptophan biosynthesis	---
FOXA1	14	164	forkhead box A1	14q12-q13	regulation of transcription	---	---

DISP2	15	164	dispatched homolog 2 (Drosophila)	15q15.1	---	---	---
CSNK2A2	16	164	casein kinase 2, alpha prime polypeptide	16p13.3-p13.2	protein kinase CK2 activity/ signal transduction	Wnt signaling pathway/Tight junction/Adherens junction	---
LOC643734	18	164	---	---	---	---	---
PLCG1	20	164	phospholipase C, gamma 1	20q12-q13.1	phosphoinositide phospholipase C activity	Cholera Infection/ Phosphatidylinositol signaling /Natural killer cell mediated cytotoxicity	---
SPEN	1	163	spen homolog, transcriptional regulator	1p36.33-p36.11	Notch signaling pathway	---	---
PCDH1	5	163	protocadherin 1 (cadherin-like 1)	5q32-q33	nervous system development	---	---
LOC340260	7	163	---	---	---	---	---
MARVELD1	10	163	MARVEL domain containing 1	10q24.2	---	---	---
CYGB	17	163	cytoglobin	17q25.3	heme binding	---	---
RAPH1	2	162	Ras association and pleckstrin homology domains 1	2q33	cytoskeleton/signal transduction	---	---
FLJ10707	3	162	---	---	---	---	---
FAM44B	5	162	family with sequence similarity	5q35.2	---	---	---
FKBP8	19	162	FK506 binding protein 8, 38kDa	19p12	isomerase activity	---	---
LIX1L	1	161	Lix1 homolog (mouse) like	1q21.1	---	---	---
TYRO3	15	161	TYRO3 protein tyrosine kinase	15q15.1-q21.1	transferase activity	---	---
MAP1LC3B	16	161	Microtubule associated protein 1 light chain 3 beta	16q24.2	autophagic vacuole/autophagy /ubiquitin cycle	---	---
PRKACA	19	161	protein kinase, cAMP-dependent, catalytic, alpha	19p13.1	cAMP-dependent protein kinase complex	Wnt signaling pathway/ Hedgehog signaling pathway/ MAPK signaling	---
GNAS	20	161	GNAS complex locus	20q13.3	G-protein coupled receptor protein signaling pathway	Long-term depression/Gap junction/Cholera	Acromegaly/McCune-Albright syndrome/
LOC340578	X	161	---	---	---	---	---
KIF21B	1	160	kinesin family member 21B	1pter-q31.3	microtubule motor activity	---	---
FLJ39653	4	160	---	---	---	---	---
LY6H	8	160	lymphocyte antigen 6 complex, locus H	8q24.3	cellular defense response/ nervous system development	---	---
LOC51145	9	160	---	---	---	---	---
USP7	16	160	ubiquitin specific peptidase 7	16p13.3	cysteine-type endopeptidase activity	---	---
ASH1L	1	159	absent, small, or homeotic-like	1q22	regulation of transcription	Tight junction	---
FLJ90575	4	159	---	---	---	---	---
GTF2E2	8	159	general transcription factor IIE, polypeptide 2, beta 34kDa	8p21-p12	general RNA polymerase II transcription factor activity complex	Basal transcription factors	---
LOC338799	12	159	---	---	---	---	---

LOC645631	16	159	---	---	---	---	---
PODXL2	3	158	podocalyxin-like 2	---	---	---	---
PFN2	3	158	profilin 2	3q25.1-q25.2	actin binding cytoskeleton organization and biogenesis	Regulation of actin cytoskeleton	---
NRF1	7	158	nuclear respiratory factor 1	7q32	generation of precursor metabolites and energy	---	---
LOC643481	11	158	---	---	---	---	---
CKAP4	12	158	cytoskeleton-associated protein 4	12q23.3	membrane fraction	---	---
MAST1	19	158	microtubule associated serine/threonine kinase 1	19p13.2	cytoskeleton organization and biogenesis/magnesium ion binding	---	---
LOC200312	22	158	---	---	---	---	---
LOC285346	3	157	---	---	---	---	---
ATXN7	3	157	ataxin 7	3p21.1-p12	visual perception	---	Spinocerebellar ataxia-7
C6orf148	6	157	chromosome 6 open reading frame 148	6q13	---	---	---
AIG1	6	157	androgen-induced 1	6q24.2	integral to membrane/membrane	---	---
LOC642730	8	157	---	---	---	---	---
SPPL3	12	157	---	---	---	---	---
ZNF219	14	157	zinc finger protein 219	14q11	/transcription factor activity	---	---
ANKRD9	14	157	ankyrin repeat domain 9	14q32.32	---	---	---
MAP2K3	17	157	mitogen-activated protein kinase kinase 3	17q11.2	MAP kinase activity	MAPK signaling pathway/Toll-like receptor signaling pathway	---
NFIC	19	157	nuclear factor I/C (CCAAT-binding transcription factor)	19p13.3	transcription from RNA polymerase II promoter	---	---
ALX3	1	156	aristaless-like homeobox 3	1p21-p13	Development	---	---
ZFAND3	6	156	zinc finger,AN1-type domain 3	6pter-p22.3	zinc ion binding	---	---
PRKACG	9	156	protein kinase, cAMP-dependent, catalytic, gamma	9q13	cAMP-dependent protein kinase activity/male gonad development	Wnt signaling pathway/Hedgehog signaling pathway	---
PPAPDC1A	10	156	phosphatidic acid phosphatase type 2 domain containing 1A	10q26.12	microtubule/microtubule-based movement/structural molecule activity	---	---
JAG2	14	156	jagged 2	14q32	Notch signaling pathway /auditory receptor cell fate commitment	Notch signaling pathway	---
TLK1	2	155	tousled-like kinase 1	2q31.1	regulation of chromatin assembly or disassembly/response to DNA damage stimulus	---	---
RREB1	6	155	ras responsive element binding protein 1	6p25	Ras protein signal transduction	---	---
MAP3K4	6	155	mitogen-activated protein kinase kinase kinase 4	6q26	JNK cascade/activation of MAPKK activity	MAPK signaling pathway	---

KCNB2	8	155	potassium voltage-gated channel, Shab-related subfamily, member 2	8q13.2	cation transport/delayed rectifier potassium channel activity	---	---
TAOK1	17	155	TAO kinase 1	17q11.2	amino acid phosphorylation/	---	---
ZNF521	18	155	zinc finger protein 521	18q11.2	---	---	---
C20orf11	20	155	chromosome 20 open reading frame 11	20q13.33	Nucleus	---	---
SLC6A8	X	155	solute carrier family 6 (neurotransmitter transporter, creatine), member 8	Xq28	neurotransmitter uptake/neurotransmitter:sodium symporter activity	---	Creatine deficiency syndrome, X-linked
PPARG	3	154	peroxisome proliferative activated receptor, gamma	3p25	generation of precursor metabolites and energy	---	Diabetes mellitus, insulin-resistant, with acanthosis nigrican
KIAA1718	7	154	---	---	---	---	---
ASTN2	9	154	astrotactin 2	9q33.1	---	---	---
FLJ45530	16	154	---	---	---	---	---
CANT1	17	154	calcium activated nucleotidase 1	17q25.3	Golgi stack /NF-kappaB cascade	Pyrimidine metabolism/Purine metabolism	---
SALL3	18	154	sal-like 3 (Drosophila)	18q23	regulation of transcription	---	---
LOC645874	3	153	---	---	---	---	---
BMP6	6	153	bone morphogenetic protein 6	6p24-p23	cartilage development/cell differentiation/cytokine activity	Hedgehog signaling pathway/TGF-beta signaling pathway	---
KDELR2	7	153	endoplasmic reticulum protein retention receptor 2	7p22.1	ER to Golgi vesicle-mediated transport	---	---
AGTPBP1	9	153	ATP/GTP binding protein 1	9q21.33	carboxypeptidase A activity/proteolysis	---	---
CPT1A	11	153	carnitine palmitoyltransferase 1A (liver)	11q13.1-q13.2	carnitine O-palmitoyltransferase activity	Fatty acid metabolism/Adipocytokine signaling pathway	CPT deficiency, hepatic, type IA
EB-1	12	153	---	---	---	---	---
CCNE1	19	153	cyclin E1	19q12	G1/S transition of mitotic cell cycle/androgen receptor binding	Cell cycle	---
RELB	19	153	v-rel reticuloendotheliosis viral oncogene homolog B,3	19q13.31-q13.32	transcription corepressor activity	---	---
KCTD3	1	152	potassium channel tetramerisation domain containing 3	1q41	---	---	---
KCMF1	2	152	potassium channel modulatory factor 1	2p11.2	---	---	---
GNL3	3	152	guanine nucleotide binding protein-like 3 (nucleolar)	3p21.1	GTP binding	---	---

PLXND1	3	152	plexin D1	3q21.3	development	---	---
FOXF2	6	152	forkhead box F2	6p25.3	sequence-specific DNA binding	---	---
LOC653748	7	152	---	---	---	---	---
C9orf10	9	152	chromosome 9 open reading frame 10	9q22.31	---	---	---
SIDT2	11	152	SID1 transmembrane family, member 2	11q23.3	integral to membrane/membrane	---	---
NOG	17	152	noggin	17q21-q22	cartilage development /nervous system development/sensory perception of sound	TGF-beta signaling pathway	Stapes ankylosis syndrome
LOC645369	18	152	---	---	---	---	---
KIF3B	20	152	kinesin family member 3B	20q11.21	anterograde axon cargo transport/determination of left/right symmetry	---	---
LOC643325	22	152	---	---	---	---	---
SHANK3	22	152	SH3 and multiple ankyrin repeat domains 3	22q13.3	protein binding	---	Chromosome 22q13.3 deletion syndrome
OTUD5	X	152	OTU domain containing 5	Xp11.23	---	---	---
DOCK7	1	151	dedicator of cytokinesis 7	1p31.3	GTPase binding/guanyl-nucleotide exchange factor activity	---	---
KCNH1	1	151	potassium voltage-gated channel subfamilyH member1	1q32-q41	calmodulin binding/cation transport/delayed rectifier potassium channel activity	---	---
UNQ6077	1	151	---	---	---	---	---
ODC1	2	151	ornithine decarboxylase 1	2p25	lyase activity/ornithine decarboxylase activity/polyamine biosynthesis	Urea cycle and metabolism of amino groups/Arginine and proline metabolism	Colonic adenoma recurrence
KCNK12	2	151	potassium channel, subfamily K, member 12	2p22-p21	potassium channel activity/ voltage-gated ion channel activity	---	---
HEG1	3	151	HEG homolog 1 (zebrafish)	3q21.2	---	---	---
CPLX1	4	151	complexin 1	4p16.3	exocytosis/neurotransmitter transport/synaptic transmission/syntaxin binding	---	---
FLJ20647	4	151	---	---	---	---	---
CSS3	5	151	---	---	---	---	---
FNDC1	6	151	fibronectin type III domain containing 1	6q25	---	ECM-receptor interaction	---
KIAA1706	7	151	---	---	---	---	---
GRB10	7	151	growth factor receptor-bound protein 10	7p12-p11.2	SH3/SH2 adaptor activity/cell-cell signaling	---	---
WDR5	9	151	WD repeat domain 5	9q34	protein binding	---	---
C10orf9	10	151	chromosome 10 open reading frame 9	10p11.21	regulation of progression through cell cycle	---	---

PHF21A	11	151	PHD finger protein 21A	11p11.2	protein binding/regulation of transcription	---	---
DRAP1	11	151	DR1-associated protein 1 (negative cofactor 2 alpha)	11q13.3	transcription corepressor activity/transcription factor activity	---	---
GNAO1	16	151	guanine nucleotide binding protein (G protein)	16q13	G-protein coupled receptor protein signaling pathway /nervous system development	Long-term depression	---
FAM57A	17	151	family with sequence similarity 57, member A	17p13.3	integral to membrane/membrane	---	---
LOC645722	17	151	---	---	---	---	---
CACNG4	17	151	calcium channel, voltage-dependent, gamma subunit 4	17q24	calcium ion binding	MAPK signaling pathway	---
TUBB4	19	151	tubulin, beta 4	19p13.3	GTP binding/ microtubule-based movement	Gap junction	---
C20orf18	20	151	chromosome 20 open reading frame 18	20p13	ubiquitin cycle	---	---
SLC24A3	20	151	solute carrier family 24, member 3	20p13	antiporter activity /symporter activity	---	---
ZNF278	22	151	zinc finger protein 278	22q12.2	DNA-dependent	---	---